

3D Registration in 30 Years: A Survey

Jiaqi Yang, Chu'ai Zhang, Zhengbao Wang, Xinyue Cao, Xuan Ouyang, Xiyu Zhang, Zhenxuan Zeng, Zhao Zeng, Borui Lu, Zhiyi Xia, Qian Zhang, Yulan Guo, *Senior Member, IEEE*, and Yanning Zhang, *Fellow, IEEE*

Abstract—3D point cloud registration is a fundamental problem in computer vision, computer graphics, robotics, remote sensing, and etc. Over the last thirty years, we have witnessed the amazing advancement in this area with numerous kinds of solutions. Although a handful of relevant surveys have been conducted, their coverage is still limited. In this work, we present a comprehensive survey on 3D point cloud registration, covering a set of sub-areas such as pairwise coarse registration, pairwise fine registration, multi-view registration, cross-scale registration, and multi-instance registration. The datasets, evaluation metrics, method taxonomy, discussions of the merits and demerits, insightful thoughts of future directions are comprehensively presented in this survey. The regularly updated project page of the survey is available at <https://github.com/Amyyyy11/3D-Registration-in-30-Years-A-Survey>.

Index Terms—3D point cloud, point cloud registration, survey, performance evaluation, dataset.

1 INTRODUCTION

ALIGNING 3D point clouds to a unified coordinate system, known as 3D point cloud registration, is a fundamental problem in numerous areas such as computer vision, computer graphics, robotics and remote sensing. Aligned point clouds offer two key results: 1) a more complete point cloud for reconstruction, information fusion, and error measurement; 2) a six-degree-of-freedom (6-DoF) pose for robust pose estimation, 3D tracking, object/place localization, and motion-flow estimation. With the development of 3D active and passive acquisition technology (e.g., Intel's RealSense, Apple's iPhone series), 3D point cloud registration has attracted an increasing research attention on this topic during the last three decades.

In particular, there are several sub-branches towards robust 3D point cloud registration, depending on either data acquisition or application scenarios (Fig. 1). From the perspective of handled data sequences, pairwise registration focuses on aligning two point clouds, while multi-view registration aligns more than two sequential or unordered multiple point clouds. From the perspective of error minimization, coarse registration roughly aligns point clouds with relatively large pose variation, while fine registration usually focuses on minimizing small residual errors. From the perspective of methodologies, early methods design hand-crafted optimization or heuristic methods, while re-

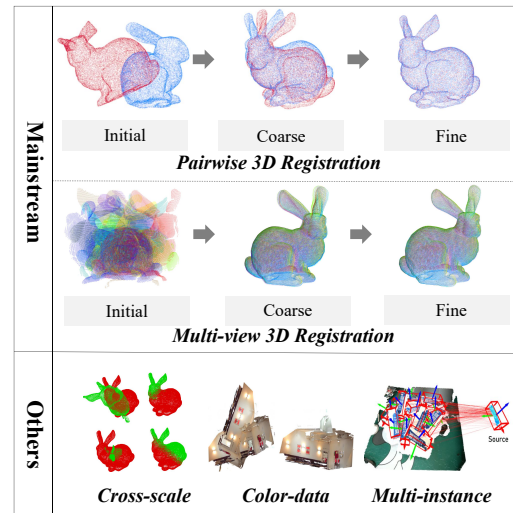


Fig. 1. Typical 3D registration problems.

cent methods resort to deep learning approaches. There are also other perspectives for investigating the registration problem, such as feature learning, correspondence learning, and robust 6-DoF pose estimation. Therefore, there are many methods and research topics in the 3D point cloud registration realm.

Existing surveys are focused on either different parts or a limited scope of point cloud registration tasks. For instance, an early review [1] covers various aspects of point cloud registration but lacks a thorough analysis of the interconnections between subfields, failing to systematically reveal the intrinsic relationships and interactions among them. A recent review [2] recaps commonly used datasets and evaluation metrics but lacks performance comparisons in unified experimental settings, failing to demonstrate the advantages and limitations of different methods under consistent conditions. As such, they fail to cover the literature from the last three decades from a more comprehensive

- This work is supported in part by National Natural Science Foundation of China (No. 62372377).
- Jiaqi Yang, Chu'ai Zhang, Zhengbao Wang, Xinyue Cao, Xuan Ouyang, Xiyu Zhang, Zhenxuan Zeng, Zhiyi Xia and Yanning Zhang are with the School of Computer Science, Northwestern Polytechnical University, China. E-mail: {cazhang, npu-wzb, caoxinyue, ouyangxuan, 2426988253, zengzhenxuan, xiazhiyi}@mail.nwpu.edu.cn; {jqyang, ynzhang}@nwpu.edu.cn.
- Zhao Zeng and Borui Lu are with the School of Electronics and Control Engineering, Chang'an University, China. E-mail: {zhaozeng, 2024232056}@chd.edu.cn.
- Qian Zhang is with School of Architecture & Urban Planning, Shenzhen University, China. E-mail: {hangfanqz}@163.com. (Corresponding author: Qian Zhang)
- Yulan Guo is with the School of Electronics and Communication Engineering, Sun Yat-Sen University, China. E-mail: {guoyulan}@sysu.edu.cn.

perspective.

To fill the gap, we present a comprehensive survey on 3D registration methods in the last decades. The major contributions are summarized as follows.

- **Thorough review and new taxonomy.** To the best of our knowledge, as shown in Fig. 2, this is the first survey paper to comprehensively review point cloud registration methods, covering a set of subareas such as pairwise coarse registration, pairwise fine registration, multi-view registration, cross-scale registration, and multi-instance registration. It offers a systematic taxonomy and a broad literature coverage.
- **Benchmark overview and performance comparison.** Popular benchmark datasets and performance evaluation metrics for point cloud registration are systematically summarized. A set of comparative results of representative state-of-the-art methods on standard benchmarks are also reported.
- **Outlook on future directions.** The traits, merits, and demerits of the existing methods have been highlighted. We also present insightful discussions on current challenges and several future research directions to inspire follow-up works in this field.

The remainder of the paper is organized as follows. Sec. 2 reviews point cloud registration datasets and evaluation metrics. Sec. 3 introduces pairwise coarse registration methods, including correspondence-based and correspondence-free approaches. Sec. 4 discusses pairwise fine registration methods, focusing on ICP-based and GMM-based methods. Sec. 5 presents multi-view coarse registration methods, covering geometric and deep learning-based approaches. Sec. 6 introduces multi-view fine registration methods, including point-based and motion-based methods. Sec. 7 introduces other registration problems, such as cross-scale, cross-source, color point cloud, and multi-instance registration. Sec. 8 discusses challenges and opportunities in the field. Finally, Sec. 9 draws conclusions.

2 BACKGROUND

2.1 Basic Concepts

Point cloud. A point cloud \mathbf{P} comprises a set of 3D points $\{\mathbf{p}_i | i = 1, 2, \dots, N\}$, where $\mathbf{p}_i \in \mathbb{R}^3$. It is a discrete representation of the 3D continuous surface, which is unorganized and permutation-insensitive.

Point cloud registration. Given a set of point clouds $\{\mathbf{P}_1, \mathbf{P}_2, \dots, \mathbf{P}_N\}$ of the same object or scene. The goal of point cloud registration is to determine multiple transformations $\{\mathbf{T}_1, \mathbf{T}_2, \dots, \mathbf{T}_N\} \in SE(3)$ composed of the corresponding rotation matrices $\{\mathbf{R}_1, \mathbf{R}_2, \dots, \mathbf{R}_N\} \in SO(3)$ and corresponding translation vectors $\{\mathbf{t}_1, \mathbf{t}_2, \dots, \mathbf{t}_N\} \in \mathbb{R}^3$: $\{\mathbf{P}_1, \mathbf{P}_2, \dots, \mathbf{P}_N\} \rightarrow \mathbf{P}_{reg}$, which aligns these point clouds to a unified coordinate system. It generates a more complete point cloud and a set of pose parameters.

2.2 Datasets

A large number of datasets have been collected to evaluate the performance of geometric and deep-learning methods

for various registration tasks. Depending on the popularity in the community, we list several standard datasets used for the registration problems investigated in this survey in Table 1.

2.3 Metrics

Various evaluation metrics have been proposed to evaluate 3D registration performance. For instance, registration recall (RR), root mean square error (RMSE), mean absolute error (MAE), mean squared error (MSE), mean isotropic error (MIE), rotation error (RE), and translation error (TE) are fundamental metrics for evaluating the accuracy performance of most registration tasks. In particular, for the multi-view coarse registration task, maximum correspondence error (MCE) is additionally used to evaluate the maximum displacement of any point on surface from its ground truth position, and empirical cumulative distribution function (ECDF) is used to evaluate the function of the error distribution.

There are also some metrics used for evaluating some modules in a registration pipeline. For instance, the recall versus precision curve (RPC) is the most frequently used metric for evaluating the performance of local descriptors. Inlier recall (IR), inlier precision (IP), and F1-score (F1) are frequently used metrics for evaluating the performance of correspondence optimization methods.

3 PAIRWISE COARSE REGISTRATION

3.1 Geometric Methods

This section summarizes the pairwise coarse registration methods based on geometric approaches, the taxonomy and chronological overview are shown in Fig. 4 and Fig. 6, respectively.

3.1.1 Correspondence-based Methods

In correspondence-based methods, as shown in Fig. 3, correspondence generation is crucial for the accuracy and robustness of the registration process.

(i) **Keypoint detection.** Its aim is to find a set of sparse yet distinctive points for matching. A comparative evaluation is available in [13]. A branch of methods detect semantically consistent 3D keypoints [22], [23], [24], which will be detailed here as they are not specifically designed for registration. We classify existing keypoint detectors for 3D registration as fixed-scale and adaptive-scale.

1) **Fixed-scale keypoint detection methods.** These detectors operate at a fixed scale when identifying keypoints or features across the entire scene, without adjusting the scale based on object size or the distance from the sensor. The main advantage of fixed-scale detectors lies in their faster processing speed and lower computational demands. These methods can be broadly divided into two categories: saliency-based and signature-based. Saliency-based keypoint detection methods [6], [25], [26], [27], [28], [29] define a saliency measure to identify regions with distinctive geometric or visual properties, often focusing on local surface variations for efficient keypoint selection. Early works by Chen et al. [25] and Castellani et al. [26] utilize local surface patches and a 3D saliency measure to

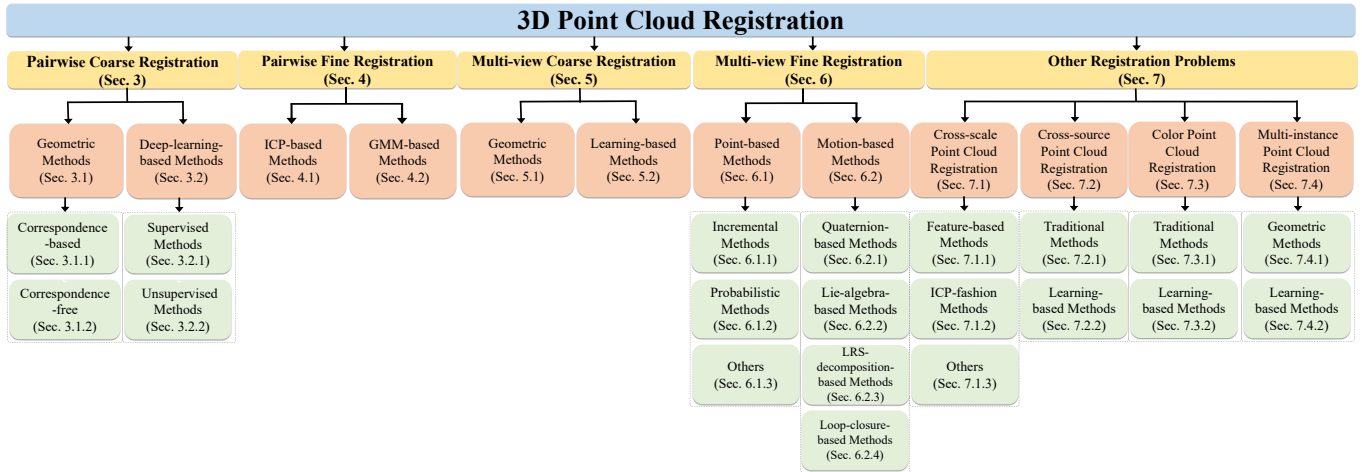


Fig. 2. A taxonomy of 3D point cloud registration methods.

TABLE 1
A summary of representative datasets for 3D registration problems.

Name	Year	# Samples	Acquisition	Type	Nuisances	Application scenario
Stanford 3D Scanning Repository [3]	1996	52	LiDAR	Object	Real noise	Pairwise fine & Multi-view & Cross-scale registration
U3M [4]	2006	496	LiDAR	Object	Limited overlap & Self-occlusion	Pairwise coarse registration
U3OR [5], [6]	2006	188	LiDAR	Indoor	Occlusion & Clutter	Pairwise coarse registration
QuLD [7]	2011	240	LiDAR	Outdoor	Occlusion & Clutter & Noise	Pairwise coarse registration
RGB-D scenes [8]	2011	300	Kinect	Indoor	Occlusion & Real noise	Pairwise fine registration
EPFL Statue [9]	2012	55	Synthetic	Object	Limited overlap & Occlusion & Real noise	Pairwise fine registration
RGB-D SLAM [10]	2012	39	Kinect	Indoor	Occlusion & Real noise	Pairwise fine registration
KITTI [11]	2012	555	LiDAR	Outdoor	Clutter & Occlusion & Real noise	Pairwise coarse & fine & Multi-view registration
ETH [12]	2012	713	LiDAR	Outdoor	Limited overlap & Clutter & Occlusion & Real noise	Pairwise coarse & fine & Multi-view registration
B3R [13]	2013	54	Synthetic	Object	Gaussian noise & Mesh decimation	Pairwise coarse registration
Space time [13]	2013	120	Synthetic	Object	Occlusion	Pairwise coarse registration
ModelNet40 [14]	2015	12311	Synthetic	Object	Partial missing data & Simulated noise	Pairwise coarse & fine & Multi-instance registration
ScanNet [15]	2017	1513	Kinect	Indoor	Occlusion & Real noise	Multi-view registration
3DMatch [16]	2017	1623	Kinect	Indoor	Occlusion & Real noise	Pairwise coarse & fine & Multi-view registration
Scan2CAD [17]	2019	1506	Synthetic	Indoor	Clutter & Occlusion & Real noise	Multi-instance registration
WHU-TLS [18]	2020	115	LiDAR	Outdoor	Point density & Clutter & Occlusion	Pairwise coarse & fine registration
3DLoMatch [19]	2021	1781	Kinect	Indoor	Limited overlap & Occlusion & Real noise	Pairwise coarse & Multi-view registration
3DCSR [1]	2021	221	LiDAR & Kinect	Indoor	Noise & Density difference & Limited overlap	Cross-source registration
NSS [20]	2023	27	Synthetic	Outdoor	Spatiotemporal changes	Pairwise coarse registration
Color3DMatch [21]	2024	1623	Kinect	Indoor	Occlusion & Real noise	Color point cloud registration
Color3DLoMatch [21]	2024	1781	Kinect	Indoor	Limited overlap & Occlusion & Real noise	Color point cloud registration

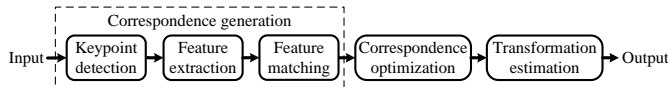


Fig. 3. Pipeline of correspondence-based 3D pairwise coarse registration.

detect keypoints in regions with significant surface shape variations. In parallel, Mian et al. [27] proposed a method for detecting keypoints with significant shape variations on 3D faces, enabling the extraction of highly descriptive, pose-invariant features. There are also methods that address specific challenges, such as scale invariance [6] and computational efficiency [28]. More recently, Teng et al. [29] introduced the centroid distance (CED) detector, which uniquely identifies keypoints in geometric and color spaces without requiring normal estimation or eigenvalue decomposition.

Signature-based keypoint detection methods [30], [31] rely on specific geometric features to identify keypoints, ensuring robustness and repeatability. For instance, Sun et al. [30] proposed a heat kernel signature (HKS) detector to

capture multi-scale neighborhood information, improving stability under shape perturbations. Zhong [31] developed the intrinsic shape signature (ISS), which provides a view-independent representation of local and semi-local regions for efficient shape matching and pose estimation. There are also several works improving ISS by Guo et al. [32] and Zhang et al. [33], respectively.

Although the above methods are efficient, they generally exhibit limited repeatability performance in complex scenes.

2) **Adaptive-scale keypoint detection methods.** These detectors dynamically adjust the scale at which keypoints are identified based on local geometry or appearance, ensuring that features are robustly captured across varying object sizes, distances, or levels of detail. An intuitive idea is to extend 2D detectors to 3D. For instance, Sipiran and Bustos [34] adapted the widely used 2D Harris operator to 3D, achieving robust keypoint detection by analyzing vertex neighborhoods. Some detectors only adapt to 3D meshes [35], [36], [37]. For instance, Zaharescu et al. [35] developed MeshDOG, a scalar field-based method that detects keypoints invariant to rotation, translation, and scale, describing features with local geometric properties. Incorporo-

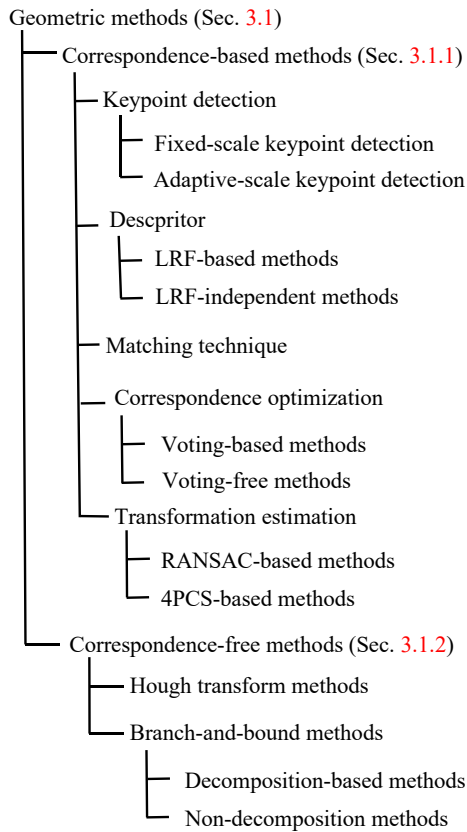


Fig. 4. Taxonomy of representative geometric methods for 3D pairwise coarse registration.

rating additional robustness, Knopp et al. [37] introduced a method combining local feature extraction with an extended SURF descriptor and a probabilistic Hough transform, significantly improving 3D shape recognition accuracy. Some detectors are designed specifically for 3D point clouds [38], [39], [40], Unnikrishnan and Hebert [39] proposed a multi-scale operator approach for direct keypoint detection from raw point clouds, avoiding predefined structures. Steder et al. [40] further enhanced keypoint detection by developing the normal aligned radial feature (NARF) method, which integrates object boundary information for better stability and precision.

Although adaptive-scale methods improve robustness against scale variations, their computational complexity sometimes limits real-time efficiency.

(ii) **Descriptors.** Once the keypoints are detected, the geometric features of the surrounding local surface can be extracted to generate a local feature descriptor. As shown in Fig. 5, depending on whether a local reference frame (LRF) is established on the local surface of the point cloud, these local feature descriptors can be further classified into two categories: LRF-based and LRF-independent. Table 2 provides an overview of the performance of methods for the description of local surface features.

1) **LRF-based methods.** These descriptors first construct an LRF in the local surface and then encode the spatial and geometric information of the surface based on the LRF. These methods can be further divided into two categories, i.e., real-valued encoding and binary feature encoding.

Real-valued encoding methods generally generate descriptors with 2D projection attributes, 3D point attributes, or 3D voxel attributes. 2D-projection-attribute-based methods [41], [42], [43], [44], [45], [46], [47], [48] project the local surface onto 2D planes to efficiently capture geometric distributions by simplifying 3D structures into 2D representations. For instance, Malassiotis and Srinivas [41] proposed snapshots, which projects the local surface onto the camera plane, while Guo et al. [42] developed the rotational projection statistics (RoPS), ensuring a more comprehensive feature encoding with multi-view projection information. Following RoPS, Yang et al. [43] introduced the rotational contour signatures (RCS), capturing multi-view information through 2D contour projections. By contrast, 3D-point-attribute-based methods [25], [49], [50], [51], [52], [53], [54], [55] utilize spatial and geometric relationships within the 3D neighborhood to describe local surface characteristics. Notable examples include the local surface patch (LSP) representation by Chen et al. [25], which encodes angular relationships into a 2D histogram, and the signature of histograms of orientations (SHOT) by Tombari et al. [49], which divides the neighborhood into subspaces for enhanced descriptiveness. 3D voxel attribute methods divide the local region into voxel grids to encode occupancy or density information, effectively representing complex spatial structures. For instance, Tang et al. [56] proposed the signature geometric centroids (SGC) descriptor, which encodes geometry using voxelized centroid-based features. Zhang et al. [53] proposed the kernel density-based descriptor (KDD), utilizing kernel density estimation to balance robustness and descriptiveness.

For binary encoding methods, they focus on simplifying the representation of geometric and spatial information in binary formats, thereby significantly reducing memory usage and accelerating feature matching. We further divide them into descriptor-space binarization and attribute-space binarization methods. For descriptor-space binarization, Prakhya et al. [57] introduced the binary signature of histograms of orientations (B-SHOT), which uses binary quantization to enhance memory efficiency and matching speed without compromising SHOT's performance. On the other hand, attribute-space binarization methods [58], [59], [60], [61], such as the local voxelized structure (LoVS) descriptor proposed by Quan et al. [58], directly compare geometric attribute values within an LRF, improving compactness and efficiency.

LRF-based methods generally exhibit superior descriptiveness performance on clean data, however, their robustness to nuisances such as noise and partial overlap is limited due to LRF's instability.

2) **LRF-independent methods.** LRF-independent descriptors capture local shape information by leveraging geometric properties of the point cloud, such as normal vectors and point densities. These methods can be broadly categorized into two main types: attribute-based statistical methods and attribute-space projection methods. Attribute-based statistical methods [62], [63], [64], [65], [66], [67], [68], [69], [70] focus on capturing the distribution characteristics of local point clouds through statistical analysis of individual attributes (e.g., distances and angles) or their combinations. These descriptors, such as the point feature histograms

(PFH) [63], fast point feature histograms (FPFH) [64], use distance relationships to describe local geometry. Some methods encode several attributes simultaneously, such as the local feature statistics histogram (LFSH) [65] and the fully attribute pair statistical histogram (FAPSH) [70]. On the other hand, attribute-space projection methods [71], [72], [73], [74], [75], [76], [77] transform the point cloud into an attribute space with structured forms, such as 3D grids or voxel grids. Some methods project on a 2D attribute space. For instance, spin image [71] and spherical spin image [73] project local point cloud data onto structured spaces, enabling better handling of occlusions and clutter. Some other methods construct a 3D attribute space for projection. For instance, the voxelization in invariant distance space (VOID) descriptor [75] uses voxelization to encode robust features by computing three invariant distance attributes for keypoints and their neighboring points.

LRF-independent methods have recently emerged as a promising and increasingly important trend for 3D local shape description.

(iii) Matching technique. The main purpose of matching is to accurately identify the corresponding matching pairs of points by comparing the feature descriptors extracted for keypoints. A common approach involves using different distance metrics to perform nearest-neighbor (NN) or nearest-neighbor distance ratio (NNDR) matching. Various distance measures have been used for this purpose, such as the Euclidean distance and the Manhattan distance [63].

To improve the matching speed, several acceleration techniques have been introduced. Some researchers focus on optimizing the search for nearest neighbors by using data structures such as 2D index tables [71]. Hash tables [5], [74], [78] employ hash functions to quickly map feature descriptors to specific locations, allowing for rapid retrieval. Locality-sensitive trees [31] group similar data points together to facilitate faster matching, and K-d trees [42], [79], [80] are commonly used to accelerate nearest-neighbor searches in high-dimensional spaces. These methods significantly improve the speed and reliability of the matching process.

(iv) Correspondence optimization. Due to descriptor limitations and challenges such as clutter and occlusions in point cloud data, initial correspondence sets often contain many incorrect matches (outliers). To address this issue, researchers have developed various optimization techniques, generally categorized as voting-based and voting-free. Table 3 provides an overview of the performance for the correspondence optimization methods.

1) **Voting-based methods.** Inspired by the success of the Hough Transform [102] in 2D image processing, early 3D methods extend this approach by transforming 3D correspondences into a Hough space for voting. For instance, Tombari and Stefano [103] aimed to detect tight clusters formed by inliers in the Hough space. To further enhance memory efficiency and precision, Woodford et al. [104] introduced intrinsic Hough and minimum-entropy Hough, refining vote filtering to make the method more suitable for 3D applications. Xing et al. [99] proposed single point correspondence voting and clustering (SCVC), predicting the transformation with a single correspondence while applying Hough voting to determine the remaining degrees of

freedom.

In recent years, methods incorporating geometric constraints have been proposed to optimize correspondences. Buch et al. [105] presented the search of inliers (SI), which utilizes low-level geometric invariants for local evaluation and covariant constraints for global voting. Based on this, Sahloul et al. [106] presented a two-stage voting scheme with dense evaluation and ranking of local and global geometric consistency. Wu et al. [107] further refined the approach by first generating a geometric consistency point pair voting set using PPF constraints, followed by selecting compatible correspondence triplets to estimate hypothesis poses, resulting in a more robust final pose voting set.

More recently, research has shifted towards exploiting the consistency between inliers in the graph space. Yang et al. [108] proposed consistency voting (CV), which evaluates the consistency of each initial correspondence against a predefined voting set based on rigidity and LRF affinity. Expanding on this idea, Yang et al. [109] developed loose-tight geometric voting (LTGV), which balances precision and recall by using complementary loose and tight geometric constraints within a dynamic voting scheme. Sun and Deng [90] proposed triple-layered voting with consensus maximization (TriVoC), which decomposes the selection of minimal 3-point sets into three layers, each employing efficient voting and correspondence sorting based on pairwise equal-length constraints. Finally, Yang et al. [95] proposed mutual voting (MV), which models graph nodes and edges as candidates and voters, refining both to achieve more reliable scoring for correspondence evaluation.

2) **Voting-free methods.** Initially, these methods optimize correspondences with feature similarities [5], [110]. Assuming correct correspondences form strongly connected clusters, methods such as spectral technique (ST) [82] and geometric consistency (GC) [25] identify matches through spectral and spatial clustering. Chen et al. [91] proposed SC^2 -PCR, which employs second-order spatial compatibility for more distinctive clustering at an early stage. Apart from clustering-based methods, some approaches leverage game theory for inlier selection. Albarelli et al. [111] introduced a game-theoretic framework to achieve fine surface registration based on global geometric compatibility. Building on this, Rodola et al. [80] introduced game theory matching (GTM), incorporating scale invariance and enhancing robustness in cluttered scenes.

Other methods focus on finding global optima in the parameter space using techniques such as branch-and-bound (BnB) [112]. For instance, Bustos and Chin [84] proposed guaranteed outlier removal (GORE), which uses geometric operations to reject outliers, with BnB as a subroutine. Aiming for efficiency rather than guaranteed global optimality, Li [89] defined correspondence matrix (CM) and augmented correspondence matrix (ACM) for tight bounding. To further accelerate GORE, Li et al. [113] presented quadratic-time GORE (QGORE), which employs a voting-based geometric consistency approach for faster upper-bound estimation while maintaining robustness and optimality.

Recent voting-free methods also aim to achieve global maximum consensus. Zhou et al. [83] proposed fast global registration (FGR), using the German-McClure loss and Graduated non-convexity (GNC) for non-convex optimiza-

TABLE 2
Performance summary of representative local feature descriptors.

Year	Method	Data Type	Category	Performance
1999	Spin image [71]	Mesh & Point cloud	LRF-independent	Rotational invariance and efficient
2001	Spherical spin images [73]	Mesh	LRF-independent	Outperforms spin image
2004	3DSC [74]	Point cloud	LRF-independent	Outperforms spin image
2007	LSP [25]	Depth image	LRF-based	Comparable to spin image, spherical spin image
	Snapshots [41]	Mesh	LRF-based	Outperforms spin image
2008	PFH [63]	Point cloud	LRF-independent	Time consuming
2009	FPFH [64]	Point cloud	LRF-independent	More time efficient than PFH
2010	SHOT [49]	Mesh	LRF-based	Outperforms spin image
2011	CSHOT [51]	Mesh	LRF-based	Outperforms SHOT
2013	RoPS [42]	Mesh	LRF-based	Outperforms spin image, LSP, SHOT
2015	B-SHOT [57]	Point cloud	LRF-based	Outperforms SHOT
	TriSI [50]	Mesh	LRF-based	Outperforms spin image, SHOT, RoPS
2016	LFSH [65]	Point cloud	LRF-independent	High efficiency and outperforms FPFH, SHOT
	CoSPAIR [52]	Point cloud	LRF-based	Outperforms FPFH, SHOT, CSHOT
2017	RCS [43]	Point cloud	LRF-based	Outperforms snapshots, SHOT, B-SHOT, RoPS, RCS
	TOLDI [44]	Point cloud	LRF-based	Outperforms snapshots, FPFH, SHOT, RoPS
	MaSH [69]	Point cloud	LRF-independent	Outperforms snapshots, FPFH, RoPS, LFSH, RCS
2018	LoVS [58]	Point cloud	LRF-based	Outperforms snapshots, FPFH, SHOT, B-SHOT, RoPS
	LPPFH [66]	Point cloud	LRF-independent	Outperforms spin image, FPFH, SHOT, RoPS
2019	SDASS [68]	Point cloud	LRF-independent	Outperforms spin image, FPFH, SHOT, RoPS, LFSH, TriSI, TOLDI
2020	HoPPF [67]	Point cloud	LRF-independent	Outperforms spin image, PFH, FPFH, SHOT, RoPS
	WHI [45]	Point cloud	LRF-based	Outperforms spin image, SHOT, RoPS, TOLDI, LFSH
2021	KDD [53]	Point cloud	LRF-based	Outperforms FPFH, SHOT, RoPS and short time consuming
2022	VOID [75]	Point cloud	LRF-independent	Outperforms spin image, snapshots, FPFH, SHOT, RoPS, RCS
	Dual spin-image [54]	Point cloud	LRF-based	Outperforms spin image, snapshots, FPFH, SHOT
	RSPP [59]	Point cloud	LRF-based	Outperforms FPFH, SHOT, RCS, TOLDI
2023	LOVC [60]	Point cloud	LRF-based	Outperforms spin image, LoVS, RoPS, TOLDI
	BWPH [61]	Point cloud	LRF-based	Outperforms LoVS, RCS, TOLDI, WHI
	TPSH [46]	Point cloud	LRF-based	Outperforms spin image, FPFH, SHOT, RoPS, TOLDI
2024	RE-LSFH [77]	Point cloud	LRF-independent	Outperforms FPFH, LFSH
	FAPSH [70]	Point cloud	LRF-independent	Outperforms spin image, SHOT, RoPS, TOLDI, TriSI, LFSH, MaSH
	LSD [47]	Point cloud	LRF-based	Outperforms spin image, TOLDI, LoVS
	PDSH [48]	Point cloud	LRF-based	Outperforms FPFH, SHOT, RoPS, RCS, TOLDI, WHI
	3DFoNR [55]	Point cloud	LRF-based	High recognition rate, robust to occlusion and noise
	M-POE [76]	Point cloud	LRF-independent	Outperforms snapshots, FPFH, SHOT, RoPS, RCS, Dual-SI

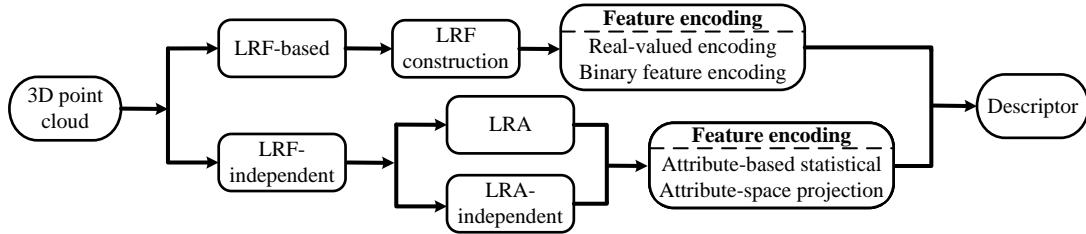


Fig. 5. Illustration of 3D local descriptor construction pipeline.

tion. In graph-theoretic frameworks, methods such as TEASER [88] and Segregator [114] use maximum cliques to prune outliers, with segregator incorporating semantic and geometric information. Lusk et al. [115] proposed CLIPPER, which relaxes combinatorial constraints for scalable and optimal solutions. Further extending these concepts, Li et al. [116] constructed an undirected graph to select preferred correspondences based on the maximum cliques of reliable edges. Qiao et al. [98] proposed G3Reg, which leverages geometric primitives and a pyramid compatibility graph to solve multiple maximum cliques. Rather than focusing solely on the maximum cliques, graph reliability outlier removal (GROR) [94] and supercore maximization and flexible thresholding (SUOFT) [97] employ reliability degrees and K-supercore concepts for robust consensus sets. Additionally, Zhang et al. [117] integrated graph signal processing to accelerate the speed of transformation estimation.

Despite these advancements, achieving optimal trade-offs between speed and accuracy remains challenging, par-

ticularly in complex scenes. Future work may focus on leveraging multi-order geometric consistency to improve robustness, accuracy, and efficiency.

(v) **Transformation estimation.** After correspondence optimization, the transformation aligning the point clouds is estimated, typically by generating candidate transformations through sampling correspondence subsets, which can be RANSAC- or 4PCS-based. Table 3 provides an overview of the performance for the transformation estimation methods.

1) **RANSAC-based methods.** Random sample consensus [81] (RANSAC) iteratively finds the parameters that fit the input data to a model while discarding outliers, as shown in Fig. 7. Over the years, many RANSAC variants have emerged, focusing on three main areas of improvement: sampling strategy, evaluation criteria, and local optimization.

Sampling Strategy: Several approaches aim to enhance the sampling process, especially when data is noisy or high-

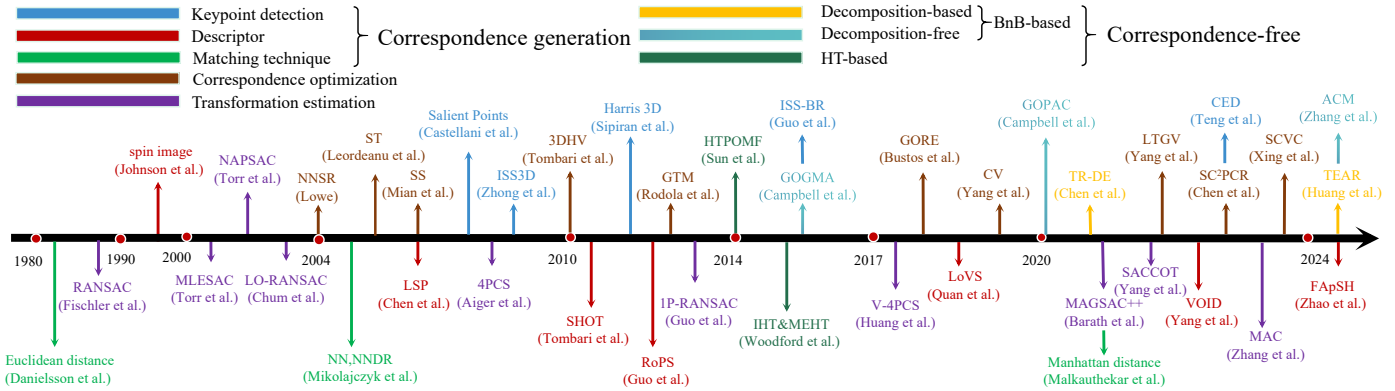


Fig. 6. Chronological overview of representative geometric 3D pairwise coarse registration methods.

TABLE 3

Comparative results of registration recall for geometric correspondence-based methods on U3M, 3DMatch, 3DLoMatch, KITTI, and ETH datasets. '-' indicates that the result is unavailable. 'Trans. Est.' and 'Corr. Opt.' refer to transformation estimation and correspondence optimization, respectively.

Year	Method	Category	U3M		3DMatch		3DLoMatch		KITTI		ETH	
			RMSE<5pr	SHOT	RE<15°	TE<0.3m	FPFH	FCGF	RE<15°	TE<0.3m	FPFH	FCGF
1981	RANASC [81]	Trans. Est.	20.77	-	64.20	88.42	-	-	74.41	98.02	-	73.33
2005	ST [82]	Corr. Opt.	-	-	55.88	86.57	-	-	-	-	-	-
2009	SAC-IA [64]	Trans. Est.	22.98	-	-	-	-	-	-	-	-	-
2016	FGR [83]	Corr. Opt.	46.77	-	40.91	78.93	5.09	-	5.23	89.54	-	18.76
2018	GORE [84]	Corr. Opt.	-	-	-	-	-	-	-	-	-	96.00
	GC-RANSAC [85]	Trans. Est.	-	-	67.65	92.05	17.01	-	48.62	78.38	73.69	85.33
2020	CG-SAC [86]	Trans. Est.	-	-	78.00	87.52	-	-	52.31	74.23	83.24	-
	MAGSAC++ [87]	Trans. Est.	-	-	-	-	-	-	-	-	-	54.67
2021	TEASER [88]	Corr. Opt.	-	-	75.48	85.77	35.15	-	46.76	91.17	94.96	-
2022	Practical $O(N^2)$ [89]	Corr. Opt.	-	-	-	-	-	-	-	-	-	100
	TriVoc [90]	Corr. Opt.	-	-	78.42	-	37.51	-	-	-	-	-
	SC ² -PCR [91]	Corr. Opt.	39.60	-	83.73	93.16	38.57	-	58.73	99.28	97.84	-
	SAC-COT [92]	Trans. Est.	48.19	-	-	-	-	-	-	-	-	-
	TR-DE [93]	Trans. Est.	-	-	-	86.99	-	-	50.4	99.10	98.20	-
2023	GROR [94]	Corr. Opt.	-	-	80.78	92.67	38.52	-	54.10	-	-	-
	MV [95]	Corr. Opt.	-	-	82.62	93.47	36.16	-	59.18	98.92	98.20	-
	MAC [96]	Trans. Est.	59.26	-	84.10	93.72	40.88	-	59.85	99.46	97.84	-
2024	SUCOFT [97]	Corr. Opt.	-	-	85.52	-	43.14	-	-	-	-	-
	G3Reg [98]	Corr. Opt.	-	-	-	-	-	-	99.46	-	-	-
	SCVC [99]	Corr. Opt.	-	-	89.44	94.43	-	-	61.30	99.80	100	-
	TEAR [100]	Trans. Est.	-	-	-	-	-	-	99.10	-	-	-
	HERE [101]	Trans. Est.	-	-	-	91.56	-	-	99.10	98.20	-	-

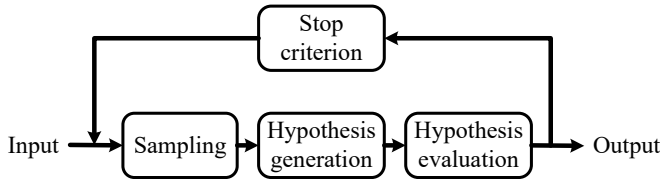


Fig. 7. The general pipeline of RANSAC-based methods for 6-DoF pose estimation.

dimensional. Torr et al. [118] proposed N adjacent points sample consensus (NAPSAC), which prioritizes adjacent points, assuming that inliers are closer together. Barath et al. [87] built on this with progressive neighborhood sampling and introduced progressive NAPSAC (P-NAPSAC). Chum and Matas [119] presented progressive sample consensus (PROSAC) that ranks correspondences to enhance the accuracy of match prediction. Following a similar idea,

Quan and Yang [86] proposed compatibility-guided sample consensus (CG-SAC) to reduce randomness by ranking correspondence pairs based on their compatibility scores. Ni et al. [120] introduced GroupSAC to optimize sampling with few inliers by focusing on promising groups. Yang et al. [92] presented sample consensus with compatibility triangles (SAC-COT) that leverages compatibility triangles (COTs) for generating accurate hypotheses. For more flexible constraints, Zhang et al. [96] introduced MAC, which relaxes the previous maximum consensus requirement by using maximal cliques, fully accounting for each local consensus to achieve accurate registration. While a rigid transformation typically requires at least three correspondences [121], some methods sample fewer. For instance, Guo et al. [122] proposed one point RANSAC (1P-RANSAC), which makes a single match with its corresponding LRF sufficient to estimate the pose transformation. Yang et al. [69] proposed 2-point based sample consensus with global constraint (2SAC-

GC), which samples two correspondences with associated local reference axes (LRAs). Alternatively, Li et al. [123] presented one-RANSAC, a method that estimates scaling and translation parameters using a single-point sample without feature information.

Evaluation Criteria: RANSAC variants also differ in the way in which they evaluate the quality of a candidate transformation. Torr et al. [124] proposed MLESAC, which employs a criterion that maximizes the likelihood rather than just the number of inliers. Chum and Matas [125] introduced optimal randomized RANSAC (R-RANSAC), which derives the optimality property through a modified sequential probability ratio test (SPRT). Rusu et al. [64] used the Huber penalty function for evaluation and proposed sample consensus initial alignment (SAC-IA). Addressing limitations in existing metrics, Yang et al. [126] proposed several metrics based on analyzing the contribution of inliers and outliers.

Local Optimization: The techniques in this area aim to refine the transformation by locally optimizing it. Chum et al. [127] proposed a locally optimized RANSAC (LO-RANSAC) to reduce the noise brought about by the minimum subset. Barath and Matas [85] introduced graph-cut RANSAC (GC-RANSAC), which applies graph-cut techniques to perform the local optimization step for more precise results.

Despite efforts to improve RANSAC, these methods often suffer from low efficiency and limited accuracy, especially in extremely low-inlier-ratio cases. Future research could focus on more robust methods to handle high-dimensional data and heavy outliers, while advancements in parallel processing and adaptive sampling could further boost RANSAC's speed and robustness.

2) **4PCS-based methods.** The four-point congruent set (4PCS) [128] method enhances registration robustness by using point sets with fixed affine ratios, sampling four coplanar points instead of random selections. Variants have been proposed to improve the efficiency: keypoint-based 4PCS (K-4PCS) [129] applies keypoint features to accelerate coplanar set matching, Super4PCS [130] considers angles and uses a 3D grid to limit search areas, and generalized 4PCS (G-4PCS) [131] extends to non-coplanar points. Combining both the advantages of Super4PCS and G-4PCS, Mohamad et al. [132] proposed super generalized 4PCS, which incorporates adaptive thresholding techniques and dynamic search space constraints. Building on Super4PCS, Huang et al. [133] incorporated volumetric information to further reduce computation time with a volumetric 4PCS (V-4PCS).

4PCS-based methods are limited by the high computational demands of identifying similar point sets and verifying transformations. Although improved variants offer faster, more accurate, and scalable registration, they still fail for real-time applications. Combining 4PCS with other correspondence optimization techniques could reduce the computational load.

3.1.2 Correspondence-free Methods

These methods perform pairwise coarse registration through optimal parameter search, eliminating the need for correspondence generation or further processing, as shown

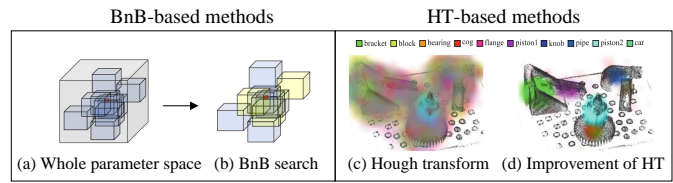


Fig. 8. Illustration of typical correspondence-free methods [134], [135].

in Fig. 8. Furthermore, correspondence-free methods can be broadly categorized into two types, i.e., Hough-transform-based (HT-based) and BnB-based.

(i) **HT-based methods.** The core idea of HT-based methods is to discretize the entire parameter space into a set of bins, subsequently selecting the bin with the highest accumulation of support from the given correspondences as the solution. Hough et al. [136] first introduced the concept of HT. Then Woodford et al. [134] introduced the intrinsic HT that reduces memory and computational requirements, and the minimum-entropy HT to improve precision and robustness, respectively. Sun et al. [137] proposed phase-only matched filtering (POMF) for the partially overlapped signal registration, which transforms the input scans into a Hough domain. However, these HT-based methods not only require significant memory and computational requirements, but also may fall into local optima. Consequently, such methods are not widely prevalent.

(ii) **BnB-based methods.** Instead of directly searching and voting as the HT-based methods, BnB-based methods recursively partition the parameter space into smaller branches, pruning those suboptimal solutions by assessing the bounds. However, the 6-DoF high-dimensional search space results in exponential time complexity. Depending on the specific acceleration techniques employed, these methods can be broadly classified into decomposition-based and decomposition-free ones.

1) **Decomposition-based methods.** They typically decompose the 6-DOF parameter space into multiple sub-problems, thereby accelerating the BnB process. Liu et al. [138] and Wang et al. [139] introduced a rotation invariant feature to decompose the transformation. However, the high non-linearity of 3-DoF rotation still limits the efficiency of BnB. Then, Chen et al. [140] proposed to decompose the 6-DoF parameter space into (2+1) and (1+2) DoF on rotation axis, an optimal solution is then obtained through a two-stage search strategy. Differently, Huang et al. [141] employed different strategies, which uses truncated entry-wise absolute residuals and heuristics-guided sampling [135] to decompose the 6-DoF problem into a set of sub-problems, respectively.

2) **Decomposition-free methods.** They typically utilize additional constraints to narrow the parameter search space, thereby accelerating the BnB process. Some methods [142], [143], [144], [145] achieve the optimal solution through the combination of BnB and existing technologies. For instance, Li et al. [143] reformulated the consensus set maximization problem as a mixed integer programming (MIP) problem, solving it via a tailored BnB method. Yang et al. [144] integrated the classic ICP method with the BnB method to solve global optimization problems. Campbell et al. [145]

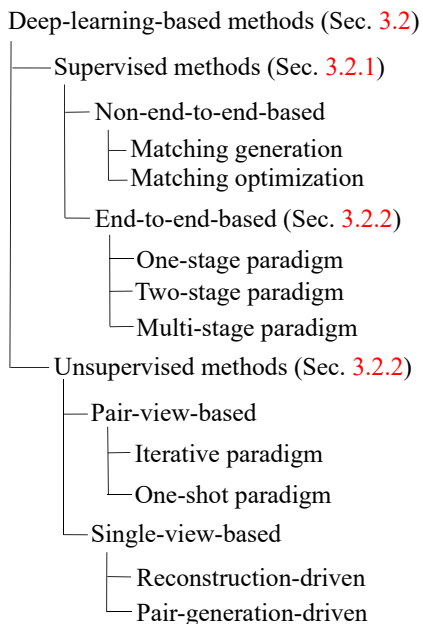


Fig. 9. Taxonomy of deep-learning-based 3D pairwise coarse registration methods.

presented the GOGMA method employing a BnB approach to solve the problem of 3D rigid Gaussian mixture alignment. In addition, some methods [146], [147], [148] aim to identify more novel and robust constraints. For instance, Olsson et al. [146] proposed a framework that utilizes various types of correspondences in conjunction with the BnB method to achieve an optimal solution for various pose and registration problems. Bustos et al. [147] introduced a novel bounding function using stereographic projections to precompute, and spatially indexed all possible point matches to solve the rotation problem. Recently, Zhang et al. [148] proposed a general technique performing a 1-DoF reduction of the space over which BnB is branching to accelerate deterministic consensus maximization. The remaining dimension is solved with an interval stabbing approach. Finally, some methods aim to address specific scenarios through the BnB method. Some BnB methods are also proposed to solve specific application problems. For instance, Cai et al. [149] presented a fast BnB approach with a polynomial-time subroutine for the 4-DOF scenario of terrestrial LiDAR scan pairs. Campbell et al. [150] employed the BnB approach to search the 6D space for camera pose and correspondence estimation, and the geometry of $SE(3)$ is used to find upper and lower bounds based on the number of inliers.

Finally, the performance of correspondence-free methods are shown in Table 4.

3.2 Deep-learning-based Methods

This section summarizes deep-learning-based pairwise coarse registration methods. The taxonomy, chronological overview, and performance comparison are shown in Fig. 9, Fig. 10 and Tab. 5.

3.2.1 Supervised Methods

Supervised learning methods for point cloud registration rely on various types of supervisory signals, such as ground-truth correspondences or transformation parameters, to train models effectively [2]. Based on the learning paradigm, the related methods can be divided into non-end-to-end-based and end-to-end-based. The former category focuses on specific stages, such as matching generation or matching optimization, while the latter models the entire point cloud registration process within a single deep learning network.

(i) **Non-end-to-end-based methods.** These methods typically focus on specific aspects of point cloud registration, such as feature extraction, correspondence searching, and outlier removal. They can be broadly divided into two categories: matching generation and matching optimization.

1) **Matching generation paradigm.** In this paradigm, the feature extraction network plays a crucial role, which is used to construct the local descriptor for matching keypoints. Similarly to traditional approaches, some methods adopt a patch-wise network that takes local patches as input and outputs descriptors. Typically, a patch-wise network requires a manual method to transform the input local patch into a rotation-invariant space before feature extraction. For instance, some approaches [189] [151] have enhanced feature compression capabilities by processing high-dimensional hand-crafted descriptors into compact, low-dimensional representations. Some other methods [16] [190] [155] utilize LRFs to extract features in a canonical pose. More recent proposals [157] [191] [192] employ rotation-equivalent networks to directly extract features from raw point clouds or voxels without relying on pre-processing.

Although patch-wise networks are effective, their fixed receptive fields can lead to the loss of high-level semantic information. To address this, some works [154] [166] [170] shift to the construction of point-wise descriptors from the entire point cloud as input. However, these methods often bypass the keypoint detection step, and instead randomly sample points for feature description. Such randomness may result in descriptors from non-salient regions, introducing noise into later matching steps. To address this problem, other approaches [193] [194] [19] [195] [169] integrate keypoint detection and descriptor extraction into a unified framework. These methods jointly predict salient scores and descriptors for all points, and then according to the scores of keypoints, using top-scored points to generate feature correspondences.

2) **Matching optimization paradigm.** In this paradigm, researchers always focus on learning an accurate transformation from input noisy feature correspondences. For instance, Pais et al. [196] designed a classification backbone to classify inlier correspondences from the initial matching, followed by [197] [158]. Lee et al. [198] and Jiang et al. [199] introduced deep learning voting methods to improve outlier rejection. Guo et al. [200] introduced a second-order consistency into the feature space. Yan et al. [183] combined a semantic segmentation network to establish multi-level semantic consistency of filtered correspondences. For robust pose estimation, Gao et al. [201] designed a lightweight learning-based pose evaluator to enhance the accuracy of pose selection in low-overlap scenarios.

TABLE 4
Performance summary of representative correspondence-free 3D pairwise coarse registration methods.

Year	Method	Data Type	Category	Performance
1962	HT [136]	Points	HT	Proposes the Hough transform
2007	box-and-ball [142]	Point cloud	BnB	Improvement of BnB using octree
2008	VTPR [146]	Point cloud	BnB	Solution with cross-type correspondences
2009	BnBMIP [143]	Points	BnB	Outperforms RANSAC
2014	bnb-M-circ [147]	Point cloud	BnB	Solve for rotation matrix only
	IHT&MEHT [134]	CAD models	HT	Improvements in memory requirements and accuracy
	HTPOMF [137]	Point cloud	HT	Outperforms ICP
2016	Go-ICP [144]	Point cloud	BnB	Suitable for applications with low real-time requirements
	GOGMA [145]	Point cloud	BnB	Outperforms Go-ICP
2018	GoTS [138]	Point cloud	BnB	Outperforms Go-ICP
2020	GOPAC [150]	CAD models	BnB	Need GPU implementation reducing runtime
2021	GPETD [139]	2D/3D data	BnB	Outperforms GOPAC
2022	TR-DE [140]	Point cloud	BnB	Outperforms PointDSC
2024	TEAR [141]	Point cloud	BnB	Suitable for large-scale point pairs
	HERE [135]	Point cloud	BnB	Competitive performance with rapid speed
	ACM [148]	Point cloud	BnB	A general strategy to speed up the BnB technique

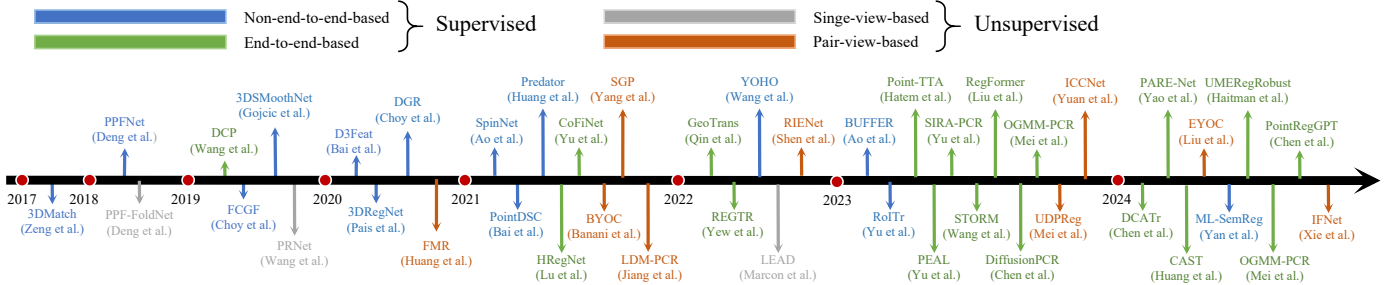


Fig. 10. Chronological overview of deep-learning-based 3D pairwise coarse registration methods.

(ii) **End-to-end-based methods.** In these methods, each stage of traditional point cloud registration is represented by distinct modules within the network, enabling it to directly output the estimated transformation. This structure better leverages the potential of deep learning technology. These methods can be roughly divided into one-stage, two-stage, and multi-stage paradigms.

1) **One-stage paradigm.** In the early stage of end-to-end point cloud registration, most methods only search the matching relationship between point clouds once or directly estimate the transformation from the input pair. For end-to-end methods that perform a single matching search, improvements have been made in areas such as feature extraction and matching optimization. For example, some approaches introduce handcrafted descriptors to enhance feature discrimination [202], while others incorporate feature interactions between point cloud pairs to improve distinctiveness and matching reliability [203] [204] [205]. Some other works [206] [175] [207] [208] directly predict overlap regions or estimated overlap scores for points to enhance the search for correspondences. To improve the reproducibility of matching points, a few works directly predict the coordinates of corresponding points for transformation estimation [209] [210]. To enhance the inlier selection process, Zhang et al. [211] and Chen et al. [212] optimized the matching matrix to increase the confidence of inlier correspondences. Other one-stage methods estimate trans-

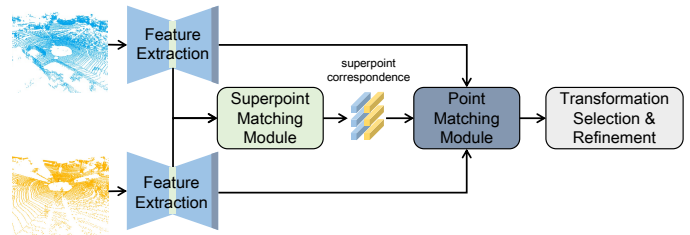


Fig. 11. The general framework for two-stage paradigm in supervised 3D pairwise coarse registration methods.

formations directly based on features. For instance, Deng et al. [213] utilized FoldingNet [214] to learn rotation-invariant and rotation-aware descriptors, which were used to search for correspondences and estimate the transformation in feature space. Subsequently, Chen et al. [215] and Jiang et al. [216] decoupled the transformation to achieve a more reliable transformation estimation.

2) **Two-stage paradigm.** The two-stage paradigm often leverages a coarse-to-fine mechanism, whose superiority has been demonstrated in image matching tasks [217]. As shown in Fig. 11, these methods typically downsample the input point clouds into superpoints, match them to obtain coarse correspondences, and then propagate these correspondences to individual points based on neighborhood relationships. They finally yield dense point correspondences.

TABLE 5

Performance comparison of deep-learning-based pairwise coarse registration methods across various datasets. ‘-’ indicates that the result is unavailable. ‘w’ in the ‘Sup.’ column indicates a supervised method, while ‘w/o’ represents unsupervised. ‘**’ signifies omitted digits.

Year	Method	Sup.	3DMatch			3DLoMatch			KITTI			ModelNet40-unseen instance				ModelNet40-unseen category			
			FMR (%)	IR (%)	RR (%)	FMR (%)	IR (%)	RR (%)	RTE (cm)	RRE (°)	RR (%)	RMSE (R)	RMSE (t)	MAE (R)	MAE (t)	RMSE (R)	RMSE (t)	MAE (R)	MAE (t)
2017	3DMatch [16]	w	59.6	-	67	-	-	-	-	-	-	-	-	-	-	-	-	-	
2018	PPFNet [151]	w	62.3	-	71	-	-	-	-	-	-	-	-	-	-	-	-	-	
	PPF-FoldNet [152]	w/o	71.82	-	-	-	-	-	-	-	-	-	-	-	-	-	-	-	
2020	DCP [153]	w	95.2	56.9	87.3	76.6	21.4	40.1	4.881	0.17	97.83	1.143385	0.001786	0.770573	0.001195	3.150191	0.005039	2.00721	0.003703
	3DSmoothNet [155]	w	94.7	37.7	80.3	63.6	11.4	33	-	-	-	-	-	-	-	-	-	-	
	PRNet [156]	w/o	-	-	-	-	-	-	-	-	-	3.199257	0.016	1.454	0.0003	3.953	0.017	1.712	0.011
	SpinNet [157]	w	97.6	47.5	88.6	75.3	20.5	59.8	9.88	0.47	99.1	-	-	-	-	-	-	-	
2021	PointDSC [158]	w	-	86.54	93.28	-	-	-	8.13	0.35	98.2	-	-	-	-	-	-	-	
	Predator [19]	w	96.6	49.9	88.3	71.7	20	54.2	6.8	0.27	99.8	-	-	-	-	-	-	-	
	HRegNet [159]	w	-	-	93.2	-	-	-	4.7	0.147	100	-	-	-	-	-	-	-	
	CoFiNet [160]	w	98.1	49.8	89.3	83.1	24.4	67.5	8.5	0.41	99.8	-	-	-	-	-	-	-	
	BYOC [161]	w/o	78.6	-	-	-	-	-	-	-	-	-	-	-	-	-	-	-	
	SGP [162]	w/o	-	-	91.4	-	-	-	-	-	-	-	-	-	-	-	-	-	
	LDM-PCR [163]	w/o	-	-	-	-	-	-	-	-	-	-	-	-	-	-	-	-	
	GeoTransformer [164]	w	97.9	71.9	92	88.3	43.5	75	7.4	0.27	99.8	3.0178	0.0028	0.2779	0.00036	-	-	-	
2022	REGTR [165]	w	-	-	92	-	-	64.8	-	-	-	-	-	-	-	-	-	-	
	YOHO [166]	w	98.2	64.4	90.8	79.4	25.9	65.2	-	-	-	-	-	-	-	-	-		
	RIENet [167]	w/o	-	-	-	-	-	-	-	-	-	0.0033	0.0000*	-	0.0059	0.0000*	-		
	LEAD [168]	w/o	95.84	-	-	-	-	-	-	-	-	-	-	-	-	-	-		
2023	BUFFER [169]	w	-	-	92.9	-	-	71.8	5.37	0.22	97.66	-	-	-	-	-	-		
	RoTr [170]	w	98	82.6	91.9	89.6	54.3	74.8	-	-	-	-	-	-	-	-	-		
	Point-TTA [171]	w	-	-	93.47	-	-	57.81	-	-	-	-	-	-	-	-	-		
	PEAL [172]	w	99	72.4	94.6	91.7	45	81.7	-	-	-	-	-	-	-	-	-		
	SIRA-PCR [173]	w	98.2	70.8	93.6	88.8	43.3	73.5	-	-	-	-	-	-	-	-	-		
	RegFormer [174]	w	-	-	-	-	-	-	8.4	0.24	99.8	-	-	-	-	-	-		
	STORM [175]	w	-	-	-	-	-	-	2.27	0.7	88.6	-	-	-	-	-	-		
	OGMM-PCR [176]	w	-	-	-	-	-	-	-	-	-	0.5892	0.0079	-	0.6309	0.0055	-		
	DiffusionPCR [177]	w	98.3	75	94.4	86.3	49.7	80	6.3	0.23	99.8	-	-	-	-	-	-		
	UDPReg [178]	w/o	-	-	91.4	-	-	64.3	-	-	-	-	-	-	-	-	-		
	ICCNNet [179]	w/o	-	-	-	-	-	-	-	-	-	0.0012	0.0000*	-	0.0022	0.0000*	-		
2024	DCATr [180]	w	98.1	76.5	92.6	87.4	48.4	76.8	6.6	0.22	99.7	-	-	-	-	-	-		
	PARE-Net [181]	w	98.5	76.9	95	88.3	47.5	80.5	4.9	0.23	99.8	-	-	-	-	-	-		
	CAST [182]	w	-	-	95.2	-	-	75.1	2.5	0.27	100	-	-	-	-	-	-		
	ML-SemReg [183]	w	-	-	93.4	-	-	5.2	0.2	98.1	-	-	-	-	-	-	-		
	UMERegRobust [184]	w	-	-	93.4	-	-	-	-	-	-	-	-	-	-	-	-		
	PointRegPT [185]	w	98.7	71.9	93.3	89.4	45.6	77.2	-	-	-	-	-	-	-	-	-		
	EYOC [186]	w/o	-	-	-	-	-	-	-	-	99.5	-	-	-	-	-	-		
	RKHS-PCR [187]	w/o	-	-	-	-	-	-	-	-	-	0.02	-	-	-	-	-		
IFNet [188]	w/o	-	-	-	-	-	-	-	-	-	0.0016	0.0000*	0.0007	0.0000*	0.0013	0.0000*	0.0006	0.0000*	

To our knowledge, CoFiNet [160] is the first to introduce this mechanism into point cloud registration, paving the way for subsequent developments. For the coarse-to-fine methods, the superpoint matching accuracy directly determines the final registration performance. Consequently, most methods focus on improving the inlier ratio of coarse correspondences. For instance, GeoTransformer [164] leverage geometric relationships to enhance the discriminative ability of superpoints, with a set of follow-up works in optimizing superpoint matching [218] [219] [182]. Other works [172] [220] [221], such as PEAL [172], incorporated explicit overlap region recognition to more effectively identify inlier correspondences. DCATr [180] introduces progressive update mechanisms to improve the spatial consistency of coarse correspondences. PosDiffNet [222], HRegNet [159] and Regformer [174] introduce multi-level correspondences to improve the inlier ratio of the coarse matching stage.

In recent years, the two-stage paradigm has been enriched by deep learning innovations from other domains. Chen et al. [173] applied transfer learning to enable generalization from synthetic to real-world scenarios. Hatem et al. [171] proposed a test-time adaptation framework with three self-supervised auxiliary tasks. Yao et al. [181] and Pertigkiozoglou et al. [223] incorporated rotation-equivariant networks to improve registration performance. Chen et al. [185] introduced generative models in data augmentation, creating various input pairs to improve training.

3) **Multi-stage paradigm.** Inspired by iterative closest point (ICP), the multi-stage paradigm registers point cloud pairs iteratively, where each iteration constitutes a forward pass of the network. After each pass, the input pairs are aligned using the estimated transformation, which acts as input for the next iteration as well.

Some methods focus on feature-based matching refinement. Wang et al. [153] and Yew et al. [224] utilized soft

matching matrices to estimate transformations, iteratively generating weighted correspondences. Diffusion models have been employed by Jiang et al. [225] and Chen et al. [177], formulating registration as a denoising process to progressively refine transformations.

Some other approaches focus on enhancing feature representations. Wu et al. [226] employed multi-level feature interactions to boost the discriminative power of learned features. Li et al. [227] proposed a semantic-aware scoring model to leverage both semantic and geometric information, highlighting regions of interest for better registration outcomes. Fu et al. [228] extended this by incorporating deep graph matching and embedding high-order geometric relationships to improve robustness against noise and outliers.

A different line of work bypasses intermediate matching and estimates transformations directly in the feature space. For instance, Aoki et al. [229] and Li et al. [230] combined the Lucas & Kanade algorithm with global feature differences for iterative alignment. Mei et al. [176] introduced probabilistic registration using Gaussian mixture models (GMMs), while FINet [231] designed a dual-branch framework for the direct regression of translation and rotation.

3.2.2 Unsupervised Methods

The supervised methods mentioned above have shown impressive performance. However, most of their success mainly depends on large amounts of ground-truth transformations between the input pairs, which significantly increases their training costs. Furthermore, obtaining accurate transformation labels can be challenging, due to sensor errors or the reliance on traditional SfM pipelines without convergence guarantees [232]. To avoid this, recent efforts have been focused on developing unsupervised registration networks. Based on the input type, unsupervised methods can be roughly divided into two categories: pair-view-based and single-view-based.

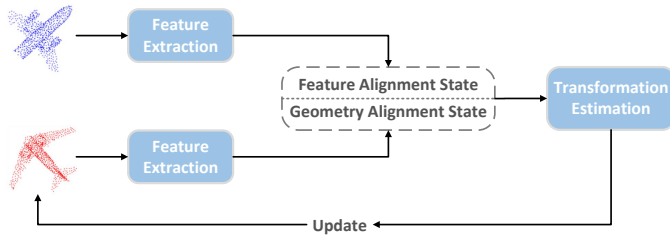


Fig. 12. The general framework for iterative paradigm in unsupervised 3D pairwise coarse registration methods.

(i) **Pair-view-based.** These methods always train the network with the pairs of point clouds and design the loss function without ground truth information. We can categorize them into two paradigms for discussion, i.e., iterative and one-shot paradigms.

1) **Iterative paradigm.** these methods are similar to the multi-stage paradigm commonly employed in supervised methods, which perform point cloud registration iteratively during both the training and inference phases. Furthermore, two strategies, i.e., feature alignment and geometric alignment, to align input pairs, as illustrated in Fig. 12.

In the feature alignment strategy, researchers [233] [234] [163] [235] typically estimate rigid transformations based on the feature projection error. These methods emphasize that the extracted feature needs to be related to the rigid pose of the input. For example, Huang et al. [233] designed an auto-encoder framework to extract geometry and transformation information, which was later followed by [234] and [163]. Yuan et al. [235] further maximized multi-hierarchical mutual information in the feature extraction module to obtain discriminative and less redundant representation. Zhang et al. [187] directly leveraged SE(3)-equivariant features for direct feature space registration.

The geometric alignment strategy, on the contrary, requires obtaining point-level correspondences to estimate the transformation using the SVD algorithm. For instance, Jiang et al. [236] introduced soft correspondences to generate pseudo-targets and incorporated the geometric alignment error into the loss function. Building on this, Shen et al. [167] proposed local neighborhood consensus and spatial consistency in pseudo-target generation and loss function definition to improve the ratio of inlier correspondences, followed by [237] [179] [238]. Jiang et al. [239] and Zheng et al. [240] combined the feature interaction mechanism between the input pairs for inlier correspondence identification. To improve efficiency, Xie et al. [188] built on a series of registration blocks. These blocks are cascaded and unfolded recurrently over time to achieve a balance between efficiency and accuracy. Meanwhile, Nie et al. [241] performed transformation estimation within a minimal set of correspondences. The iterative paradigm typically yields more precise registration results but demands greater computational resources, which is why most methods focus on object point cloud datasets.

2) **One-shot paradigm.** Unlike the iterative paradigm, this paradigm typically registers the input pair only in a one-shot manner. Consequently, these methods always focus on mining prior information or generating pseudo-labels from unlabeled data during the training process, in or-

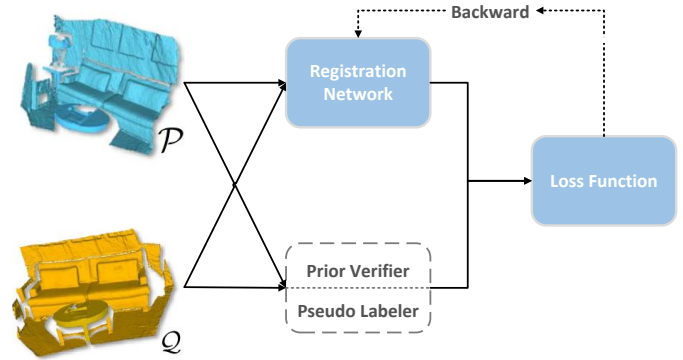


Fig. 13. The general framework for one-shot paradigm in unsupervised 3D pairwise coarse registration methods.

der to improve registration performance. This is illustrated in Fig. 13.

For pseudo-label, Yang et al. [162] and Lowens et al. [242] proposed a teacher-student framework, where the teacher module generates point-wise correspondences as pseudo-label. These labels are then filtered by a verifier to remove low-confidence correspondences before the student module training stage. Liu et al. [186] further extended this framework to distant point cloud registration in a progressive manner.

For prior information, some researchers choose to mine geometric priors. For instance, Kadam et al. [243] introduced LRF to capture transformation-invariant information and constructed matching correspondences at multiple scales based on their PointHop [244] framework. Zhang et al. [245] trained their network to align the input pair with a canonical pose. Li et al. [246] combined the orthogonality and cycle consistency of rigid transformation to guide network training. Huang et al. [247] and Mei et al. [178] utilized GMMs to model the local geometry for evaluating the quality of the registration in the loss function. Other researchers introduce semantic information, such as shape prior and color information. For instance, Hao et al. [248] and Li et al. [249] obtained the shape prior by part segmentation and shape completion for enhancing object point cloud registration performance. Banani et al. [161] [250] combined RGB-D information to assist in training their indoor point cloud registration network. Compared to the iterative paradigm, the one-shot paradigm is more flexible and better suited for diverse and complex datasets. In recent years, Liu et al. [251] extended the one-shot paradigm to large-scale LiDAR point cloud datasets.

(ii) **Single-view-based:** These methods aim to train their networks using only one point cloud as input, which eliminates the need for “paired data” and significantly reduces the difficulty of data acquisition. Based on the difference in their training strategies, these methods can be broadly categorized as reconstruction-driven and pair-generation-driven.

1) **Reconstruction-driven.** These methods usually design an auto-encoder framework to reconstruct the input data, thereby learning a compact representation of the input. For example, Deng et al. [152] developed PPF-FoldNet based on PPFNet [151] and FoldingNet [214]. This approach employs

an encoder-decoder framework, where the encoder takes the PPF representation [252] of local patches as input. With the same folding-based auto-encoder framework, Marcon et al. [168] employed spherical CNNs as the encoder to directly extract rotation-equivalent local descriptors from the original local patches of key points, ensuring the completeness of the input information.

2) **Pair-generation-driven.** These methods train the registration network by generating appropriate registration pairs from single-view inputs. For instance, Sun et al. [253] generated the registration pair by applying a random rigid transformation to the input point cloud. Wang et al. [156] simulated partial overlap scenario through random sampling. However, due to the wide variety of noise, partial overlap, and occlusion in real-world scenarios, the pair-generation paradigm struggles to produce a large number of point cloud pairs for registration under diverse conditions. In recent years, a few works [254] [185] [181] incorporate pair generation into their data augmentation pipelines to expand the dataset size for supervised learning.

3.3 Summary

We outline the development and characteristics of pairwise coarse registration methods in 3D point cloud registration as follows.

1) **Correspondence-based geometric methods.** More research attention has been shifted to correspondence optimization and transformation estimation in recent years, compared to that of geometric local feature detectors and descriptors. It is still challenging for existing methods to handle low-inlier ratio problems.

2) **Correspondence-free geometric methods.** These methods typically solve the optimal maximum consensus solution through parameter search. However, the 6-DoF high-dimensional search space results in exponential time complexity. Therefore, the BnB-based methods have increasingly popular owing to their globally optimal solution and effectiveness.

3) **Learning-based methods.** Most existing researches toward this line are supervised, achieving great accuracy improvement. However, improving the generalization ability and fostering unsupervised methods deserve further research.

4 PAIRWISE FINE REGISTRATION

Pairwise fine registration aims to precisely align two point clouds by refining transformations to minimize residual errors. The key methods are based either on ICP or GMMs. This section reviews the main methodologies for pairwise fine registration. The taxonomy, chronological overview, and performance comparison are shown in Fig. 14, Fig. 15 and Table. 6, respectively.

4.1 ICP-based Methods

ICP is first proposed by Besl and McKay [255]. It aligns point clouds by iterating between finding matching points and minimizing errors, as illustrated in Fig. 16. While the standard ICP offers a simple and effective framework, it faces challenges due to its sensitivity to noise, outliers, and the

Pairwise fine registration (Sec. 4)

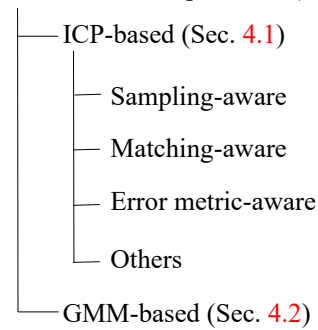


Fig. 14. Taxonomy of 3D pairwise fine registration methods.

need for good initial alignment. Subsequent improvements attempt to address these issues from different perspectives.

Sampling-aware. In the early stages of ICP development, researchers seek to optimize point selection strategies. Turk and Levoy [271] incorporated uniform sampling, and Masuda and Yokoya [272] suggested random sampling. Both sampling methods accelerated the registration process while maintaining registration accuracy. As ICP evolves, sampling-aware methods focus on keypoints selection to reduce erroneous correspondences in the matching stage, such as normal-space sampling [257] and local-geometric-feature-based sampling in [270].

Matching-aware. Improving the matching module of ICP can effectively enhance robustness against noise and outliers as well as accelerate the registration process. In terms of accelerating the matching process, Benjema and Schmitt [273] introduced the multi-z-buffer technique, which optimizes the nearest neighbor search by segmenting 3D space. Men et al. [262] accelerated matching by incorporating hue-based color information, while color-supported GICP [264] introduces color space data to improve matching accuracy and reduce computational load. Some studies focus on enhancing robustness. For example, a statistical method based on distance distribution has been used to improve matching robustness [274]. GICP [260] combines a probabilistic framework with planar structure of scans to enhance correspondences. Additionally, GFOICP [270] introduces a distance threshold that gradually shrinks with iterations during matching, and TrICP [259] incorporates the least trimmed squares method. Both methods enhance the robustness of the ICP method by eliminating incorrect correspondences.

Error-metric-aware. For ICP methods, the error metric is crucial to determine the alignment quality between two point clouds. A well-designed error metric ensures accurate convergence, reduces misalignment, and handles errors caused by noise or incomplete data.

One solution is to reduce the impact of incorrect point pairs by assigning different weights, as done in Generalized ICP [260], Sparse ICP [263] and Robust ICP [275]. For instance, robust ICP uses the Welsch function to minimize the influence of outliers while maintaining accuracy even in the presence of noise and partial overlap. Another solution involves modifying the error metric to expand the convergence basin or accelerate convergence, as done in methods such as LM-ICP [258], AA-ICP [266], and sym-

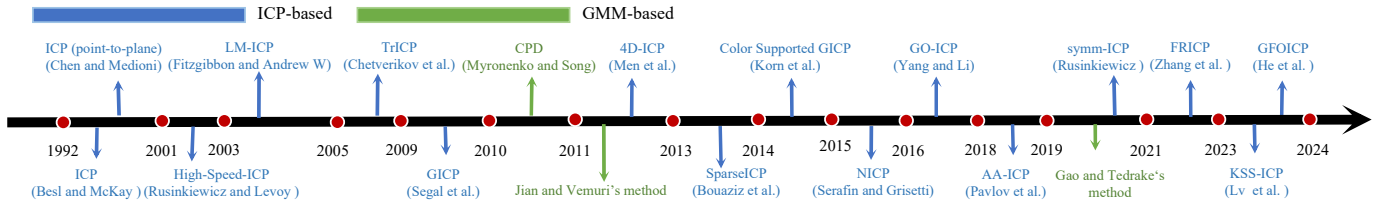


Fig. 15. Chronological overview of representative 3D pairwise fine registration methods.

TABLE 6
Performance summary of typical 3D pairwise fine registration methods.

Year	Method	Data type	Category	Performance
1992	ICP (PTP) [255]	Point cloud	ICP-based	Basic method of ICP
	ICP (PTL) [256]	Range images & Point cloud	Error metric	Basic method of ICP
2001	High-Speed-ICP [257]	Range images & Point cloud	Sampling	High efficiency
2003	LM-ICP [258]	2D/3D Point cloud	Error metric	Outperforms ICP
2005	TrICP [259]	2D/3D Point cloud	Matching	Applicable to cases with low overlap
2009	GICP [260]	Point cloud	Matching & Error metric	More robust than ICP
2010	CPD [261]	Point cloud	GMM-based	Robust to noise, outliers
2011	4D-ICP [262]	Point cloud	Matching	High efficiency
2013	SparseICP [263]	Point cloud	Error metric	Robust to outliers, incomplete data
2014	Color GICP [264]	Point cloud	Matching	More robust than GICP
2015	NICIP [265]	Point cloud	Error metric	Outperforms GICP
2016	GO-ICP [144]	Point cloud	Others	Robust to initial estimation & High efficiency
2018	AA-ICP [266]	Point cloud	Error metric	High efficiency
2019	Symmetric-ICP [267]	Point cloud	Error metric	Outperforms ICP
2021	FRICP [268]	Point cloud	Error metric	Outperforms SparseICP
2023	KSS-ICP [269]	Point cloud	Others	Robust to similarity transformations
	GFOICP [270]	Point cloud	Sampling & Error metric	Robust to noise & Outperforms AA-ICP, ICP

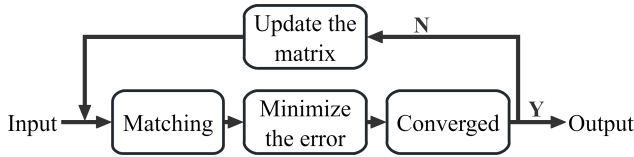


Fig. 16. The general pipeline of ICP methods.

metric ICP [267]. LM-ICP and symmetric ICP enhance the registration robustness and accelerate convergence when dealing with smooth and noisy datasets, while AA-ICP leverages historical data to accelerate registration without sacrificing accuracy.

Several methods try to incorporate geometric information into the error metric to improve ICP. For instance, point-to-plane ICP [256] utilizes the normal information of point clouds to refine the error metric from point-to-point distance to point-to-plane distance. NICIP [265] and GFOICP [270] incorporate normal vectors and curvature information into the error metric, respectively.

Others. The following methods expand on the traditional ICP method, offering broader solutions to overcome specific limitations. Go-ICP [144] uses branch-and-bound global optimization within ICP, allowing globally optimal registration throughout the entire SE(3) space, helping to avoid local minima. KSS-ICP [269] leverages Kendall shape space (KSS) to remove translation, rotation, and scaling effects, making it robust for registering point clouds with non-uniform density and noise while preserving shape invariance.

4.2 GMM-based Methods

Different to ICPs that rely on deterministic point correspondences, GMM models point sets as probabilistic distributions, framing registration as an optimization of alignment between these distributions. Specifically, GMM methods generally employ the Expectation-Maximization (EM) framework, where the E step estimates probabilistic correspondences, and the M step optimizes transformation parameters by maximizing the expected log-likelihood. This iterative process enables GMM methods to excel in handling noisy or incomplete data, sometimes offering greater flexibility and robustness compared to ICP.

Jian and Vemuri [276], [277] first introduced a method that minimizes the L_2 distance between two GMMs, achieving robust registration in the presence of noise and outliers. The coherent point drift (CPD) method [261] performs registration by maximizing the likelihood function, which replaces the L_2 norm with the KL divergence. Although these methods provide good robustness, they are generally much slower than ICP and almost incapable of scaling to large-scale point clouds, significantly limiting their practicality. To address this issue, Gao and Tedrake [278] proposed Filter-Reg, which incorporates Gaussian filters into the EM framework, reducing computational cost and enabling faster and more robust registration of large-scale point clouds while maintaining accuracy and robustness.

4.3 Summary

The following points can be found.

- 1) **ICP remains a standard paradigm.** ICP methods have formed a standard paradigm for 3D pairwise fine regis-

tration. GMM methods are less popular due to their high computational complexity and sensitivity to parameters.

2) **Geometric methods are dominating.** It is interesting that deep learning methods are rare in this area, potentially due to the difficulties in ultra-accurate error prediction.

5 MULTI-VIEW COARSE REGISTRATION

The task of multi-view coarse registration involves aligning multiple point cloud views, captured from different perspectives, into a unified coordinate system using pairwise registration as a foundation. Compared to pairwise registration, multi-view registration presents additional challenges, such as estimating multiple transformations while addressing cumulative errors and computational overhead. The chronological overview, and performance comparison are shown in Fig. 17 and Table 7, respectively.

5.1 Geometric Methods

Geometric methods utilize the intrinsic geometric properties of 3D data to establish correspondence between different views. Based on how these methods construct point cloud topological structures, multi-view point cloud coarse registration geometric methods can be categorized into spanning-tree-based and the others.

Spanning-tree-based. These methods establish connections through pairwise point cloud registration relationships, unifying the point clouds from different views into the same coordinate system. This is achieved by estimating the relative transformations between nodes to perform the overall registration.

Some methods [4], [279], [280], [281] follow a common pipeline, i.e., constructing a spanning tree by exhaustively registering all point cloud pairs. Specifically, they perform pairwise registration for all point clouds, establish connections for successful registrations to form a connected graph, calculate the spanning tree of the model graph, and finally align the nodes in each connected component using the corresponding transformations. Although these methods can achieve accurate results, their exhaustive nature makes them computationally expensive. To address this issue, several improvements have been proposed. Some approaches involve selecting a set of root nodes based on reliable pairwise registration results and iteratively match them with remaining point clouds [79], [282], [283], [284], [285]. Other methods impose additional constraints on the construction process to reduce the number of pairwise registrations. For example, Zhu et al. [286] employed the overlap rate between point clouds as a basis to judge whether a set of point clouds should be registered with each other. Mian et al. [5] and Cheng et al. [287] performed graph optimization and constructed a multi-level spanning tree hypergraph and a sparse scan graph for acceleration, respectively.

Others. Some methods are based on the perspective of shape enhancement. Guo et al. [288] initialized the seed shape by selecting the view, updated the seed shape sequentially through pairwise registration, and iteratively registered all input views during the shape growth process. Zhu et al. [289] employed reliable pairwise registration results to enhance the model shape. There are also some optimization-based methods. Huang et al. [290] and Choi et al. [291]

both modeled the relative relationships between views as a graph. The former uses a greedy method to iteratively select matching edges with high consistency, merging subgraphs until all views are globally matched. By contrast, the latter uses a global optimization strategy based on line processes to identify and eliminate incorrect pairwise alignments, ultimately achieves a global consistency. In addition, Zhou et al. [83] aligned multiple partially overlapping 3D surfaces by directly optimizing a global objective function.

5.2 Learning-based Methods

Compared to traditional geometric approaches, learning-based registration methods offer significantly improved computational efficiency while maintaining high registration accuracy. These methods leverage deep neural networks to learn more advanced and robust features, enhancing their effectiveness in diverse scenarios. Based on their implementation strategies, learning-based multi-view point cloud registration methods can be broadly categorized into two types: two-stage and end-to-end.

Two-stage. These methods perform multi-view 3D registration with two steps or networks comprising two key modules. For the former methods, they generally follow a coarse-to-fine fashion [296], [297], [299]. For instance, Wang et al. [296] designed a novel history reweighting function to update the edge weights in the pose graph and employed an iterative reweighted least squares (IRLS) scheme to optimize the residual error. Jin et al. [299] optimized the pairwise correlation matrices using a diffusion-based procedure, jointly optimizing point cloud rotation and position. Zhao et al. [297] constructed a minimum spanning tree by calculating the prediction overlap confidence and leveraged a Lie algebra-based method to optimize the residual error. For the latter methods, they typically involve two sub-networks [293], [298]. DeepMapping [293], the first unsupervised method, proposes an L-Net to estimate the pose of the input point cloud, and an M-Net to model the scene structure. It serves the LiDAR mapping problem as a binary classification problem. To cope with large-scale data, DeepMapping2 [298], proposes a place-recognition-based batch organization module to get initial poses, and then introduces a learning-based optimization module for error minimization.

End-to-end. There are still only a few end-to-end methods. As a pioneering work, Huang et al. [292] proposed a synchronization method that alternates between transform synchronization and using an iterative neural network. Gojic et al. [294] jointly learned initial pairwise alignment and global consistency refinement to improve the robustness of multi-view registration. Yew et al. [295] proposed a graph neural network to learn transformation synchronization and iteratively refined the absolute pose throughout the optimization process. To foster information interaction, Hu et al. [300] recently proposed FeatSync that allows information exchange between different stages, achieving better synchronization result.

5.3 Summary

The following points can be summarized.

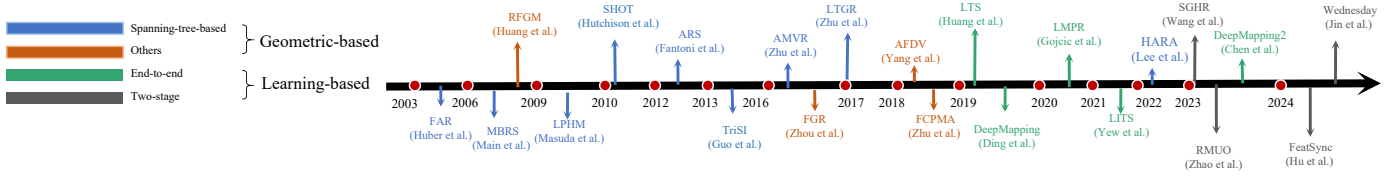


Fig. 17. Chronological overview of representative 3D multi-view coarse registration methods.

TABLE 7
Performance summary of typical 3D multi-view coarse registration methods.

Year	Method	Data Type	Category	Performance
2003	FAR [279]	Range image	Geometric	Sensitive to high symmetry
2006	MBRS [5]	Mesh	Geometric	Robust to noise
	RFGM [290]	Mesh	Geometric	Robust to matching features of different sizes
2009	LPHM [281]	Range images	Geometric	Comparable performance to spin image
2010	SHOT [280]	Mesh	Geometric	Outperforms SI, EM, PS
2012	ARS [284]	Point cloud	Geometric	Robust to noise
2013	TriSI [79]	Range image	Geometric	Outperforms SHOT, Spin image, robust to varying mesh resolutions
2016	AMVR [282]	Point cloud	Geometric	Outperforms robust to scan orders
	FGR [83]	Point cloud	Geometric	Robust to noise and fast in calculation
2017	LTGR [286]	Mesh	Geometric	Outperforms TriSI
2018	AFDV [285]	Point cloud	Geometric	Robust to data modal changes
	FCPMA [289]	Point cloud	Geometric	Speed up correspondence propagation
2019	LTS [292]	Point cloud	Learning	Outperforms the state-of-the-art transform synchronization techniques on ScanNet and Redwood
	DeepMapping [293]	Point cloud	Learning	Outperform in scene data
2020	LMPR [294]	Point cloud	Learning	Outperforms FGR
2021	LITS [295]	Point cloud	Learning	Outperforms FGR, LMPR
2022	HARA [283]	Point cloud	Geometric	Sensitive to the parameters
	SGHR [296]	Point cloud	Learning	Outperforms LMPR, LITS
	RMUO [297]	Point cloud	Learning	Comparable performance to SGHR, outperforms FGR
2023	DeepMapping2 [298]	Point cloud	Learning	Outperforms in scene data
	FeatSync [300]	Point cloud	Learning	Outperforms LMPR, LITS, RMPR
2024	FeatSync [300]	Point cloud	Learning	Test in scene data

1) **Geometry-based coarse registration methods.** These methods mainly rely on geometric features and constraints to achieve registration by constructing topological relationships between pairwise point clouds. While effective in certain scenarios, they struggle with large-scale point clouds, especially when the overlap between views is limited.

2) **Learning-based coarse registration methods.** Deep learning approaches reduce the reliance on hand-crafted features and heuristic rules, enabling more adaptable and data-driven solutions. However, most existing methods heavily rely on pairwise registration, which limits their generalization capabilities across diverse scenarios. In addition, the sensitivity to outliers can impede the identification of correct connections between views.

6 MULTI-VIEW FINE REGISTRATION

Different from multi-view coarse registration which estimates the transformations of views without initial guesses, multi-view fine registration usually relies on the coarse-aligned transformation input and aims to eliminate the cumulative residual errors. The taxonomy, chronological overview, and performance comparison are shown in Fig. 18, Fig. 19 and Table 8, respectively.

6.1 Point-based Methods

Point-based methods leverage all available point correspondence information as a constraint to refine the transformation parameters.

Multi-view fine registration (Sec. 6)

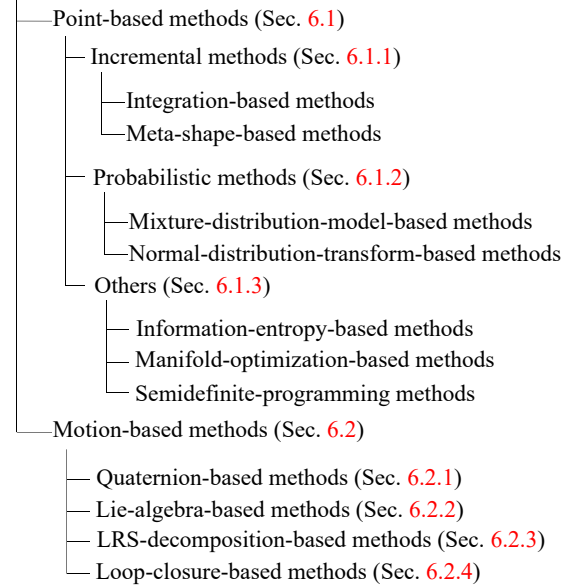


Fig. 18. Taxonomy of 3D multi-view fine registration methods.

6.1.1 Incremental Methods

These methods follow an incremental manner that merge single views to a complete point cloud.

(i) **Integration-based methods.** These methods sequentially align views to an integrated point cloud. Chen et al. [301] proposed a method to merge views sequentially using ICP, but suffers from error accumulation due to the failure of pairwise registration and the lack of global con-

straints. To address this issue, some methods improve the integration process by establishing a specifically designed graph structure [302], [303], which can provide a suitable aligned sequence. Bergevin et al. [304] developed a star-network graph to add global constraints. To further speed up this star-network, some approaches utilize z-buffer segmentation to accelerate point correspondence establishment [273], [305]. Some methods improve ICP to obtain a higher successful rate during pairwise registration, including color-enhanced [306] and incorporation of generalized Procrustes analysis [307]. For global constraints, William et al. [308] used a constant matrix for direct transformation calculation. Recently, some methods [309], [310] improve global alignment. More recently, Wu et al. [311] proposed a hierarchical method for scan-to-block integration and model assembly, which shows impressive performance on large-scale datasets.

These methods heavily rely on pairwise fine registration methods. Therefore, they exhibit limited robustness under low-overlap and noisy conditions.

(ii) **Meta-shape-based methods.** Similar to integration-based methods, meta-shape-based methods also follow an incremental manner. The main difference between these two categories is that integration-based ones (mentioned as “meta-view” [301], [303]) merge individual views, which can be seen as “real-shape”, while meta-shape sample points in each view and merge them into a seed point cloud as a new point cloud. A typical meta-shape-based method pipeline is shown in Fig. 20. Furthermore, meta-shape includes updating operations rather than the simple integration of views.

Zhu et al. [313] proposed a coarse-to-fine framework that iteratively updates the meta-shape after each view registration. Following this strategy, some methods [286], [314] also introduce the local-to-global manner to refine the meta-shape. There are also some methods [315], [316] update the meta-shape by K-means meta-shapes, employing centroids as transformation estimations. Zhang et al. [312] evaluated various meta-shape-based methods, suggesting simple yet effective modifications to improve performance. Recently, Li et al. [317] introduced a two-stage candidate retrieval process for meta-shape refinement.

Meta-shape-based methods generally achieve good accuracy performance. However, similar to integration-based methods, their convergence performance heavily depends on their pairwise registration methods used.

6.1.2 Probabilistic Methods

These methods apply probabilistic techniques to address multi-view fine registration, including mixture-distribution-model-based and normal-distribution-transform-based approaches.

(i) **Mixture-distribution-model-based methods.** Similar to pairwise fine registration, these methods model point clouds using a mixture distribution, iterating between E-step (expectation) and M-step (maximization) to estimate transformation parameters and update mixture parameters.

Evangelidis et al. [318], [319] first derived an expectation maximization (EM) manner in multi-view fine registration named JRMPC, which estimates both the GMM parameters and the transformations by mapping individual

view onto the “central” model. Zhou et al. [320] adapted GMM to model the point-wise distance. However, these methods are computationally expensive because of the need to estimate numerous parameters and the dependence on initial parameters. Some methods are proposed after JRMPC to further improve the robustness to noise by leveraging other distribution models, such as t-mixture-model (TMM) [321], hybrid mixture model combining Gaussian and Von Mises–Fisher distributions [322], Laplacian mixture model (LMM) [323]. They are demonstrated to be more robust to noise and outliers than GMM.

To reduce computational overhead, Eckart et al. [324] introduced a hierarchical Gaussian mixture model, progressively aligning smaller point clouds to optimize the scale of point set correlations. Unlike previous GMM methods such as JRMPC [319], which assume all data points are generated from a central GMM, EMPMR [325] assumes that each data point is generated from one corresponding GMM. It only requires to estimate one covariance as well as rigid transformations, which successfully reduces computational cost. In addition, LGS-CPD [326] introduces different levels of point-to-plane penalization to add local geometric information to improve GMM performance, which also applies matrix computation on GPU in the E-step for acceleration.

These mixture-based methods offer better robustness as compared with incremental methods, particularly in the presence of outliers. However, the significantly increased computation burden remains an issue.

(ii) **Normal-distribution-transform-based methods.** Normal distribution transform (NDT) was introduced by Biber et al. [327] for pairwise 3D registration, which leverages k-means clustering to approximate points in each cluster by normal distributions before registration. Zhu et al. [328] extended NDT to multi-view registration, integrating K-means clustering with Lie algebra optimization to enhance registration performance across multiple views.

6.1.3 Others

In addition to the previously mentioned methods, there are other point-based approaches, such as information-entropy-based, manifold-optimization-based methods, learning-based, and semidefinite-programming-based.

(i) **Information-entropy-based methods.** These methods rely on mutual information to measure the similarity between point sets. Methods such as entropy measures based on cumulative distribution functions (CDF) have been proposed to quantify group-wise similarities. These methods offer robust registration even in the presence of noisy or missing correspondences and provide good computational efficiency with closed-form solutions [334], [337], [345].

(ii) **Manifold-optimization-based methods.** Manifold optimization focuses on transforming the problem of multi-view registration into an optimization problem over a manifold. These approaches ensure that the rotation matrix constraints are maintained during the iterative process. It allows for the alignment of multiple point clouds without static point correspondences, which reduces computational cost and accelerates convergence [333], [346], [347].

(iii) **Semidefinite-programming-based methods.** Semidefinite programming (SDP) is used to relax the least-

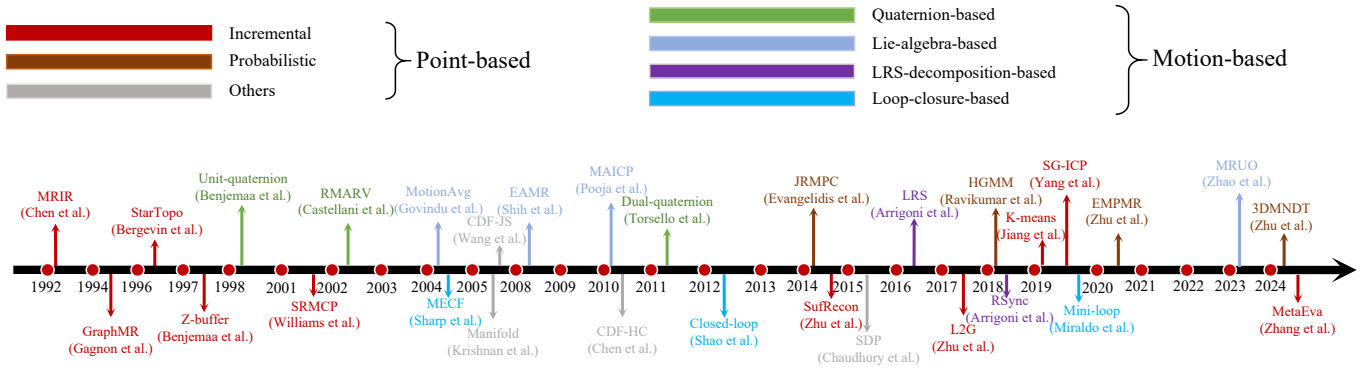


Fig. 19. Chronological overview of 3D multi-view fine registration methods.

TABLE 8
Performance summary of typical 3D multi-view fine registration methods.

Year	Method	Data type	Category	Performance
1992	MRIR [501]	Range image	Integration-based	Tests in object model
1994	GraphMR [302]	Range image	Integration-based	More balanced graph compared to MRIR; integrates 8 range views of the object into a complete model
1996	StarTopo [304]	Mesh	Integration-based	Integrates up to 20 scans
1997	Z-buffer [305]	Point cloud	Integration-based	Accelerates StarTopo using z-buffer
1998	Unit-quaternion [329]	Point cloud	Quaternion-based	Tests in object model
2001	SRMCP [308]	Point cloud	Integration-based Methods	Outperforms Unit-quaternion
2002	RMARV [330]	Acoustic range view	Quaternion-based	Outperforms MRIR
2004	MotionAvg [331]	Data-agnostic	Lie-algebra-based	Outperforms the bundle adjustment method
2004	MECF [332]	Range image	Loop-closure-based	Tests in indoor scene and object model
2005	Manifold [333]	Point cloud	Manifold-optimization-based	Outperforms StarTopo and SRMCP in object data
2006	CDF-JS [334]	Point cloud	Information-entropy-based	Tests in point cloud data, is immune to noise, and is statistically more robust than the JS
2008	EAMR [335]	Mesh	Lie-algebra-based	Outperforms MotionAvg and MECF in object data
2010	MAICP [336]	Point cloud	Lie-algebra-based	Outperforms Z-buffer and MECF in object data
2010	CDF-HC [337]	Point cloud	Information-entropy-based	Outperforms CDF-JS in point cloud data
2011	Dual-quaternion [338]	Point cloud	Quaternion-based	Outperforms in object data
2012	Closed-loop [339]	Point cloud	Loop-closure-based	Tests in generated point cloud data
2014	JRMPC [318]	Point cloud	Mixture-distribution-model-based	Outperforms SRMCP in object data
2014	SufRecon [313]	Point cloud	Meta-shape-based	Outperforms StarTopo and MotionAvg in object data
2015	SDP [340]	Point cloud	Semidefinite-programming-based	Tests in generated point cloud data
2016	LRS [341]	Point cloud	LRS-decomposition-based	Outperforms MECF, Dual-quaternion, and MotionAvg in object data
2017	L2G [286]	Point cloud	Meta-shape-based	Outperforms MAICP in object data
2018	HGMM [321]	Point cloud	Mixture-distribution-model-based	Outperforms JRMPC in object data and scene data
2018	Rsync [342]	Point cloud	LRS-decomposition-based	Outperforms in object data
2019	K-means [343]	Point cloud	Meta-shape-based	Outperforms in object data
2019	SG-ICP [314]	Point cloud	Meta-shape-based	Outperforms sequential ICP in object and scene data
2019	Mini-loop [344]	Point cloud	Loop-closure-based	Tests in scene data
2020	EMPMR [325]	Point cloud	Mixture-distribution-model-based	Outperforms MAICP, JRMPC, LRS, and K-means in object data
2023	MRUC [297]	Point cloud	Lie-algebra-based	Outperforms JRMPC in scene and object data
2024	MetaEva [312]	Point cloud	Meta-shape-based	Evaluates different variants of meta-shape methods
2024	3DMNDT [328]	Point cloud	Normal-distribution-transform-based	Outperforms MAICP, JRMPC, LRS, and K-means in object and scene data

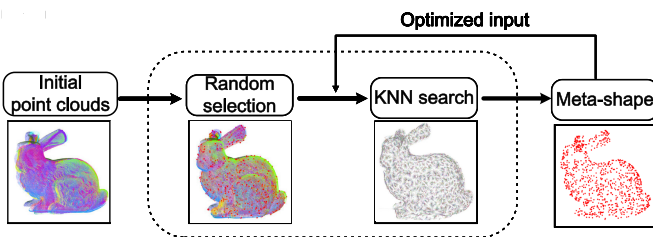


Fig. 20. Pipeline of KNN meta-shape method [312].

squares registration problem into a convex optimization, which is easier to solve. These methods leverage SDP formulations to perform global alignment across multiple views, reducing the complexity of the registration process through rank relaxation and iterative methods [340], [348], [349], [350].

6.2 Motion-based Methods

Motion-based (a.k.a transformation synchronization) approaches aim to recover the globally optimal transformation

by synchronizing a series of pairwise motions. These methods primarily rely on accurate pairwise transformations. They can be grouped into four main categories: quaternion-based, Lie-algebra-based, LRS-decomposition-based, and loop-closure-based.

6.2.1 Quaternion-based Methods

Quaternion-based methods leverage the properties of quaternions for iterative optimization of rotation and translation in point cloud registration. Several works employ unit quaternion or dual quaternions for optimizing rotations and transformations. Benjemaa and Schmitt [329] leveraged unit quaternions for optimizing rotations via an iterative process on symmetric 4×4 matrices. Fusiello et al. [351] and Castellani et al. [330] focused on parameterizing rotation in $SE(3)$ using unit quaternion. Torsello et al. [338] extended this by using dual quaternions to represent motion and distribute registration errors through a neighbor graph. These methods generally aim to improve rotational optimization through the mathematical properties of quaternions, with variations in the form of iterative processes and error distribution strategies.

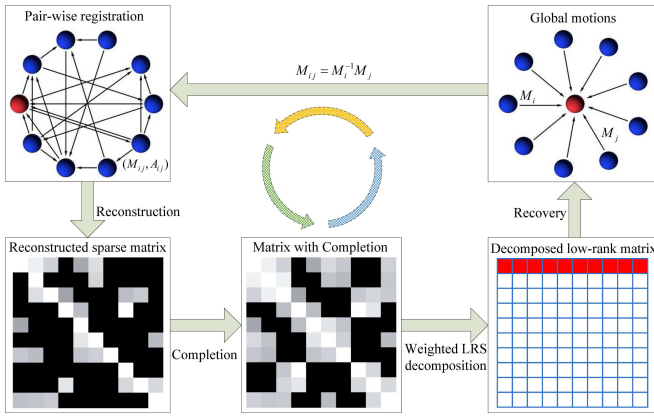


Fig. 21. An example of LRS-decomposition-based methods [361].

6.2.2 Lie-algebra-based Methods

These methods leverage Lie group and Lie algebra structures to average transformations and mitigate cumulative registration error. Govindu first introduced motion averaging (MA) [331] and its RANSAC version [352] based on Lie-algebra. Later, Govindu and Pooja [336], [353] proposed MAICP method that combines MA and ICP and utilizes Lie algebra to compute transformations after obtaining point-wise correspondences in iterations, which is followed by [354], [355]

There are also methods that improve global consistency based on graph structure, such as using Dijkstra’s algorithm for outlier rejection [356], utilizing maximum connected sub-graph to eliminate unreliable relative motions [343], [357], or leveraging cycle constraints [335]. In addition, weighting strategies are proposed [355], [358] to punish unreliable relative transformations.

To mitigate the sensitivity of the F norm to errors in previous methods, Zhu et al. [359] proposed substituting the F norm for corr-entropy. To reduce computational overhead, Bourmaud et al. [360] introduced a variational Bayesian approach to deal with large-scale problems. Zhao et al. [297] recently applied Lie algebra as a fine registration block.

While Lie-algebra-based methods are efficient, they generally require good initialization. In addition, some approaches only distribute cumulative registration errors equally among views rather than eliminating them.

6.2.3 LRS-decomposition-based Methods

Low rank sparsity (LRS) decomposition methods reformulate multi-view registration as an LRS matrix decomposition problem. They optimize transformations by separating them from noise, thereby reducing the impact of noisy data. A typical LRS-decomposition-based method pipeline is shown in Fig. 21. Arrigoni et al. [341], [342] framed registration as an LRS decomposition problem, recovering global motions from a block matrix. However, the reliability of each relative motion differs in reality. LRS assumes that all relative motions have equal reliability, which inevitably leads to accuracy degradation. To address this issue, several methods propose weighting techniques. Jin et al. [361] assigned the corresponding weights of each scan pair through TriCP for reliable and accurate relative motions. TriCP may run into the local minimum within several iterations, thus Zhang et

al. [268] incorporated angle constraints among point cloud relative motions for weighting. In addition, Wang et al. [362] introduced a weighted approach from another perspective, which utilizes spatial distribution features of point clouds extracted by spatial rasterization. To reduce computational cost, Li et al. [363] weighted the LRS method utilizing an optimization strategy based on the Lagrange multiplier. It improves registration accuracy and accelerates the process.

6.2.4 Loop-closure-based Methods

These methods establish the constraints for multi-view point cloud registration through a closed loop and optimize the relative pairwise transformation parameters between views within the closed loop. Sharp et al. [332] defined the problem as an optimization of the graph of neighboring views, and showed that the graph can be decomposed into a set of cycles. Therefore, the optimal transformation parameter for each cycle can be solved in a closed form. Recently, Miraldo et al. [344] also followed this manner that utilizes small loop constraints and fewer point-wise correspondences. To further eliminate pairwise registration error, Liu et al. [364] adapted a parametric bidirectional method to generate reversible transformations in paired overlapping areas thereby eliminating cumulative errors. Some methods [339], [365] decouple the rotation matrix and translation vector to distribute cumulative errors. These methods utilize the loop constraint in connecting graphs to optimize poses, which leads to the same problem as Lie-algebra-based methods that errors are averaged rather than eliminated.

6.3 Summary

We outline the development and characteristics of multi-view fine registration methods as follows.

- 1) **The challenge to achieve a performance balance.** Existing point-based methods deliver good accuracy, while suffer from low time-efficiency. By contrast, motion-based methods are fast but fail to eliminate small errors. Hence, it is still challenging to achieve a balance in terms of accuracy, robustness, and efficiency.
- 2) **The dependence on pairwise ICP.** The performance of point-based methods usually highly relies on the convergence accuracy of pairwise ICPs. Such dependency may inherit the limitations of ICP methods.
- 3) **Scalability to large-scale unordered data.** It is still challenging for existing methods to handle a large number of unordered point cloud views.

7 OTHER REGISTRATION PROBLEMS

Beyond pairwise and multi-view point cloud registration, there are also some other registration problems addressing specific challenges, including cross-scale registration, cross-source registration, color point cloud registration, and multi-instance registration.

7.1 Cross-scale Point Cloud Registration

Cross-scale point cloud registration additionally addresses the scale variation problem. Existing methods are mainly learning-independent, which can be further classified as

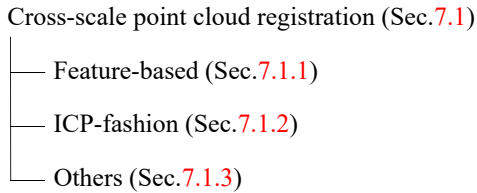


Fig. 22. Cross-scale point cloud registration approaches.

feature-based, ICP-fashion, and the others. The taxonomy, chronological overview, and performance comparison are shown in Fig. 22, Fig. 23 and Table 9, respectively.

7.1.1 Feature-based Methods

These methods extract distinctive geometric features from point clouds for the scale variation problem. Some approaches extract local features that are resilient to scale changes and local variations. For instance, Lin et al. [376] proposed the scale-invariant point feature (SIPF) for key-point detection, using a voting mechanism to strengthen multi-scale object detection. This approach is further refined through boundary extraction [386]. To enhance feature selection at varying scales, Lim and Lee [387] extended the scale-invariant feature transform (SIFT) to 3D, detecting highly repeatable features and obtaining the support radius regardless of the mesh scale. You et al. [382] presented the category-level point pair feature (CPPF) for 9D pose estimation, enabling the generalization ability across unseen objects. Some other methods combine local and global features. Mellado et al. [373] developed a growing least squares method for scale-invariant matching across noisy, multi-modal data, combining localized accuracy with global structural awareness.

7.1.2 ICP-fashion Methods

These methods minimize distances between point clouds while estimating scale, rotation, and translation parameters. Some approaches [366], [367], [369], [388] integrate scale estimation into the traditional ICP method, extending it to estimate scale alongside rotation and translation. Another category focuses on constraint optimization [368], [371], [374], [379], [380], formulating the registration problem as a high-dimensional optimization task with bounded or adaptive constraints. Additionally, some methods optimize generated correspondences [378], [381], [384], [389], [390] to enhance the resilience to outliers, noise, and partial overlaps through probabilistic models or advanced similarity measures.

7.1.3 Others

Probabilistic models such as the coherent point drift (CPD) method [261] leverage GMMs to achieve robust scale alignment in both rigid and nonrigid scenarios. On the other hand, scale characterization techniques, such as those based on principal component analysis (PCA) [372], [391], focus on matching the scale between point clouds, addressing scale variations that hinder accurate alignment. Pham et al. [370] further introduced a voting-based technique that uses invariant shape characteristics and distance ratios for scale-independent registration. Transform-based methods, such as the Fourier Mellin SOFT transform [377], address

the full degrees of freedom for global alignment. Recent innovations [385], [392] improve the robustness of the registration through advanced feature detection and noise filtering. Additionally, some methods focus on outlier rejection [88], [393] to improve registration accuracy and computational efficiency given correspondences. As a pioneering deep-learning-based solution, Gao et al. [383] proposed a high-dimensional regression network HDRNet that effectively handles scale, noise, and partial overlap.

The research toward robust cross-scale registration is at an early stage, and most works assume that the data are fully overlapped. The handling of partial data with scale and rotation variation remains to be solved.

7.2 Cross-source Point Cloud Registration

Cross-source point cloud registration is vital to merge multi-modal point clouds. The main challenge is the dramatic point distribution variation. This section reviews methodologies in cross-source point cloud registration. The taxonomy, chronological overview, and performance comparison are shown in Fig. 24, Fig. 25 and Table 10, respectively.

7.2.1 Traditional Methods

These methods can be further categorized into correspondence-based and correspondence-free.

(i) **Correspondence-based methods.** These methods generally design scale-aware descriptors for correspondence generation followed by a transformation estimator. Persad and Armenakis [403] proposed to perform registration in 2D projection images by matching scale, rotation, and translation-invariant descriptors on sparse 2D keypoints. Some methods perform registration directly in the 3D space. For instance, Peng et al. [394] proposed a two-stage matching process. It matches ensemble of shape functions (ESF) descriptors in the coarse stage, followed by ICP refinement. In a transformation-decomposition way, Li et al. [404] decomposed the full seven-parameter registration problem into three subproblems, i.e., scale, rotation, and translation, through line vectors.

(ii) **Correspondence-free methods.** These methods register point clouds by leveraging global structures or statistical models. Graph-based approaches, such as [395], apply graph matching to represent macro and micro structures. Statistical modeling and refinement methods [396], [398], [400] focus on probabilistic representations of point clouds, using models such as GMM to capture global structures and iteratively refine alignments.

7.2.2 Learning-based Methods

Learning-based methods handle noise, outliers, and density variations by designing robust feature learning modules. Huang et al. [397] introduced a feature-metric framework that bypasses correspondence search, accelerating the process while maintaining the robustness to noise. Xiong et al. [399] extended this by proposing skeletal representations to enhance topological feature encoding. Building on this, Yang et al. [401] advanced correspondence refinement through a descriptor with in-plane rotation equivalence and disparity-weighted scoring. Recently, Ma et al. [402]

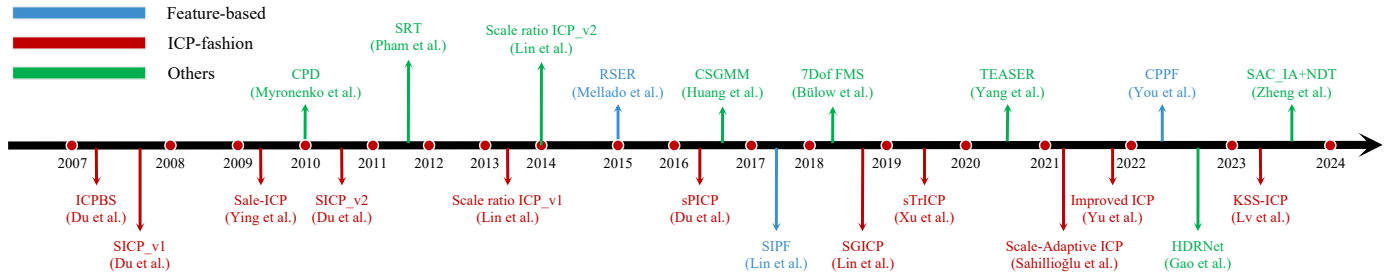


Fig. 23. Chronological overview of representative cross-scale 3D point cloud registration methods.

TABLE 9
Performance summary of typical cross-scale 3D point cloud registration methods.

Year	Method	Data Type	Category	Performance
2007	ICPBS [366]	2D shape, point cloud	ICP-fashion	Outperforms ICP and ICPS between two m-D point sets
	SICP_v1 [367]	2D shape, point cloud	ICP-fashion	General for scaling registration
2009	Scale-ICP [368]	Point cloud	ICP-fashion	Robust to large-scale stretch and noise
2010	CPD [261]	Point cloud	Others	Suitable for nonrigid point set registration
	SICP_v2 [369]	2D shape, point cloud	ICP-fashion	Independent of shape and features
2011	SRT [370]	Point cloud	Others	High computational cost
2013	Scale ratio ICP_v1 [371]	Point cloud	ICP-fashion	High computational cost
2014	Scale ratio ICP_v2 [372]	Point cloud	Others	Robust to noise
2015	RSER [373]	Multi-modal data	Feature-based	Outperforms Scale ratio ICP_v2
2016	sPICP [374]	Point cloud	ICP-fashion	Outperforms ICPBS and CPD
	CSGMM [375]	Point cloud	Others	Effective for large-scale, variable data
2017	SIPF [376]	Point cloud	Feature-based	Robust to scale invariant
2018	7Dof FMS [377]	Point cloud	Others	Robust to noise and partial overlap
	SGICP [378]	Point cloud	ICP-fashion	Enhances GICP with scale variables
2019	sTriCP [379]	2D shape, range image	ICP-fashion	Effective for both overlapping and non-overlapping point sets
2020	TEASER [88]	Point cloud	Others	Solves by a simple enumeration
2021	Scale-Adaptive ICP [380]	Point cloud	ICP-fashion	Outperforms TEASER
	Improved ICP [381]	Point cloud	ICP-fashion	Outperforms ICP, efficient without manual intervention
2022	CPPF [382]	Point cloud	Feature-based	Robust to noise
	HDRNet [383]	Point cloud	Others	Resilient to partial overlaps and noise
2023	KSS-ICP [384]	Point cloud	ICP-fashion	Invariant to similarity transformations
	SAC_IA+NDT [385]	Point cloud	Others	Outperforms ICP and NDT+ICP

TABLE 10
Performance summary of typical cross-source 3D point cloud registration methods.

Year	Method	Data Type	Category	Performance
2014	CSC2F [394]	Point cloud	Correspondence-based	Robust to density, noise, scale and occlusion differences
2017	CSGM [395]	Point cloud	Correspondence-free	Outperforms CPD
	GM-CSPC [396]	Point cloud	Correspondence-free	Outperforms CPD
2020	FMR [397]	Point cloud	Learning-based	Robust to noise, outliers and density differences
2021	OneSac [123]	Point cloud	Correspondence-based	Robust against severe outliers
2023	GCC [398]	Point cloud	Correspondence-free	Outperforms CICP, GCTR, FGR, DGR, FMR
2024	SPEAL [399]	Point cloud	Learning-based	Outperforms FGR, DGR
	VRHCF [400]	Point cloud	Correspondence-free	Outperforms GICP, GCTR, GCC
	MSReg [401]	Point cloud	Learning-based	Effective for large-scale and heterogeneous data
	FF-LOGO [402]	Point cloud	Learning-based	Outperforms CICP, GCTR, DGR, FMR, GCC

Cross-source point cloud registration (Sec.7.2)

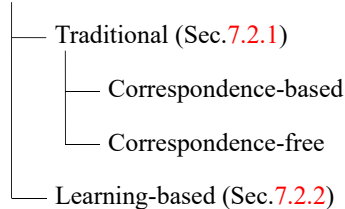


Fig. 24. Taxonomy of 3D cross-source point cloud registration approaches.

developed FF-LOGO, integrating feature filtering with local-global optimization to ensure modality-invariant feature

extraction.

Despite recent advances, it is still challenging to handle data with severe point density variation.

7.3 Color Point Cloud Registration

For point clouds acquired by RGB-D sensors, additional color cues can be leveraged for point cloud registration. Existing methods can be categorized into traditional and learning-based. The taxonomy, chronological overview, and performance comparison are shown in Fig. 26, Fig. 27 and Table 11, respectively.

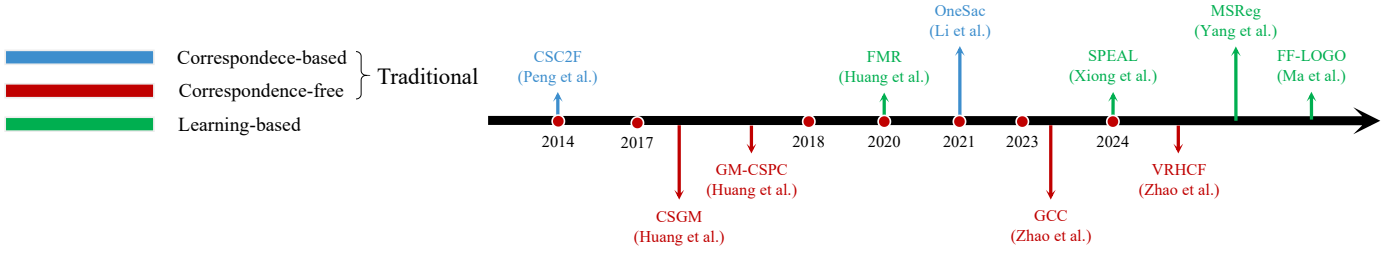


Fig. 25. Chronological overview of representative 3D cross-source point cloud registration methods.

TABLE 11
Performance summary of typical 3D color point cloud registration methods.

Year	Method	Data Type	Category	Performance
1999	Color 6D ICP [405]	Point cloud	ICP-fashion	Incorporates both 3D data and color information
2001	RSICCP [406]	Range image	ICP-fashion	Invariant to rigid transformations
2006	ICP_GAT/MAT/GCT [407]	Range image	ICP-fashion	Integrates color information in ICP variants
2011	Color 4D ICP [262]	Point cloud	ICP-fashion	Combines point range and weighted hue values
2014	Color GICP [264]	Point cloud	ICP-fashion	Robust to low-quality color images
2017	Color 3D ICP [408]	Point cloud	Hybrid-feature-based	Outperforms Color 6D ICP, Color 4D ICP, Color GICP
2018	Improved TrICP [409]	Point cloud	Hybrid-feature-based	Outperforms TrICP
2020	IKCP [410]	Point cloud	ICP-fashion	Outperforms Color 6D ICP, Color 3D ICP, Color GICP
2022	PCR-CG [411]	Point cloud	Learning-based	Outperforms Color 3D ICP
	SOD+BCD+MCC [412]	Point cloud	Others	Addresses data degradation and uneven distribution
	ImLoveNet [413]	Point cloud, color image	Learning-based	Tackles the challenge of low-confidence features
	LLT [414]	Point cloud, RGB-D image	Learning-based	Addresses challenges in multi-modal integration for registration
2023	IMFNet [415]	Point cloud, image	Learning-based	Integrates weighted texture information
	PointMBF [416]	Point cloud, RGB-D image	Learning-based	Outperforms LLT
2024	PointDSCC [417]	Point cloud	Learning-based	Outperforms Color 3D ICP, Color GICP
	SemReg [418]	Point cloud, 2D image	Learning-based	Outperforms PCR-CG
	RGBD-Glue [419]	Point cloud	Learning-based	Outperforms LLT, PointMBF
	ColorPCR [21]	Point cloud	Learning-based	Addresses challenges in low-overlap point cloud registration

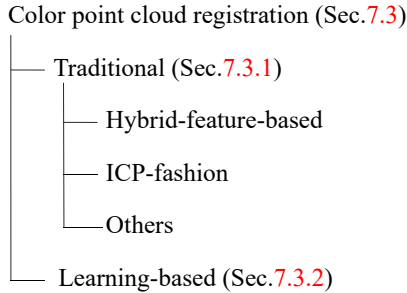


Fig. 26. Taxonomy of 3D color point cloud registration methods.

7.3.1 Traditional Methods

We further classify them as Hybrid-feature-based, ICP-fashion, and the others.

(i) **Hybrid-feature-based methods.** Hybrid-feature-based methods enhance point cloud registration by combining color, texture, and geometric features to establish correspondences. It can be categorized into two groups: traditional-feature-based and color-enhanced-feature-based. Traditional-feature-based approaches [409], [420], [421] primarily rely on classical feature extraction techniques and traditional methods for integrating color cues into the registration process. Color-enhanced-feature-based approaches [408], [422] refine geometric feature matching by incorporating color for enhanced robustness.

(ii) **ICP-fashion methods.** ICP-fashion methods adapt the ICP method by incorporating color and other features to improve registration accuracy. Early works [405], [406], [407] incorporate invariant attributes and color range images to strengthen matching. Later, Men et al. [262] and Korn et al. [264] combined geometry with hue and $L^*A^*B^*$ color

space to accelerate convergence and improve transformation accuracy. More recently, Choi et al. [410], [423] refined pose and depth using color-supported soft matching, addressing depth errors with adaptive cost functions.

(iii) **Others.** Recent advances in color point cloud registration focus on improving robustness under challenging conditions. Liu et al. [424] used a genetic algorithm to improve the robustness of the registration under changing lighting conditions. Wan et al. [412] applied salient object detection and bidirectional color distance for precise structural registration.

7.3.2 Learning-based Methods

These methods can be further categorized into three main approaches: 2D-3D fusion, RGB-D fusion and hierarchical fusion. 2D-3D fusion approaches, such as PCR-CG [411], ImLoveNet [413] and SemReg [418], integrate color features from 2D images with 3D geometry to enhance registration performance. RGB-D fusion approaches [414], [416], [417], [419], [425] focus on combining RGB and depth data to exploit their complementary strengths for better correspondence estimation. Hierarchical fusion approaches, such as IMFNet [415], ColorPCR [21] and [426], improve registration by combining multi-level fusion strategies and enhancing feature interpretability.

7.4 Multi-instance Point Cloud Registration

Multi-instance point cloud registration estimates transformations of multiple instances in the scene. However, this process comes with challenges such as the ambiguity of correspondences from different instances, occlusions,

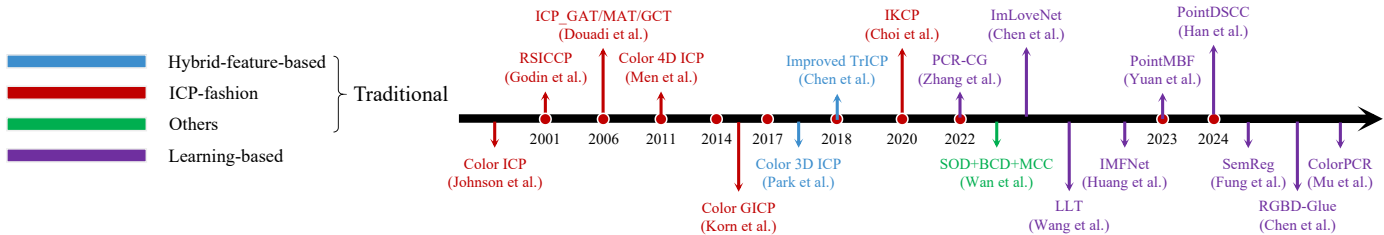


Fig. 27. Chronological overview of representative 3D color point cloud registration methods.

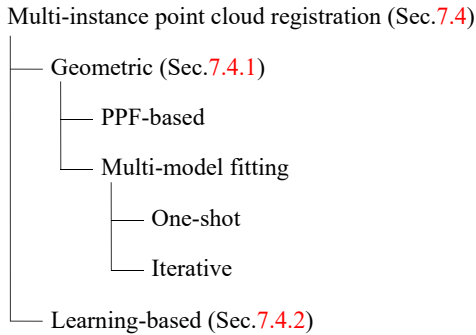


Fig. 28. Taxonomy of 3D multi-instance point cloud registration methods.

and noise. Research in this area generally falls into two categories: geometric and learning-based. The taxonomy, chronological overview, and performance comparison are shown in Fig. 28, Fig. 29 and Table 12, respectively.

7.4.1 Geometric Methods

Geometric methods leverage spatial and structural information to align multiple instances within a scene. These approaches can be categorized into point-pair-features-based (PPF-based) and multi-modal fitting techniques.

(i) **PPF-based methods.** Early multi-instance registration methods focus on correspondence-free techniques for object recognition and pose estimation. They leverage PPF to encode geometric relationships between points, efficiently estimating multiple poses. Drost et al. [427] laid the foundation by introducing a global model description and a fast voting scheme to generate pose hypotheses efficiently. Building on this, many follow-ups have been proposed. Vidal et al. [450] introduced surface information to improve feature extraction as a preprocessing step. In the modeling stage, various strategies [428], [429], [430], [432], [437], [438] are developed to optimize feature discrimination. In the voting stage, Guo et al. [440] proposed a center voting strategy based on geometric relationships to improve pose hypothesis generation. In addition, Vock et al. [451] developed an efficient hypothesis validation method to reduce false positives. In a coarse-to-fine fashion, Birdal et al. [433] and Yue et al. [444] combined initial segmentation with progressively refined pose estimation.

(ii) **Multi-model fitting methods.** These methods estimate model parameters from data points generated by multiple models. They can be broadly classified into two categories: one-shot and iterative.

1) **One-shot manner.** These methods estimate model parameters in a single step for efficient fitting. Clustering-based approaches, such as T-Linkage [431], focus on group-

ing correspondences to detect model instances. Magri and Fusiello [434] developed RansaCov, formulating the problem as set coverage, effectively managing intersecting structures and outliers. Optimization-based methods, such as Multi-X [435], employ optimization techniques for multi-class and multi-instance fitting. Some other methods direct clustering transformation hypotheses. An example is ECC [442], which directly groups noisy correspondences via compatibility matrices.

2) **Iterative manner.** Iterative methods successively register instances. Baráth et al. [436], [441] iteratively improved multi-model parameter estimation by combining hypothesis generation with optimization techniques. Cao et al. [445] introduced the first iterative framework IBI specifically designed for 3D multi-instance registration, which mines consistent seed correspondences to guide inlier recovery. Later, Yu et al. [448] enhanced clustering efficiency and robustness without known cluster number under an iterative paradigm.

7.4.2 Learning-based Methods

Learning-based methods have progressed to address challenges such as clutter, occlusion, and overlapping instances. Some methods learn correspondences from data or learn multiple registration poses from correspondences. For instance, CONSAC [439] learns sampling weights to guide RANSAC, and PointMC [447] learns correspondences to performance pose clustering. In addition, PointCLM [443] estimates multi-instance registration poses from correspondences with contrastive learning. A recent trend is end-to-end learning. MIRETR [446] proposes a coarse-to-fine transformer-based approach to extract instance-aware correspondences and predict registration poses. Recently, 3DFM-Net [449] introduces a novel framework that first focuses on object proposals and then performs instance-level registration.

7.5 Summary

The following points can be summarized.

1) **Cross-scale registration.** Geometric methods are still the mainstream approaches. Simultaneously addressing scale and partial overlap issues remains a challenge.

2) **Cross-source registration.** Recent deep-learning-based methods show powerful ability. However, it is still challenging to align cross-source point clouds with significant point distribution variation.

3) **Color point cloud registration.** A recent trend is to guide geometric registration with color cues for either performance boosting or supervision signal reduction.

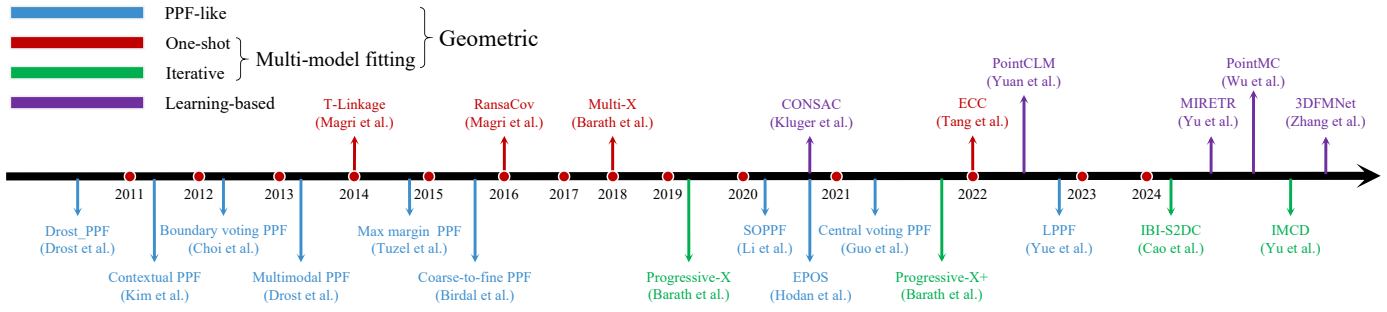


Fig. 29. Chronological overview of representative 3D multi-instance point cloud registration methods.

TABLE 12
Performance summary of typical 3D multi-instance point cloud registration methods.

Year	Method	Data Type	Category	Performance
2010	Drost_PPF [427]	Point cloud	PPF-based	Robust to noise and clutter
2011	Contextual PPF [428]	Range image	PPF-based	Outperforms Drost_PPF
2012	Boundary voting PPF [429]	CAD model	PPF-based	Exploits boundary information, suitable for planar objects
	Multimodal PPF [430]	Range image	PPF-based	Combines intensity and depth data, invariant to scale and rotation
2014	T-Linkage [431]	Point cloud, image pair	One-shot	Outperforms J-Linkage
	Max margin PPF [432]	Point cloud, 3D model	PPF-based	Outperforms Drost_PPF, suitable for self-similar and planar surfaces
2015	Coarse-to-fine PPF [433]	Point cloud, depth image	PPF-based	Outperforms Drost_PPF
2016	RansaCov [434]	Image pair	One-shot	Outperforms J-Linkage, T-Linkage
2018	Multi-X [435]	Image pair	One-shot	Outperforms T-Linkage
2019	Progressive-X [436]	Point cloud, image pair	Iterative	Outperforms T-Linkage, RansaCov, Multi-X
2020	SOPPF [437]	Point cloud	PPF-based	Outperforms Drost_PPF
	EPOS [438]	RGB image	PPF-based	Outperforms Drost_PPF
	CONSAC [439]	Image pair	Learning-based	Outperforms T-Linkage, RansaCov, Multi-X, Progressive-X
2021	Central voting PPF [440]	Point cloud, image	PPF-based	Outperforms Drost_PPF
	Progressive-X+ [441]	Image pair	Iterative	Outperforms T-Linkage, RansaCov, Multi-X, Progressive-X, CONSAC
2022	ECC [442]	Point cloud	One-shot	Outperforms T-Linkage, Progressive-X, CONSAC
	PointCLM [443]	Point cloud	Learning-based	Outperforms T-Linkage, RansaCov, CONSAC, ECC
	LPPF [444]	Point cloud	PPF-based	Robust to noise, fast convergence
2024	IBI-S2DC [445]	Point cloud	Iterative	Outperforms T-Linkage, Progressive-X, CONSAC, ECC, PointCLM
	MIRETR [446]	Point cloud	Learning-based	Outperforms T-Linkage, RansaCov, ECC, PointCLM
	PointMC [447]	Point cloud	Learning-based	Outperforms T-Linkage, RansaCov, CONSAC, ECC, PointCLM
	IMCD [448]	Point cloud	Iterative	Outperforms ECC, PointCLM
	3DFMNet [449]	Point cloud	Learning-based	Outperforms T-Linkage, RansaCov, ECC, PointCLM, MIRETR

4) **Multi-instance registration.** End-to-end learning methods have shown better performance than methods learning with correspondences only. Both bottom-up and top-down methods have shown their own merits.

8 CHALLENGES AND OPPORTUNITIES

Although we have witnessed great success towards robust 3D point cloud registration in the last decades, there are still several critical issues requiring future research attention.

- 1) **Push unsupervised registration to the limit.** The point cloud registration problem, in its nature, is an optimization problem. Although fully-supervised methods have achieved great success in recent years, unsupervised methods are more applicable in real-world applications and are very promising when combined with geometric constraints. We have witnessed a few unsupervised methods at present; their performance is even comparable with supervised methods, motivating us to explore the performance upper bound.
- 2) **End-to-end learning or hybrid solutions.** End-to-end learning is a well-known fashion to tackle 2D vision problems. Following this trend, a number of end-to-end registration frameworks emerge. However, a recent work demonstrates that a decoupled

framework (e.g., learned features with geometrical estimators) surpasses state-of-the-art methods, and enables better generalization ability. As such, this problem should be investigated more deeply to give an answer to the 3D registration community.

- 3) **Robust transformation estimation with extremely scare inliers.** Correspondence-based registration methods are frequently revisited due to their promising performance and robustness. Since the invention of RANSAC, many follow-ups have been proposed. However, the problem is extremely ill-posed in the presence of scares inliers, and existing methods still fail to achieve robust results. New datasets and experimental settings toward this direction deserve more attention.
- 4) **Ultra-small residual registration error elimination.** For fine registration, ICP and its variants are arguably de facto choices. An interesting observation is that most fine registration works tend to tackle the problem of global registration, while current state-of-the-art coarse registration methods could already present a good initial guess. In many industrial and measuring applications, ultra-small residual error elimination in the presence of noise, weak-geometric features is of great demand. However, existing fine registration methods struggle to

deal with such situation.

- 5) **Multi-view registration in the wild.** Current multi-view registration methods assume that the object/scene-of-interest are static, the scanning overlap are ensured, and the scanned data are controlled. Performing multi-view registration with point cloud sequences captured from a dynamic and unknown scene, remains an open problem.
- 6) **The registration of 3D Gaussians.** 3D Gaussian representations open a new era for rendering and 3D reconstruction. In large scene rendering problems, a few trails on registering 3D Gaussians have been made. We believe there are many interesting problems to be explored, given mature point cloud registration solutions and new 3D representations.
- 7) **Cross-scale 3D registration is challenging.** The scale factor sometimes is ambiguous in applications such as autonomous navigation and robotics, the problem is even more challenging when other nuisances exist simultaneously. However, we find that most of the research efforts have been paid compared to the standard registration problem without scale variation. This direction is more challenging.
- 8) **Registration with large pretrained models.** Large pretrained models have advanced the multi-modal generation tasks greatly. The strong generation ability of large pretrained model enables shape completion. This is supposed to improve the registration performance for low-and-non-overlapping data.

9 CONCLUSIONS

This paper provides a comprehensive overview of 3D point cloud registration methods in the last three decades, covering a broad area of registration problems. We have presented a comprehensive taxonomy and performance comparison of reviewed methods. The traits, merits, and demerits of these methods have been summarized. Finally, several future research directions have been discussed.

ACKNOWLEDGMENTS

The authors would like thank Dr. Siwen Quan for the discussion during the work.

REFERENCES

- [1] X. Huang, G. Mei, J. Zhang, and R. Abbas, "A comprehensive survey on point cloud registration," *arXiv*, 2021.
- [2] M. Lyu, J. Yang, Z. Qi, R. Xu, and J. Liu, "Rigid pairwise 3d point cloud registration: a survey," *PR*, p. 110408, 2024.
- [3] B. Curless and M. Levoy, "A volumetric method for building complex models from range images," in *Proc. SIGGRAPH*. ACM, 1996, pp. 303–312.
- [4] A. S. Mian, M. Bennamoun, and R. A. Owens, "A novel representation and feature matching algorithm for automatic pairwise registration of range images," *IJCV*, vol. 66, no. 1, pp. 19–40, 2006.
- [5] A. S. Mian, M. Bennamoun, and R. Owens, "Three-dimensional model-based object recognition and segmentation in cluttered scenes," *TPAMI*, vol. 28, no. 10, pp. 1584–1601, 2006.
- [6] A. Mian, M. Bennamoun, and R. Owens, "On the repeatability and quality of keypoints for local feature-based 3d object retrieval from cluttered scenes," *IJCV*, vol. 89, pp. 348–361, 2010.
- [7] B. Taati and M. Greenspan, "Local shape descriptor selection for object recognition in range data," *CVIU*, vol. 115, no. 5, pp. 681–694, 2011.
- [8] K. Lai, L. Bo, and D. Fox, "Unsupervised feature learning for 3d scene labeling," in *Proc. ICRA*. IEEE, 2014, pp. 3050–3057.
- [9] EPFL Computer Graphics and Geometry Laboratory, "EPFL statue model repository," 2012. [Online]. Available: https://lgg.epfl.ch/statues_dataset.php
- [10] J. Sturm, N. Engelhard, F. Endres, W. Burgard, and D. Cremers, "A benchmark for the evaluation of rgb-d slam systems," in *Proc. IROS*. IEEE, 2012, pp. 573–580.
- [11] A. Geiger, P. Lenz, and R. Urtasun, "Are we ready for autonomous driving? the kitti vision benchmark suite," in *Proc. CVPR*. IEEE, 2012, pp. 3354–3361.
- [12] F. Pomerleau, M. Liu, F. Colas, and R. Siegwart, "Challenging data sets for point cloud registration algorithms," *IJRR*, pp. 1705–1711, 2012.
- [13] F. Tombari, S. Salti, and L. Di Stefano, "Performance evaluation of 3d keypoint detectors," *IJCV*, vol. 102, no. 1-3, pp. 198–220, 2013.
- [14] Z. Wu, S. Song, A. Khosla, F. Yu, L. Zhang, X. Tang, and J. Xiao, "3d shapenets: A deep representation for volumetric shapes," in *Proc. CVPR*. IEEE, 2015, pp. 1912–1920.
- [15] A. Dai, A. X. Chang, M. Savva, M. Halber, T. Funkhouser, and M. Nießner, "ScanNet: Richly-annotated 3d reconstructions of indoor scenes," in *Proc. CVPR*. IEEE, 2017, pp. 5828–5839.
- [16] A. Zeng, S. Song, M. Nießner, M. Fisher, J. Xiao, and T. Funkhouser, "3dmatch: Learning local geometric descriptors from rgb-d reconstructions," in *Proc. CVPR*. IEEE, 2017, pp. 1802–1811.
- [17] A. Avetisyan, M. Dahnert, A. Dai, M. Savva, A. X. Chang, and M. Nießner, "Scan2cad: Learning cad model alignment in rgb-d scans," in *Proc. CVPR*. IEEE, 2019, pp. 2614–2623.
- [18] Z. Dong, F. Liang, B. Yang, Y. Xu, Y. Zang, J. Li, Y. Wang, W. Dai, H. Fan, J. Hyyppä *et al.*, "Registration of large-scale terrestrial laser scanner point clouds: A review and benchmark," *ISPRS*, vol. 163, pp. 327–342, 2020.
- [19] S. Huang, Z. Gojcic, M. Usvyatsov, A. Wieser, and K. Schindler, "Predator: Registration of 3d point clouds with low overlap," in *Proc. CVPR*. IEEE, 2021, pp. 4267–4276.
- [20] T. Sun, Y. Hao, S. Huang, S. Savarese, K. Schindler, M. Pollefeys, and I. Armeni, "Nothing stands still: A spatiotemporal benchmark on 3d point cloud registration under large geometric and temporal change," *arXiv*, 2023.
- [21] J. Mu, L. Bie, S. Du, and Y. Gao, "Colorpcr: Color point cloud registration with multi-stage geometric-color fusion," in *Proc. CVPR*. IEEE, 2024, pp. 21 061–21 070.
- [22] N. Chen, L. Liu, Z. Cui, R. Chen, D. Ceylan, C. Tu, and W. Wang, "Unsupervised learning of intrinsic structural representation points," in *Proc. CVPR*. IEEE, 2020, pp. 9121–9130.
- [23] T. Jakab, R. Tucker, A. Makadia, J. Wu, N. Snavely, and A. Kanazawa, "Keypointformer: Unsupervised 3d keypoint discovery for shape control," in *Proc. CVPR*, 2021, pp. 12783–12792.
- [24] H. Yuan, C. Zhao, S. Fan, J. Jiang, and J. Yang, "Unsupervised learning of 3d semantic keypoints with mutual reconstruction," in *Proc. ECCV*. Springer, 2022, pp. 534–549.
- [25] H. Chen and B. Bhanu, "3d free-form object recognition in range images using local surface patches," *Pattern Recognit Lett*, vol. 28, no. 10, pp. 1252–1262, 2007.
- [26] U. Castellani, M. Cristani, S. Fantoni, and V. Murino, "Sparse points matching by combining 3d mesh saliency with statistical descriptors," in *Proc. CGF*, vol. 27, no. 2. Wiley Online Library, 2008, pp. 643–652.
- [27] A. S. Mian, M. Bennamoun, and R. Owens, "Keypoint detection and local feature matching for textured 3d face recognition," *IJCV*, vol. 79, pp. 1–12, 2008.
- [28] R. B. Rusu and S. Cousins, "3d is here: Point cloud library (pcl)," in *Proc. ICRA*. IEEE, 2011, pp. 1–4.
- [29] H. Teng, D. Chatziparaschis, X. Kan, A. K. Roy-Chowdhury, and K. Karydis, "Centroid distance keypoint detector for colored point clouds," in *Proc. WACV*, 2023, pp. 1196–1205.
- [30] J. Sun, M. Ovsjanikov, and L. Guibas, "A concise and provably informative multi-scale signature based on heat diffusion," in *Proc. CGF*, vol. 28, no. 5. Wiley Online Library, 2009, pp. 1383–1392.
- [31] Y. Zhong, "Intrinsic shape signatures: A shape descriptor for 3d object recognition," in *Proc. ICCV Workshops*. IEEE, 2009, pp. 689–696.

- [32] Y. Guo, M. Bennamoun, F. Sohel, M. Lu, J. Wan, and N. M. Kwok, "A comprehensive performance evaluation of 3d local feature descriptors," *IJCV*, vol. 116, pp. 66–89, 2016.
- [33] Z. Zhang, J. Tang, L. Niu, B. Su, Y. Feng, Y. Sheng, S. Lin, and X. Cheng, "Point cloud registration method based on 3dmatch network and improved iss algorithm," in *ISCCER*. IEEE, 2022, pp. 161–166.
- [34] I. Sipiran and B. Bustos, "Harris 3d: a robust extension of the harris operator for interest point detection on 3d meshes," *TVC*, vol. 27, pp. 963–976, 2011.
- [35] A. Zaharescu, E. Boyer, K. Varanasi, and R. Horaud, "Surface feature detection and description with applications to mesh matching," in *Proc. CVPR*. IEEE, 2009, pp. 373–380.
- [36] E. Akagunduz and I. Ulusoy, "3d object representation using transform and scale invariant 3d features," in *Proc. ICCV*. IEEE, 2007, pp. 1–8.
- [37] J. Knopp, M. Prasad, G. Willems, R. Timofte, and L. Van Gool, "Hough transform and 3d surf for robust three dimensional classification," in *Proc. ECCV*. Springer, 2010, pp. 589–602.
- [38] J. Novatnack and K. Nishino, "Scale-dependent/invariant local 3d shape descriptors for fully automatic registration of multiple sets of range images," in *Proc. ECCV*. Springer, 2008, pp. 440–453.
- [39] R. Unnikrishnan and M. Hebert, "Multi-scale interest regions from unorganized point clouds," in *Proc. CVPR*. IEEE, 2008, pp. 1–8.
- [40] B. Steder, R. B. Rusu, K. Konolige, and W. Burgard, "Point feature extraction on 3d range scans taking into account object boundaries," in *Proc. ICRA*. IEEE, 2011, pp. 2601–2608.
- [41] S. Malassiotis and M. G. Strintzis, "Snapshots: A novel local surface descriptor and matching algorithm for robust 3d surface alignment," *TPAMI*, vol. 29, no. 7, pp. 1285–1290, 2007.
- [42] Y. Guo, F. Sohel, M. Bennamoun, M. Lu, and J. Wan, "Rotational projection statistics for 3d local surface description and object recognition," *IJCV*, vol. 105, pp. 63–86, 2013.
- [43] J. Yang, Q. Zhang, K. Xian, Y. Xiao, and Z. Cao, "Rotational contour signatures for both real-valued and binary feature representations of 3d local shape," *CVIU*, vol. 160, pp. 133–147, 2017.
- [44] J. Yang, Q. Zhang, Y. Xiao, and Z. Cao, "Toldi: An effective and robust approach for 3d local shape description," *PR*, vol. 65, pp. 175–187, 2017.
- [45] T. Sun, G. Liu, S. Liu, F. Meng, L. Zeng, and R. Li, "An efficient and compact 3d local descriptor based on the weighted height image," *Inf. Sci.*, vol. 520, pp. 209–231, 2020.
- [46] X. Liu, A. Li, J. Sun, and Z. Lu, "Trigonometric projection statistics histograms for 3d local feature representation and shape description," *PR*, vol. 143, p. 109727, 2023.
- [47] W. Tao, T. Lu, X. Chen, Z. Chen, W. Li, and M. Pang, "A local shape descriptor designed for registration of terrestrial point clouds," *TGRS*, 2024.
- [48] H. Shujuan, W. Shuangshuang, C. Lei, X. Feng, S. Chao, and Z. Wenjuan, "A 3d local feature description algorithm based on point distribution," *Comput. Electr. Eng.*, vol. 118, p. 109341, 2024.
- [49] F. Tombari, S. Salti, and L. Di Stefano, "Unique signatures of histograms for local surface description," in *Proc. ECCV*. Springer, 2010, pp. 356–369.
- [50] Y. Guo, F. Sohel, M. Bennamoun, J. Wan, and M. Lu, "A novel local surface feature for 3d object recognition under clutter and occlusion," *Inf. Sci.*, vol. 293, pp. 196–213, 2015.
- [51] F. Tombari, S. Salti, and L. Di Stefano, "A combined texture-shape descriptor for enhanced 3d feature matching," in *Proc. ICIP*. IEEE, 2011, pp. 809–812.
- [52] K. B. Logoglu, S. Kalkan, and A. Temizel, "Cospair: colored histograms of spatial concentric surflet-pairs for 3d object recognition," *Rob Auton Syst*, vol. 75, pp. 558–570, 2016.
- [53] Y. Zhang, C. Li, B. Guo, C. Guo, and S. Zhang, "Kdd: A kernel density based descriptor for 3d point clouds," *PR*, vol. 111, p. 107691, 2021.
- [54] D. L. Bibissi, J. Yang, S. Quan, and Y. Zhang, "Dual spin-image: A bi-directional spin-image variant using multi-scale radii for 3d local shape description," *CG*, vol. 103, pp. 180–191, 2022.
- [55] P. Joshi, V. Mukherjee, P. Garg, and V. Kumar, "3dhonr: A 3d object recognition using an efficient and fast low-dimensional 3d descriptor for a real-time application," in *Proc. ARSO*. IEEE, 2024, pp. 177–181.
- [56] K. Tang, P. Song, and X. Chen, "Signature of geometric centroids for 3d local shape description and partial shape matching," in *ACCV*. Springer, 2017, pp. 311–326.
- [57] S. M. Prakhya, B. Liu, and W. Lin, "B-shot: A binary feature descriptor for fast and efficient keypoint matching on 3d point clouds," in *Proc. IROS*. IEEE, 2015, pp. 1929–1934.
- [58] S. Quan, J. Ma, F. Hu, B. Fang, and T. Ma, "Local voxelized structure for 3d binary feature representation and robust registration of point clouds from low-cost sensors," *Inf. Sci.*, vol. 444, pp. 153–171, 2018.
- [59] Z. Yan, H. Wang, X. Liu, Q. Ning, and Y. Lu, "Binary feature description of 3d point cloud based on retina-like sampling on projection planes," *Machines*, vol. 10, no. 11, p. 984, 2022.
- [60] W. Tao, S. Xu, W. Huang, S. Hu, and M. Pang, "A distinctive binary descriptor and 2-point ransacwc for point cloud registration," *IEEE J-STARS*, 2023.
- [61] Z. Du, Y. Zuo, X. Song, Y. Wang, X. Hong, and J. Wu, "Efficient and accurate registration with bwph descriptor for low-quality point clouds," *Opt. Express*, vol. 31, no. 23, pp. 39307–39322, 2023.
- [62] N. J. Mitra and A. Nguyen, "Estimating surface normals in noisy point cloud data," in *Proc. SCG*, 2003, pp. 322–328.
- [63] R. B. Rusu, N. Blodow, Z. C. Marton, and M. Beetz, "Aligning point cloud views using persistent feature histograms," in *Proc. IROS*. IEEE, 2008, pp. 3384–3391.
- [64] R. B. Rusu, N. Blodow, and M. Beetz, "Fast point feature histograms (fpfh) for 3d registration," in *Proc. ICRA*. IEEE, 2009, pp. 3212–3217.
- [65] J. Yang, Z. Cao, and Q. Zhang, "A fast and robust local descriptor for 3d point cloud registration," *Inf. Sci.*, vol. 346, pp. 163–179, 2016.
- [66] A. G. Buch, D. Kraft, S. Robotics, and D. Odense, "Local point pair feature histogram for accurate 3d matching," in *BMVC*, 2018, p. 143.
- [67] H. Zhao, M. Tang, and H. Ding, "Hoppf: A novel local surface descriptor for 3d object recognition," *PR*, vol. 103, p. 107272, 2020.
- [68] B. Zhao, X. Le, and J. Xi, "A novel sclass descriptor for fully encoding the information of a 3d local surface," *Inf. Sci.*, vol. 483, pp. 363–382, 2019.
- [69] J. Yang, Q. Zhang, and Z. Cao, "Multi-attribute statistics histograms for accurate and robust pairwise registration of range images," *Neurocomputing*, vol. 251, pp. 54–67, 2017.
- [70] B. Zhao, Z. Wang, X. Chen, X. Fang, and Z. Jia, "Fapsh: An effective and robust local feature descriptor for 3d registration and object recognition," *PR*, vol. 151, p. 110354, 2024.
- [71] A. E. Johnson and M. Hebert, "Using spin images for efficient object recognition in cluttered 3d scenes," *TPAMI*, vol. 21, no. 5, pp. 433–449, 1999.
- [72] G. Hetzel, B. Leibe, P. Levi, and B. Schiele, "3d object recognition from range images using local feature histograms," in *Proc. CVPR*, vol. 2. IEEE, 2001, pp. II–394.
- [73] S. Ruiz-Correa, L. G. Shapiro, and M. Melia, "A new signature-based method for efficient 3-d object recognition," in *Proc. CVPR*, vol. 1. IEEE, 2001, pp. I–I.
- [74] A. Frome, D. Huber, R. Kolluri, T. Bülow, and J. Malik, "Recognizing objects in range data using regional point descriptors," in *Proc. ECCV*. Springer, 2004, pp. 224–237.
- [75] J. Yang, S. Fan, Z. Huang, S. Quan, W. Wang, and Y. Zhang, "Void: 3d object recognition based on voxelization in invariant distance space," *TVC*, vol. 39, no. 7, pp. 3073–3089, 2023.
- [76] C. Zhang, Y. Wang, Q. Wu, J. Zheng, J. Yang, S. Quan, and Y. Zhang, "Multi-scale point pair normal encoding for local feature description and 3d object recognition," *JEI*, vol. 33, no. 4, pp. 043005–043005, 2024.
- [77] L. Fang, T. Li, Y. Lin, S. Zhou, and W. Yao, "A radiometric correction based optical modeling approach to removing reflection noise in tls point clouds of urban scenes," *arXiv preprint arXiv:2407.02830*, 2024.
- [78] F. Stein and G. Medioni, "Structural indexing: Efficient 3-d object recognition," *TPAMI*, vol. 14, no. 2, pp. 125–145, 1992.
- [79] Y. Guo, F. Sohel, M. Bennamoun, M. Lu, and J. Wan, "Trisi: A distinctive local surface descriptor for 3d modeling and object recognition," in *Proc. GRAPP*, vol. 2. Scitepress, 2013, pp. 86–93.
- [80] E. Rodolà, A. Albarelli, F. Bergamasco, and A. Torsello, "A scale independent selection process for 3d object recognition in cluttered scenes," *IJCV*, vol. 102, no. 1-3, pp. 129–145, 2013.
- [81] M. A. Fischler and R. C. Bolles, "Random sample consensus: a paradigm for model fitting with applications to image analysis

- and automated cartography," *Commun. ACM*, vol. 24, no. 6, pp. 381–395, 1981.
- [82] M. Leordeanu and M. Hebert, "A spectral technique for correspondence problems using pairwise constraints," in *Proc. ICCV*, vol. 2. IEEE, 2005, pp. 1482–1489.
- [83] Q.-Y. Zhou, J. Park, and V. Koltun, "Fast global registration," in *Proc. ECCV*. Springer, 2016, pp. 766–782.
- [84] A. P. Bustos and T.-J. Chin, "Guaranteed outlier removal for point cloud registration with correspondences," *TPAMI*, vol. 40, no. 12, pp. 2868–2882, 2017.
- [85] D. Barath and J. Matas, "Graph-cut ransac: Local optimization on spatially coherent structures," *TPAMI*, vol. 44, no. 9, pp. 4961–4974, 2021.
- [86] S. Quan and J. Yang, "Compatibility-guided sampling consensus for 3-d point cloud registration," *TGRS*, vol. 58, no. 10, pp. 7380–7392, 2020.
- [87] D. Barath, J. Noskova, M. Ivashechkin, and J. Matas, "Magsac++, a fast, reliable and accurate robust estimator," in *Proc. CVPR*, 2020, pp. 1304–1312.
- [88] H. Yang, J. Shi, and L. Carlone, "Teaser: Fast and certifiable point cloud registration," *Trans. Robot.*, vol. 37, no. 2, pp. 314–333, 2020.
- [89] J. Li, "A practical $o(n^2)$ outlier removal method for correspondence-based point cloud registration," *TPAMI*, vol. 44, no. 8, pp. 3926–3939, 2021.
- [90] L. Sun and L. Deng, "Trivoc: Efficient voting-based consensus maximization for robust point cloud registration with extreme outlier ratios," *Robotics Auton. Lett.*, vol. 7, no. 2, pp. 4654–4661, 2022.
- [91] Z. Chen, K. Sun, F. Yang, L. Guo, and W. Tao, "Sc²-pcr++: Rethinking the generation and selection for efficient and robust point cloud registration," *TPAMI*, vol. 45, no. 10, pp. 12358–12376, 2023.
- [92] J. Yang, Z. Huang, S. Quan, Z. Qi, and Y. Zhang, "Sac-cot: Sample consensus by sampling compatibility triangles in graphs for 3-d point cloud registration," *TGRS*, vol. 60, pp. 1–15, 2021.
- [93] W. Chen, H. Li, Q. Nie, and Y.-H. Liu, "Deterministic point cloud registration via novel transformation decomposition," in *Proc. CVPR*, 2022, pp. 6348–6356.
- [94] L. Yan, P. Wei, H. Xie, J. Dai, H. Wu, and M. Huang, "A new outlier removal strategy based on reliability of correspondence graph for fast point cloud registration," *TPAMI*, vol. 45, no. 7, pp. 7986–8002, 2022.
- [95] J. Yang, X. Zhang, S. Fan, C. Ren, and Y. Zhang, "Mutual voting for ranking 3d correspondences," *TPAMI*, 2023.
- [96] X. Zhang, J. Yang, S. Zhang, and Y. Zhang, "3d registration with maximal cliques," in *Proc. CVPR*, 2023, pp. 17745–17754.
- [97] L. Sun, "Sucoft: Robust point cloud registration based on guaranteed supercore maximization and flexible thresholding," *TGRS*, 2024.
- [98] Z. Qiao, Z. Yu, B. Jiang, H. Yin, and S. Shen, "G3reg: Pyramid graph-based global registration using gaussian ellipsoid model," *Trans. Autom. Sci. Eng.*, 2024.
- [99] X. Xing, Z. Lu, Y. Wang, and J. Xiao, "Efficient single correspondence voting for point cloud registration," *TIP*, 2024.
- [100] T. Huang, L. Peng, R. Vidal, and Y.-H. Liu, "Scalable 3d registration via truncated entry-wise absolute residuals," in *Proc. CVPR*, 2024, pp. 27477–27487.
- [101] T. Huang, H. Li, L. Peng, Y. Liu, and Y.-H. Liu, "Efficient and robust point cloud registration via heuristics-guided parameter search," *TPAMI*, 2024.
- [102] J. Illingworth and J. Kittler, "A survey of the hough transform," *Comput. Vis. Graph. Image Process*, vol. 44, no. 1, pp. 87–116, 1988.
- [103] F. Tombari and L. Di Stefano, "Object recognition in 3d scenes with occlusions and clutter by hough voting," in *Proc. PSIVT*. IEEE, 2010, pp. 349–355.
- [104] O. J. Woodford, M.-T. Pham, A. Maki, F. Perbet, and B. Stenger, "Demisting the hough transform for 3d shape recognition and registration," *IJCV*, vol. 106, pp. 332–341, 2014.
- [105] A. G. Buch, Y. Yang, N. Krüger, and H. G. Petersen, "In search of inliers: 3d correspondence by local and global voting," in *Proc. CVPR*. IEEE, 2014, pp. 2075–2082.
- [106] H. Sahloul, S. Shirafuji, and J. Ota, "An accurate and efficient voting scheme for a maximally all-inlier 3d correspondence set," *TPAMI*, vol. 43, no. 7, pp. 2287–2298, 2020.
- [107] L. Wu, R. Jia, K. Zhong, Z. Li, J. Shang, and H. Luo, "A robust and accurate post-validation voting scheme for ranking 3d correspondences," in *Proc. ICCAI*, 2022, pp. 618–624.
- [108] J. Yang, Y. Xiao, Z. Cao, and W. Yang, "Ranking 3d feature correspondences via consistency voting," *PR Lett.*, vol. 117, pp. 1–8, 2019.
- [109] J. Yang, J. Chen, S. Quan, W. Wang, and Y. Zhang, "Correspondence selection with loose-tight geometric voting for 3-d point cloud registration," *TGRS*, vol. 60, pp. 1–14, 2022.
- [110] D. G. Lowe, "Distinctive image features from scale-invariant keypoints," *IJCV*, vol. 60, pp. 91–110, 2004.
- [111] A. Albarelli, E. Rodola, and A. Torsello, "A game-theoretic approach to fine surface registration without initial motion estimation," in *Proc. CVPR*. IEEE, 2010, pp. 430–437.
- [112] C. Olsson, F. Kahl, and M. Oskarsson, "Branch-and-bound methods for euclidean registration problems," *TPAMI*, vol. 31, no. 5, pp. 783–794, 2008.
- [113] J. Li, P. Shi, Q. Hu, and Y. Zhang, "Qgore: Quadratic-time guaranteed outlier removal for point cloud registration," *TPAMI*, vol. 45, no. 9, pp. 11136–11151, 2023.
- [114] P. Yin, S. Yuan, H. Cao, X. Ji, S. Zhang, and L. Xie, "Segregator: Global point cloud registration with semantic and geometric cues," in *Proc. ICRA*. IEEE, 2023, pp. 2848–2854.
- [115] P. C. Lusk, K. Fathian, and J. P. How, "Clipper: A graph-theoretic framework for robust data association," in *Proc. ICRA*. IEEE, 2021, pp. 13828–13834.
- [116] R. Li, X. Yuan, S. Gan, R. Bi, S. Gao, W. Luo, and C. Chen, "An effective point cloud registration method based on robust removal of outliers," *TGRS*, 2024.
- [117] Y. Zhang, H. Zhao, H. Li, and S. Chen, "Fastmac: Stochastic spectral sampling of correspondence graph," in *Proc. CVPR*, 2024, pp. 17857–17867.
- [118] P. H. Torr, S. J. Nasuto, and J. M. Bishop, "Napsac: High noise, high dimensional robust estimation-it's in the bag," in *BMVC*, vol. 2, 2002, p. 3.
- [119] O. Chum and J. Matas, "Matching with prosac-progressive sample consensus," in *Proc. CVPR*, vol. 1. IEEE, 2005, pp. 220–226.
- [120] K. Ni, H. Jin, and F. Dellaert, "Groupsac: Efficient consensus in the presence of groupings," in *Proc. ICCV*. IEEE, 2009, pp. 2193–2200.
- [121] C. S. Chen, Y. P. Hung, and J. B. Cheng, "Ransac-based darces: A new approach to fast automatic registration of partially overlapping range images," *TPAMI*, vol. 21, no. 11, pp. 1229–1234, 1999.
- [122] Y. Guo, M. Bennamoun, F. Sohel, M. Lu, and J. Wan, "An integrated framework for 3-d modeling, object detection, and pose estimation from point-clouds," *TIM*, vol. 64, no. 3, pp. 683–693, 2014.
- [123] J. Li, Q. Hu, and M. Ai, "Point cloud registration based on one-point ransac and scale-annealing biweight estimation," *TGRS*, vol. 59, no. 11, pp. 9716–9729, 2021.
- [124] P. H. Torr and A. Zisserman, "Mlesac: A new robust estimator with application to estimating image geometry," *Comput. Vis. Image Und.*, vol. 78, no. 1, pp. 138–156, 2000.
- [125] O. Chum and J. Matas, "Optimal randomized ransac," *TPAMI*, vol. 30, no. 8, pp. 1472–1482, 2008.
- [126] J. Yang, Z. Huang, S. Quan, Q. Zhang, Y. Zhang, and Z. Cao, "Toward efficient and robust metrics for ransac hypotheses and 3d rigid registration," *TCSVT*, vol. 32, no. 2, pp. 893–906, 2021.
- [127] O. Chum, J. Matas, and J. Kittler, "Locally optimized ransac," in *PR*. Springer, 2003, pp. 236–243.
- [128] D. Aiger, N. J. Mitra, and D. Cohen-Or, "4-points congruent sets for robust pairwise surface registration," in *Proc. SIGGRAPH*, 2008, pp. 1–10.
- [129] P. W. Theiler, J. D. Wegner, and K. Schindler, "Keypoint-based 4-points congruent sets—automated marker-less registration of laser scans," *ISPRS J. Photogramm. Remote Sens.*, vol. 96, pp. 149–163, 2014.
- [130] N. Mellado, D. Aiger, and N. J. Mitra, "Super 4pcs fast global pointcloud registration via smart indexing," in *Proc. CGF*, vol. 33, no. 5. Wiley Online Library, 2014, pp. 205–215.
- [131] M. Mohamad, D. Rappaport, and M. Greenspan, "Generalized 4-points congruent sets for 3d registration," in *Proc. 3DV*, vol. 1. IEEE, 2014, pp. 83–90.
- [132] M. Mohamad, M. T. Ahmed, D. Rappaport, and M. Greenspan, "Super generalized 4pcs for 3d registration," in *Proc. 3DV*. IEEE, 2015, pp. 598–606.
- [133] J. Huang, T.-H. Kwok, and C. Zhou, "V4pcs: Volumetric 4pcs algorithm for global registration," *J. Mech. Des.*, vol. 139, no. 11, p. 111403, 2017.

- registration by progressive distance extension," in *Proc. CVPR*, 2024, pp. 20816–20826.
- [187] R. Zhang, Z. Zhou, M. Sun, O. Ghasemalizadeh, C.-H. Kuo, R. Eustice, M. Ghaffari, and A. Sen, "Correspondence-free se (3) point cloud registration in rkhs via unsupervised equivariant learning," *arXiv*, 2024.
- [188] Y. Xie, B. Wang, S. Li, and J. Zhu, "Iterative feedback network for unsupervised point cloud registration," *RAL*, 2024.
- [189] M. Khoury, Q.-Y. Zhou, and V. Koltun, "Learning compact geometric features," in *Proc. ICCV*, 2017, pp. 153–61.
- [190] F. Poiesi and D. Boscaini, "Learning general and distinctive 3d local deep descriptors for point cloud registration," *TPAMI*, vol. 45, no. 3, pp. 3979–3985, 2022.
- [191] B. Zhao, Q. Liu, Z. Wang, X. Chen, Z. Jia, and D. Liang, "Ha-tinet: Learning a distinctive and general 3d local descriptor for point cloud registration," *TVCG*, 2024.
- [192] G. Zhao, Z. Guo, X. Wang, and H. Ma, "Spherenet: Learning a noise-robust and general descriptor for point cloud registration," *TGRS*, 2023.
- [193] X. Bai, Z. Luo, L. Zhou, H. Fu, L. Quan, and C.-L. Tai, "D3feat: Joint learning of dense detection and description of 3d local features," in *Proc. CVPR*, 2020, pp. 6359–6367.
- [194] Z. J. Yew and G. H. Lee, "3dfeat-net: Weakly supervised local 3d features for point cloud registration," in *Proc. ECCV*, 2018, pp. 607–623.
- [195] F. Lu, G. Chen, Y. Liu, Z. Qu, and A. Knoll, "Rskdd-net: Random sample-based keypoint detector and descriptor," in *Proc. NeurIPS*, 2020, pp. 21 297–21 308.
- [196] G. D. Pais, S. Ramalingam, V. M. Govindu, J. C. Nascimento, R. Chellappa, and P. Miraldo, "3dregnet: A deep neural network for 3d point registration," in *Proc. CVPR*, 2020, pp. 7193–7203.
- [197] C. Choy, W. Dong, and V. Koltun, "Deep global registration," in *Proc. CVPR*, 2020, pp. 2514–2523.
- [198] J. Lee, S. Kim, M. Cho, and J. Park, "Deep hough voting for robust global registration," in *Proc. ICCV*, 2021, pp. 15 994–16 003.
- [199] H. Jiang, Z. Dang, Z. Wei, J. Xie, J. Yang, and M. Salzmann, "Robust outlier rejection for 3d registration with variational bayes," in *Proc. CVPR*, 2023, pp. 1148–1157.
- [200] S. Guo, F. Tang, B. Liu, Y. Fu, and Y. Wu, "An accurate outlier rejection network with higher generalization ability for point cloud registration," *RAL*, vol. 8, no. 8, pp. 4649–4656, 2023.
- [201] J. Gao, C. Wang, Z. Ding, S. Chen, S. Xin, C. Tu, and W. Wang, "Deep-pe: A learning-based pose evaluator for point cloud registration," *arXiv*, 2024.
- [202] K. Slimani, C. Achard, and B. Tamadazte, "Rocnet++: Triangle-based descriptor for accurate and robust point cloud registration," *PR*, vol. 147, p. 110108, 2024.
- [203] K. Fischer, M. Simon, F. Olsner, S. Milz, H.-M. Gross, and P. Mader, "Stickypillars: Robust and efficient feature matching on point clouds using graph neural networks," in *Proc. CVPR*, 2021, pp. 313–323.
- [204] Y. Li and T. Harada, "Leopard: Learning partial point cloud matching in rigid and deformable scenes," in *Proc. CVPR*, 2022, pp. 5554–5564.
- [205] G. Chen, M. Wang, L. Yuan, Y. Yang, and Y. Yue, "Rethinking point cloud registration as masking and reconstruction," in *Proc. ICCV*, 2023, pp. 17717–17727.
- [206] A.-Q. Cao, G. Puy, A. Boulch, and R. Marlet, "Pcam: Product of cross-attention matrices for rigid registration of point clouds," in *Proc. ICCV*, 2021, pp. 13 229–13 238.
- [207] Y. Wu, Y. Zhang, X. Fan, M. Gong, Q. Miao, and W. Ma, "Inenet: Inliers estimation network with similarity learning for partial overlapping registration," *TCSVT*, vol. 33, no. 3, pp. 1413–1426, 2022.
- [208] F. Cao, L. Wang, and H. Ye, "Sharpconv: A novel graph method with plug-and-play sharpening convolution for point cloud registration," *TCSVT*, 2024.
- [209] W. Lu, G. Wan, Y. Zhou, X. Fu, P. Yuan, and S. Song, "Deepvcv: An end-to-end deep neural network for point cloud registration," in *Proc. ICCV*, 2019, pp. 12–21.
- [210] D. Lee, O. C. Hamsici, S. Feng, P. Sharma, and T. Gernoth, "Deeppro: Deep partial point cloud registration of objects," in *Proc. ICCV*, 2021, pp. 5683–5692.
- [211] Z. Zhang, J. Sun, Y. Dai, D. Zhou, X. Song, and M. He, "End-to-end learning the partial permutation matrix for robust 3d point cloud registration," in *Proc. AAAI*, vol. 36, no. 3, 2022, pp. 3399–3407.
- [212] G. Chen, M. Wang, Q. Zhang, L. Yuan, T. Liu, and Y. Yue, "Deep interactive full transformer framework for point cloud registration," in *Proc. ICRA*. IEEE, 2023, pp. 2825–2832.
- [213] H. Deng, T. Birdal, and S. Ilic, "3d local features for direct pairwise registration," in *Proc. CVPR*, 2019, pp. 3244–3253.
- [214] Y. Yang, C. Feng, Y. Shen, and D. Tian, "Foldingnet: Point cloud auto-encoder via deep grid deformation," in *Proc. CVPR*, 2018, pp. 206–215.
- [215] Z. Chen, F. Yang, and W. Tao, "Detarnet: Decoupling translation and rotation by siamese network for point cloud registration," in *Proc. AAAI*, vol. 36, no. 1, 2022, pp. 401–409.
- [216] H. Jiang, Z. Dang, S. Gu, J. Xie, M. Salzmann, and J. Yang, "Center-based decoupled point-cloud registration for 6d object pose estimation," in *Proc. ICCV*, 2023, pp. 3427–3437.
- [217] J. Sun, Z. Shen, Y. Wang, H. Bao, and X. Zhou, "Loftr: Detector-free local feature matching with transformers," in *Proc. CVPR*, 2021, pp. 8922–8931.
- [218] G. Chen, M. Wang, Y. Yang, L. Yuan, and Y. Yue, "Fast and robust point cloud registration with tree-based transformer," in *Proc. ICRA*. IEEE, 2024, pp. 773–780.
- [219] H. Cao, Y. Wang, and D. Li, "Dms: Low-overlap registration of 3d point clouds with double-layer multi-scale star-graph," *TVCG*, 2024.
- [220] Z. Wang, X. Xu, Y. Yao, N. Li, and Y. Liu, "Okr-net: Overlapping keypoints registration network for large-scale lidar point clouds," *RAL*, 2023.
- [221] Z. Zhao, J. Kang, L. Feng, J. Liang, Y. Ren, and B. Wu, "Lfa-net: Enhanced pointnet and assignable weights transformer network for partial-to-partial point cloud registration," *TCSVT*, 2024.
- [222] R. She, S. Wang, Q. Kang, K. Zhao, Y. Song, W. P. Tay, T. Geng, and X. Jian, "Posdiffnet: Positional neural diffusion for point cloud registration in a large field of view with perturbations," in *Proc. AAAI*, vol. 38, no. 1, 2024, pp. 231–239.
- [223] S. Pertigkiozoglou, E. Chatzipantazis, and K. Daniilidis, "Biequiformer: Bi-equivariant representations for global point cloud registration," *arXiv*, 2024.
- [224] Z. J. Yew and G. H. Lee, "Rpm-net: Robust point matching using learned features," in *Proc. CVPR*, 2020, pp. 11 824–11 833.
- [225] H. Jiang, M. Salzmann, Z. Dang, J. Xie, and J. Yang, "Se (3) diffusion model-based point cloud registration for robust 6d object pose estimation," in *Proc. NeurIPS*, 2024.
- [226] B. Wu, J. Ma, G. Chen, and P. An, "Feature interactive representation for point cloud registration," in *Proc. ICCV*, 2021, pp. 5530–5539.
- [227] Q. Li, C. Wang, C. Wen, and X. Li, "Deepsir: Deep semantic iterative registration for lidar point clouds," *PR*, vol. 137, p. 109306, 2023.
- [228] K. Fu, S. Liu, X. Luo, and M. Wang, "Robust point cloud registration framework based on deep graph matching," in *Proc. CVPR*, 2021, pp. 8893–8902.
- [229] Y. Aoki, H. Goforth, R. A. Srivatsan, and S. Lucey, "Pointnetlk: Robust & efficient point cloud registration using pointnet," in *Proc. CVPR*, 2019, pp. 7163–7172.
- [230] X. Li, J. K. Pontes, and S. Lucey, "Pointnetlk revisited," in *Proc. CVPR*, 2021, pp. 12763–12772.
- [231] H. Xu, N. Ye, G. Liu, B. Zeng, and S. Liu, "Finet: Dual branches feature interaction for partial-to-partial point cloud registration," in *Proc. AAAI*, vol. 36, no. 3, 2022, pp. 2848–2856.
- [232] J. L. Schonberger and J.-M. Frahm, "Structure-from-motion revisited," in *Proc. CVPR*, 2016, pp. 4104–4113.
- [233] X. Huang, G. Mei, and J. Zhang, "Feature-metric registration: A fast semi-supervised approach for robust point cloud registration without correspondences," in *Proc. CVPR*, 2020, pp. 11 366–11 374.
- [234] D. Liu, C. Chen, C. Xu, R. C. Qiu, and L. Chu, "Self-supervised point cloud registration with deep versatile descriptors for intelligent driving," *TITS*, vol. 24, no. 9, pp. 9767–9779, 2023.
- [235] Y. Yuan, Y. Wu, M. Yue, M. Gong, X. Fan, W. Ma, and Q. Miao, "Learning discriminative features via multi-hierarchical mutual information for unsupervised point cloud registration," *TCSVT*, 2024.
- [236] H. Jiang, Y. Shen, J. Xie, J. Li, J. Qian, and J. Yang, "Sampling network guided cross-entropy method for unsupervised point cloud registration," in *Proc. ICCV*, 2021, pp. 6128–6137.
- [237] P. Shi, J. Zhang, H. Cheng, J. Wang, Y. Zhou, C. Zhao, and J. Zhu, "Overlap bias matching is necessary for point cloud registration," *arXiv*, 2023.

- [238] F. Yu, Z. Xiao, Z. Chen, L. Liu, M. Jiang, X. Liu, X. Hu, and T. Peng, "Amcnet: Adaptive matching constraint for unsupervised point cloud registration," in *Proc. CGI*. Springer, 2023, pp. 56–68.
- [239] Y. Jiang, B. Zhou, X. Liu, Q. Li, and C. Cheng, "Gtinet: Global topology-aware interactions for unsupervised point cloud registration," *TCSVT*, 2024.
- [240] C. Zheng, M. Ma, Z. Chen, H. Chen, W. Wang, and M. Wei, "Regiformer: Unsupervised point cloud registration via geometric local-to-global transformer and self augmentation," *TGRS*, 2024.
- [241] J. Nie, X. Lu, Z. Shen, and Y. Wang, "Singlereg: An unsupervised registration method for point cloud with good generalization performance," *TIM*, 2024.
- [242] C. Löwens, T. Funke, A. Wagner, and A. P. Condurache, "Unsupervised point cloud registration with self-distillation," *arXiv*, 2024.
- [243] P. Kadam, M. Zhang, S. Liu, and C.-C. J. Kuo, "R-pointhop: A green, accurate, and unsupervised point cloud registration method," *TIP*, vol. 31, pp. 2710–2725, 2022.
- [244] M. Zhang, H. You, P. Kadam, S. Liu, and C.-C. J. Kuo, "Pointhop: An explainable machine learning method for point cloud classification," *TMM*, vol. 22, no. 7, pp. 1744–1755, 2020.
- [245] Z. Zhang, J. Sun, Y. Dai, D. Zhou, X. Song, and M. He, "A representation separation perspective to correspondence-free unsupervised 3-d point cloud registration," *TGRS*, vol. 19, pp. 1–5, 2021.
- [246] L. Li, H. Fu, and M. Ovsjanikov, "Wsdsc: Weakly supervised 3d local descriptor learning for point cloud registration," *TVCG*, vol. 29, no. 7, pp. 3368–3379, 2022.
- [247] X. Huang, S. Li, Y. Zuo, Y. Fang, J. Zhang, and X. Zhao, "Unsupervised point cloud registration by learning unified gaussian mixture models," *RAL*, vol. 7, no. 3, pp. 7028–7035, 2022.
- [248] Y. Hao and Y. Fang, "3d unsupervised region-aware registration transformer," in *Proc. ICIP*. IEEE, 2023, pp. 2780–2784.
- [249] X. Li, L. Wang, and Y. Fang, "Unsupervised category-specific partial point set registration via joint shape completion and registration," *TVCG*, vol. 29, no. 7, pp. 3251–3265, 2022.
- [250] M. El Banani, L. Gao, and J. Johnson, "Unsupervisedr&r: Unsupervised point cloud registration via differentiable rendering," in *Proc. CVPR*, 2021, pp. 7129–7139.
- [251] J. Liu, X. Lv, X. Gong, Y. Liang, and J. Hyypää, "An unsupervised learning network for large-scale lidar point clouds registration," *TVT*, 2024.
- [252] T. Birdal and S. Ilic, "Point pair features based object detection and pose estimation revisited," in *Proc. 3DV*. IEEE, 2015, pp. 527–535.
- [253] L. Sun, Z. Zhang, R. Zhong, D. Chen, L. Zhang, L. Zhu, Q. Wang, G. Wang, J. Zou, and Y. Wang, "A weakly supervised graph deep learning framework for point cloud registration," *TGRS*, vol. 60, pp. 1–12, 2022.
- [254] S. Horache, J.-E. Deschaut, and F. Goulette, "3d point cloud registration with multi-scale architecture and unsupervised transfer learning," in *Proc. 3DV*. IEEE, 2021, pp. 1351–1361.
- [255] P. J. Besl and N. D. McKay, "Method for registration of 3-d shapes," *IEEE Transactions on Pattern Analysis and Machine Intelligence*, vol. 14, no. 2, pp. 239–256, 1992.
- [256] Y. Chen and G. Medioni, "Object modelling by registration of multiple range images," *Image Vis Comput*, vol. 10, no. 3, pp. 145–155, 1992.
- [257] S. Rusinkiewicz and M. Levoy, "Efficient variants of the icp algorithm," in *Proc. 3DIM*, 2001, pp. 145–152.
- [258] A. W. Fitzgibbon, "Robust registration of 2d and 3d point sets," *Image and Vision Computing*, vol. 21, no. 13, pp. 1145–1153, 2003.
- [259] D. Chetverikov, D. Stepanov, and P. Krsek, "Robust euclidean alignment of 3d point sets: the trimmed iterative closest point algorithm," *Image Vis Comput*, vol. 23, no. 3, pp. 299–309, 2005.
- [260] A. Segal, D. Haehnel, and S. Thrun, "Generalized-icp." in *Proc. Robot Sci Syst*, vol. 2, no. 4. Seattle, WA, 2009, p. 435.
- [261] A. Myronenko and X. Song, "Point set registration: Coherent point drift," *TPAMI*, vol. 32, no. 12, pp. 2262–2275, 2010.
- [262] H. Men, B. Gebre, and K. Pochiraju, "Color point cloud registration with 4d icp algorithm," in *Proc. ICRA*. IEEE, 2011, pp. 1511–1516.
- [263] S. Bouaziz, A. Tagliasacchi, and M. Pauly, "Sparse iterative closest point," in *Proc. CGF*, vol. 32, no. 5. Wiley Online Library, 2013, pp. 113–123.
- [264] M. Korn, M. Holzkoth, and J. Pauli, "Color supported generalized-icp," in *Proc. VISAPP*, vol. 3. IEEE, 2014, pp. 592–599.
- [265] J. Serafin and G. Grisetti, "Nipc: Dense normal based point cloud registration," in *Proc. IROS*. IEEE, 2015, pp. 742–749.
- [266] A. L. Pavlov, G. W. Ovschinnikov, D. Y. Derbyshev, D. Tsetserukou, and I. V. Oseledets, "Aa-icp: Iterative closest point with anderson acceleration," in *Proc. ICRA*. IEEE, 2018, pp. 3407–3412.
- [267] S. Rusinkiewicz, "A symmetric objective function for icp," *TOG*, vol. 38, no. 4, pp. 1–7, 2019.
- [268] X. Zhang, Y. Zhang, C. Qu, and Z. Tan, "Fast and robust motion averaging via angle constraints of multi-view range scans," *J. Eng.*, vol. 2021, no. 2, pp. 104–113, 2021.
- [269] C. Lv, W. Lin, and B. Zhao, "Kss-icp: point cloud registration based on kendall shape space," *TIP*, vol. 32, pp. 1681–1693, 2023.
- [270] L. He, S. Wang, Q. Hu, Q. Cai, M. Li, Y. Bai, K. Wu, and B. Xiang, "Gfoicp: Geometric feature optimized iterative closest point for 3d point cloud registration," *TGRS*, 2023.
- [271] G. Turk and M. Levoy, "Zippered polygon meshes from range images," in *Proc. SIGGRAPH*, 1994, pp. 311–318.
- [272] T. Masuda and N. Yokoya, "A robust method for registration and segmentation of multiple range images," *Comput Vis Image Underst*, vol. 61, no. 3, pp. 295–307, 1995.
- [273] R. Benjema and F. Schmitt, "Fast global registration of 3d sampled surfaces using a multi-z-buffer technique," *Image Vis Comput*, vol. 17, no. 2, pp. 113–123, 1999.
- [274] Z. Zhang, "Iterative point matching for registration of free-form curves and surfaces," *IJCV*, vol. 13, no. 2, pp. 119–152, 1994.
- [275] J. Zhang, Y. Yao, and B. Deng, "Fast and robust iterative closest point," *TPAMI*, vol. 44, no. 7, pp. 3450–3466, 2021.
- [276] B. Jian and B. C. Vemuri, "A robust algorithm for point set registration using mixture of gaussians," in *Proc. ICCV*, vol. 2. IEEE, 2005, pp. 1246–1251.
- [277] —, "Robust point set registration using gaussian mixture models," *TPAMI*, vol. 33, no. 8, pp. 1633–1645, 2010.
- [278] W. Gao and R. Tedrake, "Filterreg: Robust and efficient probabilistic point-set registration using gaussian filter and twist parameterization," in *Proc. CVPR*, 2019, pp. 11 095–11 104.
- [279] D. F. Huber and M. Hebert, "Fully automatic registration of multiple 3d data sets," *IVC*, vol. 21, no. 7, pp. 637–650, 2003.
- [280] S. Salti, F. Tombari, and L. Di Stefano, "Shot: Unique signatures of histograms for surface and texture description," *CVIU*, vol. 125, pp. 251–264, 2014.
- [281] T. Masuda, "Log-polar height maps for multiple range image registration," *CVIU*, vol. 113, no. 11, pp. 1158–1169, 2009.
- [282] J. Zhu, L. Zhu, Z. Li, C. Li, and J. Cui, "Automatic multi-view registration of unordered range scans without feature extraction," *Neurocomputing*, vol. 171, pp. 1444–1453, 2016.
- [283] S. H. Lee and J. Civera, "Hara: A hierarchical approach for robust rotation averaging," in *Proc. CVPR*, 2022, pp. 15756–15765.
- [284] S. Fantoni, U. Castellani, and A. Fusiello, "Accurate and automatic alignment of range surfaces," in *Proc. ICIP*, 2012, pp. 73–80.
- [285] J. Yang, Y. Xiao, and Z. Cao, "Aligning 2.5d scene fragments with distinctive local geometric features and voting-based correspondences," *TCSVT*, vol. 29, no. 3, pp. 714–729, 2018.
- [286] J. Zhu, L. Zhu, Z. Jiang, X. Bai, Z. Li, and L. Wang, "Local to global registration of multi-view range scans using spanning tree," *Comput. Electr. Eng.*, vol. 58, pp. 477–488, 2017.
- [287] X. Cheng, Y. Liu, M. Zhang, and S. Yan, "Incremental multiview point cloud registration," *arXiv*, 2024.
- [288] Y. Guo, F. Sohel, M. Bennamoun, J. Wan, and M. Lu, "An accurate and robust range image registration algorithm for 3d object modeling," *TMM*, vol. 16, no. 5, pp. 1377–1390, 2014.
- [289] J. Zhu, S. Xu, Z. Jiang, S. Pang, J. Wang, and Z. Li, "Multi-view registration of unordered range scans by fast correspondence propagation of multi-scale descriptors," *arXiv*, 2018.
- [290] Q.-X. Huang, S. Flöry, N. Gelfand, M. Hofer, and H. Pottmann, "Reassembling fractured objects by geometric matching," *ToG*, vol. 25, no. 3, pp. 569–578, Jul. 2006.
- [291] S. Choi, Q.-Y. Zhou, and V. Koltun, "Robust reconstruction of indoor scenes," in *Proc. CVPR*, 2015, pp. 5556–5565.
- [292] X. Huang, Z. Liang, X. Zhou, Y. Xie, L. J. Guibas, and Q. Huang, "Learning Transformation Synchronization," in *Proc. CVPR*, 2019, pp. 8074–8083.
- [293] L. Ding and C. Feng, "Deepmapping: Unsupervised map estimation from multiple point clouds," in *Proc. CVPR*, 2019, pp. 8642–8651.

- [294] Z. Gojčić, C. Zhou, J. D. Wegner, L. J. Guibas, and T. Birdal, "Learning Multiview 3D Point Cloud Registration," in *Proc. CVPR*, 2020, pp. 1756–1766.
- [295] Z. J. Yew and G. H. Lee, "Learning iterative robust transformation synchronization," in *Proc. 3DV*, 2021, pp. 1206–1215.
- [296] H. Wang, Y. Liu, Z. Dong, Y. Guo, Y.-S. Liu, W. Wang, and B. Yang, "Robust multiview point cloud registration with reliable pose graph initialization and history reweighting," in *Proc. CVPR*, 2023, pp. 9506–9515.
- [297] J. Zhao, Q. Zhu, Y. Wang, W. Peng, H. Zhang, and J. Mao, "Registration of multiview point clouds with unknown overlap," *TMM*, 2023.
- [298] C. Chen, X. Liu, Y. Li, L. Ding, and C. Feng, "Deepmapping2: Self-supervised large-scale lidar map optimization," in *Proc. CVPR*, 2023, pp. 9306–9316.
- [299] S. Jin, I. Armeni, M. Pollefeys, and D. Baráth, "Multiway point cloud mosaicking with diffusion and global optimization," in *Proc. CVPR*, 2024, pp. 20838–20849.
- [300] Y. Hu, B. Li, C. Xu, S. Saydam, and W. Zhang, "Featsync: 3d point cloud multiview registration with attention feature-based refinement," *Neurocomputing*, vol. 600, p. 128088, 2024.
- [301] Y. Chen and G. Medioni, "Object modelling by registration of multiple range images," *IVC*, vol. 10, no. 3, pp. 145–155, 1992.
- [302] H. Gagnon, M. Soucy, R. Bergevin, and D. Laurendeau, "Registration of multiple range views for automatic 3-d model building," in *Proc. CVPR*. IEEE, 1994, pp. 581–586.
- [303] K. Pulli, "Multiview registration for large data sets," in *Proc. 2nd Int. Conf. 3-D Digit. Imaging Model.* IEEE, 1999, pp. 160–168.
- [304] R. Bergevin, M. Soucy, H. Gagnon, and D. Laurendeau, "Towards a general multi-view registration technique," *TPAMI*, vol. 18, no. 5, pp. 540–547, 1996.
- [305] R. Benjema and F. Schmitt, "Fast global registration of 3d sampled surfaces using a multi-z-buffer technique," in *Proc. ICRA*, 1997, pp. 113–120.
- [306] A. E. Johnson and S. B. Kang, "Registration and integration of textured 3d data," *IVC*, vol. 17, no. 2, pp. 135–147, 1999.
- [307] R. Toldo, A. Beinat, F. Crosilla *et al.*, "Global registration of multiple point clouds embedding the generalized procrustes analysis into an icp framework," in *Proc. 3DPVT*, vol. 2, 2010, p. 5.
- [308] J. Williams and M. Bennamoun, "Simultaneous registration of multiple corresponding point sets," *CVIU*, vol. 81, no. 1, pp. 117–142, 2001.
- [309] S. Fantoni, U. Castellani, and A. Fusiello, "Accurate and automatic alignment of range surfaces," in *Proc. 3DIMPVT*. IEEE, 2012, pp. 73–80.
- [310] Y. Tang and J. Feng, "Hierarchical multiview rigid registration," *CGF*, vol. 34, no. 5, pp. 77–87, 2015.
- [311] H. Wu, L. Yan, H. Xie, P. Wei, and J. Dai, "A hierarchical multiview registration framework of tfs point clouds based on loop constraint," *ISPRS*, vol. 195, pp. 65–76, 2023.
- [312] S. Zhang, J. Yang, Z. Qi, and Y. Zhang, "Toward meta-shape based multi-view 3d point cloud registration: An evaluation," *TCSVT*, 2023.
- [313] J. Zhu, Z. Li, S. Du, L. Ma, and T. Zhang, "Surface reconstruction via efficient and accurate registration of multiview range scans," *Opt. Eng.*, vol. 53, no. 10, pp. 102104–102104, 2014.
- [314] J. Yang, Y. Xiao, and Z. Cao, "Aligning 2.5 d scene fragments with distinctive local geometric features and voting-based correspondences," *TCSVT*, vol. 29, no. 3, pp. 714–729, 2018.
- [315] J. Zhu, Z. Jiang, G. D. Evangelidis, C. Zhang, S. Pang, and Z. Li, "Efficient registration of multi-view point sets by k-means clustering," *Inf. Sci.*, vol. 488, pp. 205–218, 2019.
- [316] R. Guo, J. Chen, and L. Wang, "Hierarchical k-means clustering for registration of multi-view point sets," *Comput. Electr. Eng.*, vol. 94, p. 107321, 2021.
- [317] S. Li, J. Zhu, Y. Xie, and M. Zhu, "Incremental multiview point cloud registration with two-stage candidate retrieval," *arXiv*, 2024.
- [318] G. D. Evangelidis, D. Kounades-Bastian, R. Horaud, and E. Z. Psarakis, "A generative model for the joint registration of multiple point sets," in *Proc. ECCV*. Springer, 2014, pp. 109–122.
- [319] G. D. Evangelidis and R. Horaud, "Joint alignment of multiple point sets with batch and incremental expectation-maximization," *TPAMI*, vol. 40, no. 6, pp. 1397–1410, 2017.
- [320] Y. Zhou, S. Xu, C. Jin, and Z. Guo, "Multiple point sets registration based on expectation maximization algorithm," *Comput. Electr. Eng.*, vol. 70, pp. 1–11, 2018.
- [321] N. Ravikumar, A. Gooya, S. Çimen, A. F. Frangi, and Z. A. Taylor, "Group-wise similarity registration of point sets using student's t-mixture model for statistical shape models," *MEDIA*, vol. 44, pp. 156–176, 2018.
- [322] Z. Min, J. Wang, and M. Q.-H. Meng, "Joint rigid registration of multiple generalized point sets with hybrid mixture models," *TASE*, vol. 17, no. 1, pp. 334–347, 2019.
- [323] J. Zhang, M. Zhao, X. Jiang, and D.-M. Yan, "Robust multi-view registration of point sets with laplacian mixture model," in *Proc. ACPR*. Springer, 2021, pp. 547–561.
- [324] B. Eckart, K. Kim, and J. Kautz, "Hgmr: Hierarchical gaussian mixtures for adaptive 3d registration," in *Proc. ECCV*. Springer, 2018, pp. 705–721.
- [325] J. Zhu, R. Guo, Z. Li, J. Zhang, and S. Pang, "Registration of multi-view point sets under the perspective of expectation-maximization," *TIP*, vol. 29, pp. 9176–9189, 2020.
- [326] W. Liu, H. Wu, and G. S. Chirikjian, "Lsg-cpd: Coherent point drift with local surface geometry for point cloud registration," in *Proc. ICCV*, 2021, pp. 15293–15302.
- [327] P. Biber and W. Straßer, "The normal distributions transform: A new approach to laser scan matching," in *Proc. IROS*, vol. 3. IEEE, 2003, pp. 2743–2748.
- [328] J. Zhu, J. Mu, C.-B. Yan, D. Wang, and Z. Li, "3dmndt: 3d multi-view registration method based on the normal distributions transform," *TASE*, vol. 21, no. 1, pp. 488–501, 2022.
- [329] R. Benjema and F. Schmitt, "A solution for the registration of multiple 3d point sets using unit quaternions," in *Proc. ECCV*. Springer, 1998, pp. 34–50.
- [330] U. Castellani, A. Fusiello, and V. Murino, "Registration of multiple acoustic range views for underwater scene reconstruction," *CVIU*, vol. 87, no. 1-3, pp. 78–89, 2002.
- [331] V. M. Govindu, "Lie-algebraic averaging for globally consistent motion estimation," in *Proc. CVPR*, vol. 1. IEEE, 2004, pp. I–I.
- [332] G. C. Sharp, S. W. Lee, and D. K. Wehe, "Multiview registration of 3d scenes by minimizing error between coordinate frames," *TPAMI*, vol. 26, no. 8, pp. 1037–1050, 2004.
- [333] S. Krishnan, P. Y. Lee, J. B. Moore, S. Venkatasubramanian *et al.*, "Global registration of multiple 3d point sets via optimization-on-a-manifold," in *Proc. SGP*. Citeseer, 2005, pp. 187–196.
- [334] F. Wang, B. C. Vemuri, and A. Rangarajan, "Groupwise point pattern registration using a novel cdf-based jensen-shannon divergence," in *Proc. CVPR*, vol. 1. IEEE, 2006, pp. 1283–1288.
- [335] S.-W. Shih, Y.-T. Chuang, and T.-Y. Yu, "An efficient and accurate method for the relaxation of multiview registration error," *TIP*, vol. 17, no. 6, pp. 968–981, 2008.
- [336] A. Pooja and V. M. Govindu, "A multi-view extension of the icp algorithm," in *Proc. 7th Ind. Conf. Comput. Vis. Graph. Image Process.*, 2010, pp. 235–242.
- [337] T. Chen, B. C. Vemuri, A. Rangarajan, and S. J. Eisenschenk, "Group-wise point-set registration using a novel cdf-based havrda-charvát divergence," *IJCV*, vol. 86, pp. 111–124, 2010.
- [338] A. Torsello, E. Rodolà, and A. Albarelli, "Multiview registration via graph diffusion of dual quaternions," in *Proc. CVPR*. IEEE, 2011, pp. 2441–2448.
- [339] X. Shao, Y. Shi, Y. Duan, H. Zhao, and R. Shibasaki, "Closed-loop multiple view registration," in *Proc. ROBIO*. IEEE, 2012, pp. 452–457.
- [340] K. N. Chaudhury, Y. Khoo, and A. Singer, "Global registration of multiple point clouds using semidefinite programming," *SIAM J. Optim.*, vol. 25, no. 1, pp. 468–501, 2015.
- [341] F. Arrigoni, B. Rossi, and A. Fusiello, "Global registration of 3d point sets via lrs decomposition," in *Proc. ECCV*. Springer, 2016, pp. 489–504.
- [342] F. Arrigoni, B. Rossi, P. Fragneto, and A. Fusiello, "Robust synchronization in so (3) and se (3) via low-rank and sparse matrix decomposition," *CVIU*, vol. 174, pp. 95–113, 2018.
- [343] Z. Jiang, J. Zhu, Y. Li, J. Wang, Z. Li, and H. Lu, "Simultaneous merging multiple grid maps using the robust motion averaging," *J. Intell. Robot. Syst.*, vol. 94, pp. 655–668, 2019.
- [344] P. Miraldo, S. Saha, and S. Ramalingam, "Minimal solvers for mini-loop closures in 3d multi-scan alignment," in *Proc. CVPR*. IEEE, 2019, pp. 9699–9708.
- [345] L. G. Sanchez Giraldo, E. Hasanbelliu, M. Rao, and J. C. Principe, "Group-wise point-set registration based on renyi's second order entropy," in *Proc. CVPR*. IEEE, 2017, pp. 6693–6701.

- [346] S. Krishnan, P. Y. Lee, J. B. Moore, and S. Venkatasubramanian, "Optimisation-on-a-manifold for global registration of multiple 3d point sets," *IJISTA*, vol. 3, no. 3-4, pp. 319–340, 2007.
- [347] F. Bonarrigo and A. Signoroni, "Global registration of large collections of range images with an improved optimization-on-a-manifold approach," *IVC*, vol. 32, no. 6-7, pp. 437–451, 2014.
- [348] S. M. Ahmed and K. N. Chaudhury, "Global multiview registration using non-convex admn," in *Proc. ICIP*. IEEE, 2017, pp. 987–991.
- [349] S. M. Ahmed, N. R. Das, and K. N. Chaudhury, "Least-squares registration of point sets over se (d) using closed-form projections," *CVIU*, vol. 183, pp. 20–32, 2019.
- [350] J. P. Iglesias, C. Olsson, and F. Kahl, "Global optimality for point set registration using semidefinite programming," in *Proc. CVPR*. IEEE, 2020, pp. 8287–8295.
- [351] A. Fusiello, U. Castellani, L. Ronchetti, and V. Murino, "Model acquisition by registration of multiple acoustic range views," in *Proc. ECCV*. Springer, 2002, pp. 805–819.
- [352] V. M. Govindu, "Robustness in motion averaging," in *Proc. ACCV*. Springer, 2006, pp. 457–466.
- [353] V. M. Govindu and A. Pooja, "On averaging multiview relations for 3d scan registration," *TIP*, vol. 23, no. 3, pp. 1289–1302, 2013.
- [354] J. Zhu, L. Zhu, Z. Jiang, Z. Li, C. Li, and F. Zhang, "Scaling registration of multiview range scans via motion averaging," *J. Electron. Imaging*, vol. 25, no. 4, pp. 043 021–043 021, 2016.
- [355] R. Guo, J. Zhu, Y. Li, D. Chen, Z. Li, and Y. Zhang, "Weighted motion averaging for the registration of multi-view range scans," *Multimed. Tools. Appl.*, vol. 77, pp. 10 651–10 668, 2018.
- [356] D. S. Pankaj and R. R. Nidamanuri, "Robust algorithm for multiview registration," *IET Comput. Vis.*, vol. 11, no. 1, pp. 96–103, 2017.
- [357] Z. Jiang, J. Zhu, Z. Lin, Z. Li, and R. Guo, "3d mapping of outdoor environments by scan matching and motion averaging," *Neurocomputing*, vol. 372, pp. 17–32, 2020.
- [358] U. Bhattacharya and V. M. Govindu, "Efficient and robust registration on the 3d special euclidean group," in *Proc. ICCV*. IEEE, 2019, pp. 5885–5894.
- [359] J. Zhu, J. Hu, H. Lu, B. Chen, Z. Li, and Y. Li, "Robust motion averaging under maximum correntropy criterion," in *Proc. ICRA*. IEEE, 2021, pp. 5283–5288.
- [360] G. Bourmaud, "Online variational bayesian motion averaging," in *Proc. ECCV*. Springer, 2016, pp. 126–142.
- [361] C. Jin, J. Zhu, Y. Li, S. Pang, L. Chen, and J. Wang, "Multi-view registration based on weighted lrs matrix decomposition of motions," *IET Comput. Vis.*, vol. 13, no. 4, pp. 376–384, 2019.
- [362] S. Wang, H.-Y. Sun, H.-C. Guo, L. Du, and T.-J. Liu, "Multi-view laser point cloud global registration for a single object," *Sensors*, vol. 18, no. 11, p. 3729, 2018.
- [363] Z. Li, J. Liu, Z. Tian, J. Zhu, C. Li, and S. Du, "Adaptive weighted motion averaging with low-rank sparse for robust multi-view registration," *Neurocomputing*, vol. 413, pp. 230–239, 2020.
- [364] Y. Liu, W. Zhou, Z. Yang, J. Deng, and L. Liu, "Globally consistent rigid registration," *Graph. Models*, vol. 76, no. 5, pp. 542–553, 2014.
- [365] X. Shao, Y. Shi, H. Zhao, X. Li, and R. Shibasaki, "Efficient closed-loop multiple-view registration," *Trans. Intell. Transp. Syst.*, vol. 15, no. 6, pp. 2524–2538, 2014.
- [366] S. Du, N. Zheng, S. Ying, and J. Wei, "Icp with bounded scale for registration of md point sets," in *Proc. ICME*. IEEE, 2007, pp. 1291–1294.
- [367] S. Du, N. Zheng, S. Ying, Q. You, and Y. Wu, "An extension of the icp algorithm considering scale factor," in *Proc. ICIP*, vol. 5. IEEE, 2007, pp. V–193.
- [368] S. Ying, J. Peng, S. Du, and H. Qiao, "A scale stretch method based on icp for 3d data registration," *IEEE T-ASE*, vol. 6, no. 3, pp. 559–565, 2009.
- [369] S. Du, N. Zheng, L. Xiong, S. Ying, and J. Xue, "Scaling iterative closest point algorithm for registration of m-d point sets," *JVCI*, vol. 21, no. 5-6, pp. 442–452, 2010.
- [370] M.-T. Pham, O. J. Woodford, F. Perbet, A. Maki, B. Stenger, and R. Cipolla, "A new distance for scale-invariant 3d shape recognition and registration," in *Proc. ICCV*. IEEE, 2011, pp. 145–152.
- [371] B. Lin, T. Tamaki, B. Raytchev, K. Kaneda, and K. Ichii, "Scale ratio icp for 3d point clouds with different scales," in *Proc. ICIP*. IEEE, 2013, pp. 2217–2221.
- [372] B. Lin, T. Tamaki, F. Zhao, B. Raytchev, K. Kaneda, and K. Ichii, "Scale alignment of 3d point clouds with different scales," *Mach Vision Appl*, vol. 25, pp. 1989–2002, 2014.
- [373] N. Mellado, M. Dellepiane, and R. Scopigno, "Relative scale estimation and 3d registration of multi-modal geometry using growing least squares," *TVCG*, vol. 22, no. 9, pp. 2160–2173, 2015.
- [374] S. Du, J. Liu, B. Bi, J. Zhu, and J. Xue, "New iterative closest point algorithm for isotropic scaling registration of point sets with noise," *JVCI*, vol. 38, pp. 207–216, 2016.
- [375] X. Huang, J. Zhang, Q. Wu, L. Fan, and C. Yuan, "A coarse-to-fine algorithm for registration in 3d street-view cross-source point clouds," in *Proc. DICTA*. IEEE, 2016, pp. 1–6.
- [376] B. Lin, F. Wang, F. Zhao, and Y. Sun, "Scale invariant point feature (sipf) for 3d point clouds and 3d multi-scale object detection," *Neural Comput Appl*, vol. 29, no. 5, pp. 1209–1224, 2018.
- [377] H. Bülow and A. Birk, "Scale-free registrations in 3d: 7 degrees of freedom with fourier mellin soft transforms," *IJCV*, vol. 126, pp. 731–750, 2018.
- [378] B. Lin, F. Wang, and Y. Sun, "Sgicp-based point cloud scale estimation and alignment algorithm," *Computer Applications and Software*, vol. 35, no. 5, pp. 202–207, 2018.
- [379] S. Xu, J. Zhu, Y. Li, J. Wang, and H. Lu, "Effective scaling registration approach by imposing emphasis on scale factor," *Electron Lett*, vol. 54, no. 7, pp. 422–424, 2018.
- [380] Y. Sahillioğlu and L. Kavan, "Scale-adaptive icp," *Graph Models*, vol. 116, p. 101113, 2021.
- [381] P. Yu, Y. Yang, A. Tian, C. Du, X. Liu, B. Pei, K. Gu, Y. Guo, and S. Che, "An improved icp point cloud registration algorithm based on three-points congruent sets," in *Proc. AIAM*. IEEE, 2021, pp. 407–411.
- [382] Y. You, R. Shi, W. Wang, and C. Lu, "Cpfp: Towards robust category-level 9d pose estimation in the wild," in *Proc. CVPR*. IEEE, 2022, pp. 6866–6875.
- [383] J. Gao, Y. Zhang, Z. Liu, and S. Li, "Hdrnet: High-dimensional regression network for point cloud registration," in *Proc. CGF*, vol. 42, no. 1. Wiley Online Library, 2023, pp. 33–46.
- [384] C. Lv, W. Lin, and B. Zhao, "Kss-icp: point cloud registration based on kendall shape space," *TIP*, vol. 32, pp. 1681–1693, 2023.
- [385] C. Zheng and B. Liu, "Cross-source point cloud registration algorithm based on multiple filters," in *Proc. EITCE*, 2023, pp. 686–691.
- [386] B. Lin, F. Wang, Y. Sun, W. Qu, Z. Chen, and S. Zhang, "Boundary points based scale invariant 3d point feature," *JVCI*, vol. 48, pp. 136–148, 2017.
- [387] J. Lim and K. Lee, "3d object recognition using scale-invariant features," *TVC*, vol. 35, pp. 71–84, 2019.
- [388] T. Zinßer, J. Schmidt, and H. Niemann, "Point set registration with integrated scale estimation," in *Proc. ICPR*. IEEE, 2005, pp. 116–119.
- [389] Z. Wu, H. Chen, S. Du, M. Fu, N. Zhou, and N. Zheng, "Correntropy based scale icp algorithm for robust point set registration," *Pattern Recogn.*, vol. 93, pp. 14–24, 2019.
- [390] A. Chen, J. Zhuang, and X. Han, "An improved icp algorithm for 3d point cloud registration," in *Proc. PRML*. IEEE, 2022, pp. 205–210.
- [391] T. Tamaki, S. Tanigawa, Y. Ueno, B. Raytchev, and K. Kaneda, "Scale matching of 3d point clouds by finding key scales with spin images," in *Proc. ICPR*. IEEE, 2010, pp. 3480–3483.
- [392] X. Lian and Y. Bai, "3d-sift point cloud registration method integrating curvature information," in *Proc. ICCT*. IEEE, 2023, pp. 181–186.
- [393] Y. Wang, S. Li, Y. Yang, and Q. Shu, "Scale point cloud registration algorithm based on oriented bounding," *Laser Journal*, vol. 43, no. 1, p. 7, 2022.
- [394] F. Peng, Q. Wu, L. Fan, J. Zhang, Y. You, J. Lu, and J.-Y. Yang, "Street view cross-sourced point cloud matching and registration," in *Proc. ICIP*. IEEE, 2014, pp. 2026–2030.
- [395] X. Huang, J. Zhang, L. Fan, Q. Wu, and C. Yuan, "A systematic approach for cross-source point cloud registration by preserving macro and micro structures," *TIP*, vol. 26, no. 7, pp. 3261–3276, 2017.
- [396] X. Huang, J. Zhang, Q. Wu, L. Fan, and C. Yuan, "A coarse-to-fine algorithm for matching and registration in 3d cross-source point clouds," *TCSVT*, vol. 28, no. 10, pp. 2965–2977, 2017.
- [397] X. Huang, G. Mei, and J. Zhang, "Feature-metric registration: A fast semi-supervised approach for robust point cloud registration

- without correspondences," in *Proc. CVPR*. IEEE, 2020, pp. 11 366–11 374.
- [398] M. Zhao, X. Huang, J. Jiang, L. Mou, D.-M. Yan, and L. Ma, "Accurate registration of cross-modality geometry via consistent clustering," *TVCG*, 2023.
- [399] K. Xiong, M. Zheng, Q. Xu, C. Wen, S. Shen, and C. Wang, "Speal: Skeletal prior embedded attention learning for cross-source point cloud registration," in *Proc. AAAI*, vol. 38, no. 6, 2024, pp. 6279–6287.
- [400] G. Zhao, Z. Du, Z. Guo, and H. Ma, "Vrhcf: Cross-source point cloud registration via voxel representation and hierarchical correspondence filtering," *arXiv*, 2024.
- [401] X. Yang, H. Wang, Z. Dong, Y. Liu, Y. Li, and B. Yang, "A novel method for registration of mls and stereo reconstructed point clouds," *TGRS*, 2024.
- [402] N. Ma, M. Wang, Y. Han, and Y.-J. Liu, "Ff-logo: Cross-modality point cloud registration with feature filtering and local to global optimization," in *Proc. ICRA*. IEEE, 2024, pp. 744–750.
- [403] R. A. Persad and C. Armenakis, "Automatic co-registration of 3d multi-sensor point clouds," *Isprs J Photogram*, vol. 130, pp. 162–186, 2017.
- [404] J. Li, Q. Hu, and M. Ai, "Point cloud registration based on one-point ransac and scale-annealing biweight estimation," *TGRS*, vol. 59, no. 11, pp. 9716–9729, 2021.
- [405] A. E. Johnson and S. B. Kang, "Registration and integration of textured 3d data," *IVC*, vol. 17, no. 2, pp. 135–147, 1999.
- [406] G. Godin, D. Laurendeau, and R. Bergevin, "A method for the registration of attributed range images," in *Proc. 3DIM*. IEEE, 2001, pp. 179–186.
- [407] L. Douadi, M.-j. Aldon, and A. Crosnier, "Pair-wise registration of 3d/color data sets with icp," in *Proc. IROS*. IEEE, 2006, pp. 663–668.
- [408] J. Park, Q.-Y. Zhou, and V. Koltun, "Colored point cloud registration revisited," in *Proc. ICCV*. IEEE, 2017, pp. 143–152.
- [409] W. Chen, Y. Yang, D. Fan, Z. Chen, and Q. Kou, "Registration of color point cloud by combining with color moments information," in *Proc. SMC*. IEEE, 2018, pp. 2102–2108.
- [410] O. Choi, M.-G. Park, and Y. Hwang, "Iterative k-closest point algorithms for colored point cloud registration," *Sensors*, vol. 20, no. 18, p. 5331, 2020.
- [411] Y. Zhang, J. Yu, X. Huang, W. Zhou, and J. Hou, "Pcr-cg: Point cloud registration via deep explicit color and geometry," in *Proc. ECCV*. Springer, 2022, pp. 443–459.
- [412] T. Wan, S. Du, W. Cui, R. Yao, Y. Ge, C. Li, Y. Gao, and N. Zheng, "Rgb-d point cloud registration based on salient object detection," *TNNLS*, vol. 33, no. 8, pp. 3547–3559, 2021.
- [413] H. Chen, Z. Wei, Y. Xu, M. Wei, and J. Wang, "Imlovenet: Misaligned image-supported registration network for low-overlap point cloud pairs," in *Proc. SIGGRAPH*. ACM, 2022, pp. 1–9.
- [414] Z. Wang, X. Huo, Z. Chen, J. Zhang, L. Sheng, and D. Xu, "Improving rgb-d point cloud registration by learning multi-scale local linear transformation," in *Proc. ECCV*. Springer, 2022, pp. 175–191.
- [415] X. Huang, W. Qu, Y. Zuo, Y. Fang, and X. Zhao, "Imfnet: Interpretable multimodal fusion for point cloud registration," *RAL*, vol. 7, no. 4, pp. 12323–12330, 2022.
- [416] M. Yuan, K. Fu, Z. Li, Y. Meng, and M. Wang, "Pointmbf: A multi-scale bidirectional fusion network for unsupervised rgb-d point cloud registration," in *Proc. ICCV*. IEEE, 2023, pp. 17 694–17 705.
- [417] T. Han, R. Zhang, J. Kan, R. Dong, X. Zhao, and S. Yao, "A point cloud registration framework with color information integration," *Remote Sensing*, vol. 16, no. 5, p. 743, 2024.
- [418] S. Fung, X. Lu, D. d. S. Edirimuni, W. Pan, X. Liu, and H. Li, "Semreg: Semantics constrained point cloud registration," in *Proc. ECCV*. Springer, 2025, pp. 293–310.
- [419] C. Chen, X. Jia, Y. Zheng, and Y. Qu, "Rgb-d-glue: General feature combination for robust rgb-d point cloud registration," *arXiv*, 2024.
- [420] Q. Ye, H. Liu, and Y. Lin, "Study of rgb-d point cloud registration method guided by color information," in *Proc. CIOP*, vol. 10964. SPIE, 2018, pp. 616–624.
- [421] T. Wan, S. Du, Y. Xu, G. Xu, Z. Li, B. Chen, and Y. Gao, "Rgb-d point cloud registration via infrared and color camera," *Multimed Tools Appl*, vol. 78, pp. 33 223–33 246, 2019.
- [422] Y. Yang, W. Chen, M. Wang, D. Zhong, and S. Du, "Color point cloud registration based on supervoxel correspondence," *IEEE Access*, vol. 8, pp. 7362–7372, 2020.
- [423] O. Choi and W. Hwang, "Colored point cloud registration by depth filtering," *Sensors*, vol. 21, no. 21, p. 7023, 2021.
- [424] D. Liu, D. Hong, S. Wang, and Y. Chen, "Genetic algorithm-based optimization for color point cloud registration," *Front Bioeng Biotech*, vol. 10, p. 923736, 2022.
- [425] W. Zhou, L. Ren, J. Yu, N. Qu, and G. Dai, "Boosting rgb-d point cloud registration via explicit position-aware geometric embedding," *RAL*, 2024.
- [426] C. Yan, M. Feng, Z. Wu, Y. Guo, W. Dong, Y. Wang, and A. Mian, "Discriminative correspondence estimation for unsupervised rgb-d point cloud registration," *TCSVT*, 2024.
- [427] B. Drost, M. Ulrich, N. Navab, and S. Ilic, "Model globally, match locally: Efficient and robust 3d object recognition," in *Proc. CVPR*. IEEE, 2010, pp. 998–1005.
- [428] E. Kim and G. Medioni, "3d object recognition in range images using visibility context," in *Proc. IROS*. IEEE, 2011, pp. 3800–3807.
- [429] C. Choi, Y. Taguchi, O. Tuzel, M.-Y. Liu, and S. Ramalingam, "Voting-based pose estimation for robotic assembly using a 3d sensor," in *Proc. ICRA*. IEEE, 2012, pp. 1724–1731.
- [430] B. Drost and S. Ilic, "3d object detection and localization using multimodal point pair features," in *Proc. 3DIMPVT*. IEEE, 2012, pp. 9–16.
- [431] L. Magri and A. Fusiello, "T-linkage: A continuous relaxation of j-linkage for multi-model fitting," in *Proc. CVPR*. IEEE, 2014, pp. 3954–3961.
- [432] O. Tuzel, M.-Y. Liu, Y. Taguchi, and A. Raghunathan, "Learning to rank 3d features," in *Proc. ECCV*. Springer, 2014, pp. 520–535.
- [433] T. Birdal and S. Ilic, "Point pair features based object detection and pose estimation revisited," in *Proc. 3DV*. IEEE, 2015, pp. 527–535.
- [434] L. Magri and A. Fusiello, "Multiple model fitting as a set coverage problem," in *Proc. CVPR*. IEEE, 2016, pp. 3318–3326.
- [435] D. Barath and J. Matas, "Multi-class model fitting by energy minimization and mode-seeking," in *Proc. ECCV*. Springer, 2018, pp. 221–236.
- [436] —, "Progressive-x: Efficient, anytime, multi-model fitting algorithm," in *Proc. ICCV*. IEEE, 2019, pp. 3780–3788.
- [437] D. Li, H. Wang, N. Liu, X. Wang, and J. Xu, "3d object recognition and pose estimation from point cloud using stably observed point pair feature," *IEEE Access*, vol. 8, pp. 44 335–44 345, 2020.
- [438] T. Hodan, D. Barath, and J. Matas, "Epos: Estimating 6d pose of objects with symmetries," in *Proc. CVPR*. IEEE, 2020, pp. 11 703–11 712.
- [439] F. Kluger, E. Brachmann, H. Ackermann, C. Rother, M. Y. Yang, and B. Rosenhahn, "Consac: Robust multi-model fitting by conditional sample consensus," in *Proc. CVPR*. IEEE, 2020, pp. 4634–4643.
- [440] J. Guo, X. Xing, W. Quan, D.-M. Yan, Q. Gu, Y. Liu, and X. Zhang, "Efficient center voting for object detection and 6d pose estimation in 3d point cloud," *TIP*, vol. 30, pp. 5072–5084, 2021.
- [441] D. Barath, D. Rozumny, I. Eichhardt, L. Hajder, and J. Matas, "Progressive-x+: Clustering in the consensus space," *arXiv*, vol. 1, no. 2, 2021.
- [442] W. Tang and D. Zou, "Multi-instance point cloud registration by efficient correspondence clustering," in *Proc. CVPR*. IEEE, 2022, pp. 6667–6676.
- [443] M. Yuan, Z. Li, Q. Jin, X. Chen, and M. Wang, "Pointclm: A contrastive learning-based framework for multi-instance point cloud registration," in *Proc. ECCV*. Springer, 2022, pp. 595–611.
- [444] X. Yue, Z. Liu, J. Zhu, X. Gao, B. Yang, and Y. Tian, "Coarse-fine point cloud registration based on local point-pair features and the iterative closest point algorithm," *Appl Intell*, vol. 52, no. 11, pp. 12 569–12 583, 2022.
- [445] X. Cao, X. Zhang, Y. Cheng, Z. Qi, Y. Zhang, and J. Yang, "Instance by instance: An iterative framework for multi-instance 3d registration," *arXiv*, 2024.
- [446] Z. Yu, Z. Qin, L. Zheng, and K. Xu, "Learning instance-aware correspondences for robust multi-instance point cloud registration in cluttered scenes," in *Proc. CVPR*. IEEE, 2024, pp. 19 605–19 614.
- [447] Y. Wu, Y. Yuan, X. Fan, M. Gong, H. Li, M. Zhang, Q. Miao, W. Ma et al., "Pointmc: Multi-instance point cloud registration based on maximal cliques," in *Proc. ICML*.
- [448] Z. Yu, Q. Zheng, C. Zhu, and K. Xu, "Efficient and accurate multi-instance point cloud registration with iterative main cluster detection," in *Proc. Eurographics (Short Papers)*, 2024.

- [449] L. Zhang, L. Hui, B. Li, Y. Dai *et al.*, “3d focusing-and-matching network for multi-instance point cloud registration,” in *Proc. NeurIPS*, 2024.
- [450] J. Vidal, C.-Y. Lin, X. Lladó, and R. Martí, “A method for 6d pose estimation of free-form rigid objects using point pair features on range data,” *Sensors*, vol. 18, no. 8, p. 2678, 2018.
- [451] R. Vock, A. Dieckmann, S. Ochmann, and R. Klein, “Fast template matching and pose estimation in 3d point clouds,” *Comput Graph*, vol. 79, pp. 36–45, 2019.